

NASA TECHNICAL NOTE



NASA TN D-5499

*C. 1*

NASA TN D-5499



LOAN COPY: RETURN TO  
AFWL (WL0L-2)  
KIRTLAND AFB, N MEX

## SUPERSONIC LIFTING CAPABILITIES OF LARGE-ANGLE CONES

*by James F. Campbell and Dorothy T. Howell*

*Langley Research Center*

*Langley Station, Hampton, Va.*



0132136

1. Report No. NASA TN D-5499	2. Government Accession No.	3. Recipient's Catalog No.	
4. Title and Subtitle  SUPERSONIC LIFTING CAPABILITIES OF LARGE-ANGLE CONES		5. Report Date October 1969	
		6. Performing Organization Code	
7. Author(s)  James F. Campbell and Dorothy T. Howell		8. Performing Organization Report No. L-6833	
		10. Work Unit No. 124-07-23-04-23	
9. Performing Organization Name and Address  NASA Langley Research Center Hampton, Va. 23365		11. Contract or Grant No.	
		13. Type of Report and Period Covered  Technical Note	
12. Sponsoring Agency Name and Address  National Aeronautics and Space Administration Washington, D.C. 20546		14. Sponsoring Agency Code	
15. Supplementary Notes			
16. Abstract  <p>An analysis has been made of the supersonic lifting capabilities of large-angle cones. Experimental data used for this investigation were obtained on wind-tunnel models at Mach numbers from 1.41 to 4.63 for a Reynolds number of <math>0.8 \times 10^6</math> based on model base diameter. Cone semiapex angles ranged from <math>40^\circ</math> to <math>90^\circ</math> (disk).</p> <p>Results of this study indicated that transverse displacement of the center of gravity vertically from the vehicle longitudinal center line is an effective method of producing trim lift on large-angle cones, the trim lifting capability increasing with increase in cone semiapex angle. An increase in cone semiapex angle decreases the transverse center-of-gravity displacement required to achieve a given value of trim lift-drag ratio, and correspondingly lowers trim angle of attack, and increases trim drag. Transverse displacement of the center of gravity up to 4 percent of the base diameter from the longitudinal center line results in continual decreases in trim drag to values that are about 80 percent of the trim drag obtained for the center of gravity located on the longitudinal center line. For all combinations of cone semiapex angle and transverse center-of-gravity location, trim drag is essentially constant at Mach numbers greater than 2. Rearward longitudinal displacement of the center of gravity from the cone base to 10 percent of the base diameter has little or no effect on the trim aerodynamic characteristics obtained by transverse center-of-gravity shift for cones with semiapex angles equal to or greater than <math>70^\circ</math>.</p>			
17. Key Words Suggested by Author(s) Lifting entry Large-angle cones Aerodynamic characteristics		18. Distribution Statement  Unclassified - Unlimited	
19. Security Classif. (of this report) Unclassified	20. Security Classif. (of this page) Unclassified	21. No. of Pages 65	22. Price* \$3.00

\*For sale by the Clearinghouse for Federal Scientific and Technical Information  
Springfield, Virginia 22151

# SUPERSONIC LIFTING CAPABILITIES OF LARGE-ANGLE CONES

By James F. Campbell and Dorothy T. Howell  
Langley Research Center

## SUMMARY

An analysis has been made of the supersonic lifting capabilities of large-angle cones. Experimental data used for this investigation were obtained on wind-tunnel models at Mach numbers from 1.41 to 4.63 for a Reynolds number of  $0.8 \times 10^6$  based on model base diameter. Cone semiapex angles ranged from  $40^\circ$  to  $90^\circ$  (disk).

Results of this study indicated that transverse displacement of the center of gravity vertically from the vehicle longitudinal center line is an effective method of producing trim lift on large-angle cones, the trim lifting capability increasing with increase in cone semiapex angle. An increase in cone semiapex angle decreases the transverse center-of-gravity displacement required to achieve a given value of trim lift-drag ratio, and correspondingly lowers trim angle of attack, and increases trim drag. Transverse displacement of the center of gravity up to 4 percent of the base diameter from the longitudinal center line results in continual decreases in trim drag to values that are about 80 percent of the trim drag obtained for the center of gravity located on the longitudinal center line. For all combinations of cone semiapex angle and transverse center-of-gravity location, trim drag is essentially constant at Mach numbers greater than 2. Rearward longitudinal displacement of the center of gravity from the cone base to 10 percent of the base diameter has little or no effect on the trim aerodynamic characteristics obtained by transverse center-of-gravity shift for cones with semiapex angles equal to or greater than  $70^\circ$ .

## INTRODUCTION

The mission of placing an unmanned scientific payload on the surface of Mars is receiving the continued attention of the National Aeronautics and Space Administration. Exploratory studies, such as those of references 1 and 2, have provided the basis for the present concept of a probe/lander which is an entry vehicle having a ballistic coefficient low enough to assure proper aerodynamic retardation to an altitude and Mach number at which a terminal deceleration system (such as a parachute) can be deployed. Entry into the tenuous Martian atmosphere demands that much of the entry weight be used for vehicle structure and heat shield, thus severely limiting the allowable payload weight. This

is particularly the case for a direct ballistic entry from an interplanetary trajectory (ref. 3).

Regardless of which entry mode is employed, direct or out of orbit, a lifting entry compared with a ballistic entry, can increase substantially the weight allotted as payload (ref. 4) while allowing a relaxation of the constraints imposed by terminal-decelerator deployment; for example, the Mach number would be lower for a given deployment altitude. References 4 and 5 demonstrate the significant advantages over the ballistic entry that can be achieved with only small amounts of lift (lift-drag ratio of about 0.3). The trajectory alternatives and payload growth potential afforded by a lifting entry make it desirable to investigate the lifting capabilities of one of the leading candidates for the entry vehicle shape, the large-angle cone.

The purpose of the present study is to determine the lifting capabilities of large-angle cones at supersonic speeds. Trim lift was produced on the cone bodies by vertically displacing the center of gravity from the vehicle longitudinal center line; these transverse displacements were at distances of 1, 2, 3, and 4 percent of the base diameter. The experimental wind-tunnel data used for this investigation are published in references 6 and 7 and were obtained at Mach numbers from 1.41 to 4.63 for a Reynolds number of  $0.8 \times 10^6$  based on model base diameter. Cone semiapex angles ranged from  $40^\circ$  to  $90^\circ$  (disk).

## SYMBOLS

$C_D$	drag coefficient
$C_m$	pitching-moment coefficient
$C_{m_\alpha}$	slope of pitching-moment curve
$d$	base diameter
$L/D$	lift-drag ratio
$M$	free-stream Mach number
$x, z$	longitudinal and vertical coordinates of center of gravity, origin at center of cone base (see fig. 1)
$\alpha$	angle of attack

$\theta_c$  cone semiapex angle

Subscript:

trim conditions at trim angle of attack

## EXPERIMENTAL DATA

The experimental wind-tunnel data used for the present study are reported in references 6 and 7 and were obtained for cone models with semiapex angles of  $40^\circ$ ,  $50^\circ$ ,  $60^\circ$ ,  $70^\circ$ ,  $80^\circ$ , and  $90^\circ$  (disk). These models, illustrated in figure 1, had no nose or shoulder bluntness. Mach numbers at which the data were obtained ranged from 1.41 to 4.63 for a Reynolds number of  $0.8 \times 10^6$  based on model base diameter.

The aerodynamic coefficients published in references 6 and 7 are referred to a center-of-gravity location at the center of the cone base ( $x/d = z/d = 0$ ). These same data are presented herein along with data resulting from transverse displacement of the center of gravity at the base plane ( $x/d = 0$ ) to locations vertically below the center line and at distances of 1, 2, 3, and 4 percent of the base diameter from the center line. Data are also presented for longitudinal displacement of the center of gravity along the center line ( $z/d = 0$ ) to locations 5 and 10 percent of the base diameter behind the base plane. (See fig. 1.)

The reader will note that for high-drag vehicles, such as the large-angle cones discussed herein and the Apollo vehicle discussed in reference 8, a center-of-gravity location above the center line results in a negative trim angle of attack (nose-down condition), which produces a positive  $L/D$ . Since most of the experimental data of references 6 and 7 were obtained at positive angles of attack, it was necessary to displace the center of gravity below the center line so that the desired aerodynamic characteristics at trim could be obtained. Because the aerodynamic characteristics of a cone are symmetrical about  $\alpha = 0^\circ$ , this technique of obtaining trim aerodynamic characteristics will not affect the conclusions of this study.

## RESULTS AND DISCUSSION

### Effects of Transverse Displacement of Center of Gravity

The longitudinal aerodynamic characteristics resulting from transverse displacement of the center of gravity along the base plane ( $x/d = 0$ ) are presented in figures 2 to 7 for the range of test Mach numbers and cone semiapex angles. The  $C_D$  and

$L/D$  values shown are for  $z/d = 0$  only, but since body forces are independent of center-of-gravity location, these values are representative of the forces existing for all the center-of-gravity locations. The dashed lines represent extrapolated data and are presented to illustrate  $(L/D)_{\text{trim}}$  values attainable at angles of attack greater than those at which experimental data were obtained.

The data indicate that all the cones are statically stable  $(-C_{m\alpha})$  throughout the angle-of-attack range with the center of gravity located in the base plane. Generally, the largest drag values occur at  $\alpha = 0^\circ$ ; increasing angle of attack causes a decrease in  $C_D$  and  $L/D$  (or an increase in  $-L/D$  as it will be referred to in the subsequent discussion). The effect of increasing transverse displacement of the center of gravity is to produce a progressive increase in trim angle of attack and corresponding decreases in trim  $C_D$  and increases in  $-(L/D)_{\text{trim}}$ . The stability at trim angles of attack remains practically unchanged from that at zero angle of attack.

The effects of  $z/d$  on the trim aerodynamic characteristics are summarized in figure 8 for the range of cone semiapex angles at each Mach number. These summary data indicate that transverse center-of-gravity displacement is an effective method of producing trim lift-drag ratio for most cone semiapex angles,  $L/D$  values being obtained in excess of 0.3, a value which was shown in references 4 and 5 to have significant effects on vehicle trajectory and allowable payload weight. The effectiveness of producing  $(L/D)_{\text{trim}}$  by shifting the center of gravity increases with increased cone semiapex angle so that for a given center-of-gravity location, the largest  $-(L/D)_{\text{trim}}$  value is obtained by the  $90^\circ$  cone. The sign of  $(L/D)_{\text{trim}}$  for the  $40^\circ$  cone changes from positive at  $M = 4.63$  (fig. 8(f)) to minus at the lower Mach numbers. This dependence of the sign of  $(L/D)_{\text{trim}}$  on Mach number is not desirable for a lifting entry, particularly from the standpoint of a simplified control system, that is, no roll control (ref. 8). This trend would be alleviated somewhat by nose bluntness (ref. 9), which would be present on the actual flight vehicle. The summary data of figure 8 also show that trim drag decreases with increase in  $z/d$  for all the cone semiapex angles,  $(C_D)_{\text{trim}}$  values for  $z/d = 0.04$  being about 80 percent of those for  $z/d = 0$ . The effects of center-of-gravity location on the variation of trim aerodynamic characteristics with cone semiapex angle are illustrated in figure 9 for  $M = 4.63$ . For a given  $z/d$ , an increase in cone semiapex angle leads to higher trim angles of attack, except for the  $40^\circ$  cone, with corresponding increases in trim drag and  $-(L/D)_{\text{trim}}$ .

The effects of Mach number on the trim aerodynamic characteristics of the  $60^\circ$  and  $70^\circ$  cones are presented in figure 10. The trim  $C_D$  values are seen to remain essentially constant at Mach numbers greater than 2 for all center-of-gravity locations. Likewise, trim angle of attack and  $(L/D)_{\text{trim}}$  are generally insensitive to Mach number for values of  $z/d$  up to 0.02. For larger  $z/d$  values, a decrease in Mach number

results in an increase in trim angle of attack and an associated increase in  $-(L/D)_{\text{trim}}$ . These trends of trim aerodynamic characteristics with Mach number are shown in figure 11 to apply for all the cone semiapex angles except for the  $40^\circ$  and  $50^\circ$  cones, which experience some increase in  $\alpha_{\text{trim}}$  and  $-(L/D)_{\text{trim}}$  for  $z/d = 0.02$ . The fact that the smallest  $\alpha_{\text{trim}}$  occurs at the highest Mach number is advantageous in minimizing flow asymmetry in that region of the flight trajectory where the spacecraft would encounter the maximum heating and structural loads.

The combinations of cone semiapex angle and transverse center-of-gravity location necessary to achieve given trim values of  $L/D$  are presented in figure 12 for  $M = 4.63$  along with the resulting values of trim angle of attack and trim drag. These results demonstrate in obvious fashion that a cone with a larger semiapex angle requires smaller center-of-gravity displacement to achieve a given value of trim  $L/D$ , trims at a lower angle of attack, and has higher trim drag, all of which are advantageous trends for lifting entry. An example of lifting capability is provided by the  $70^\circ$  cone which attains a value of  $-(L/D)_{\text{trim}}$  of 0.4 with a  $z/d$  value of 0.04. This center-of-gravity location amounts to a displacement of 4.8 inches (12.2 cm) from the center line of a 10-foot-diameter (3.05-m) flight vehicle, this payload diameter being acceptable to a Titan IIC/Centaur launch vehicle. The Mach number effects previously discussed should be recalled in noting that the combinations of cone semiapex angle and center-of-gravity location presented in figure 12 for  $M = 4.63$  provide conservative estimates of the lifting capabilities of the cones at lower Mach numbers, particularly if  $z/d$  is greater than 0.02.

#### Effects of Longitudinal Displacement of Center of Gravity

The preceding discussion has indicated that larger cone semiapex angles provide the aerodynamic advantages of increased lifting capability coupled with higher drag. Utilizing a larger semiapex angle, however, reduces the amount of cone volume available for packaging the instrumented lander and equipment associated with entry and thus shifts the entry vehicle center of gravity rearward. The center of gravity would be located at or behind the base of the cones with the largest semiapex angles. For this reason it is desirable to take a cursory look at the effects of longitudinal center-of-gravity displacement on the aerodynamics of the family of cones of the present study.

The pitching-moment characteristics resulting from the longitudinal displacement of the center of gravity along the cone center line ( $z/d = 0$ ) are presented in figures 13 to 18 for the range of test Mach numbers and cone semiapex angles. The  $C_D$  and  $L/D$  variations with angle of attack are not shown in these figures since they are independent of center-of-gravity location and have been presented previously in figures 2 to 7.

All the cones are stable with the center of gravity located at the base ( $x/d = 0$ ). Displacing the center of gravity rearward from the base results in a decrease in cone stability, the largest decrease occurring on the  $40^\circ$  cone and leading to an unstable condition with the center of gravity located farthest aft ( $x/d = -0.10$ ). The decrease in cone stability with rearward displacement of center of gravity diminishes with increase in cone semiapex angle, the stability of the  $90^\circ$  cone (fig. 18) being unaffected by center-of-gravity movement. These results would be expected since a longitudinal shift of the center-of-gravity location would yield increments of pitching moment produced by a normal force and an incremental moment arm, where normal force is largest for the  $40^\circ$  cone and goes to zero for the  $90^\circ$  cone (ref. 6).

The effects of transverse center-of-gravity displacement on trim aerodynamics for the cones with  $x/d = 0$  were discussed previously and would apply here for the largest semiapex-angle cones ( $\theta_c \geq 70^\circ$ ) having more rearward center-of-gravity locations; this is because the stability levels of these large-angle cones are relatively unaffected by longitudinal center-of-gravity displacement. For semiapex angles less than  $70^\circ$ , the decrease in stability with rearward center-of-gravity displacement would result in an increase in trim angle of attack and a corresponding decrease in  $(C_D)_{\text{trim}}$  and increase in  $-(L/D)_{\text{trim}}$  from those trim values obtained with the center of gravity located in the base plane ( $x/d = 0$ ).

Little or no effect of Mach number is evident in these data.

## CONCLUSIONS

An analysis has been made of the supersonic lifting capabilities of large-angle cones. Experimental data used for this investigation were obtained on wind-tunnel models at Mach numbers from 1.41 to 4.63 for a Reynolds number of  $0.8 \times 10^6$  based on model base diameter. Cone semiapex angles ranged from  $40^\circ$  to  $90^\circ$  (disk). Results of this study lead to the following conclusions:

1. Transverse displacement of the center of gravity vertically from the vehicle longitudinal center line is an effective method of producing trim lift on large-angle cones, the trim lifting capability increasing with increase in cone semiapex angle.
2. Increase in cone semiapex angle decreases the transverse center-of-gravity displacement required to achieve a given value of trim lift-drag ratio, and correspondingly lowers trim angle of attack, and increases trim drag.
3. Transverse displacement of the center of gravity up to 4 percent of the base diameter from the longitudinal center line results in continual decreases in trim drag to values that are about 80 percent of the trim drag values obtained for the center of gravity located on the longitudinal center line.



4. For all combinations of cone semiapex angle and transverse center-of-gravity location, trim drag is essentially constant at Mach numbers greater than 2.

5. Rearward longitudinal displacement of the center of gravity from the cone base to 10 percent of the base diameter has little or no effect on the trim aerodynamic characteristics obtained by transverse center-of-gravity shift for cones with semiapex angles equal to or greater than  $70^{\circ}$ .

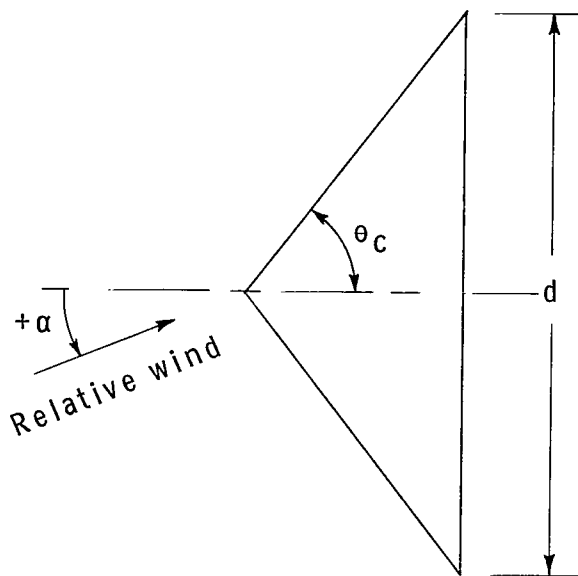
Langley Research Center,

National Aeronautics and Space Administration,

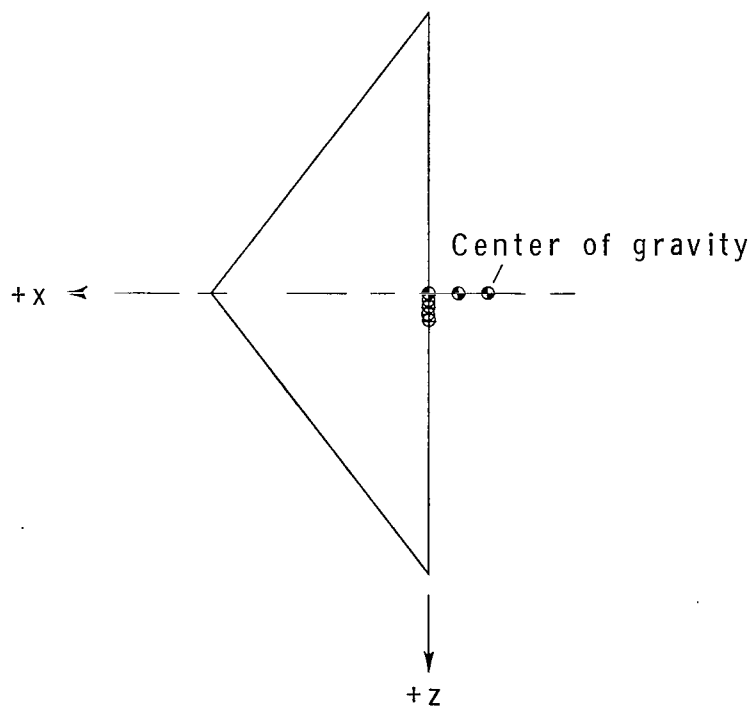
Langley Station, Hampton, Va., September 4, 1969.

## REFERENCES

1. Roberts, Leonard: Entry Into Planetary Atmospheres. Astronaut. Aeronaut., vol. 2, no. 10, Oct. 1964, pp. 22-29.
2. Eggers, Alfred J., Jr.; and Cohen, Nathaniel B.: Progress and Problems in Atmosphere Entry. Atmosphere Entry, Vol. 1 of AIAA Selected Reprint Series, Alfred J. Eggers, Jr., ed., [1967], pp. 110-128.
3. Wiltshire, Raymond S.: Study of Direct Versus Orbital Entry for Mars Missions - Vol. II: Parametric Studies, Final Analysis, and Conceptual Designs. NASA CR-66660, 1968.
4. McLellan, Charles H.; and Pritchard, E. Brian: Use of Lift to Increase Payload of Unmanned Martian Landers. J. Spacecraft Rockets, vol. 3, no. 9, Sept. 1966, pp. 1421-1425.
5. Harrison, Edwin F.; and Slocumb, Travis H., Jr.: Evaluation of Entry and Terminal Deceleration Systems for Unmanned Martian Landers. Paper presented at AIAA Entry Vehicle Systems and Technology Conference (Williamsburg, Va.), Dec. 1968.
6. Campbell, James F.; and Howell, Dorothy T.: Supersonic Aerodynamics of Large-Angle Cones. NASA TN D-4719, 1968.
7. Campbell, James F.: Supersonic Aerodynamic Characteristics and Shock Standoff Distances for Large-Angle Cones With and Without Cylindrical Afterbodies. NASA TN D-5334, 1969.
8. Crowder, R. S.; and Moote, J. D.: Apollo Entry Aerodynamics. J. Spacecraft Rockets, vol. 6, no. 3, Mar. 1969, pp. 302-307.
9. Owens, Robert V.: Aerodynamic Characteristics of Spherically Blunted Cones at Mach Numbers From 0.5 to 5.0. NASA TN D-3088, 1965.

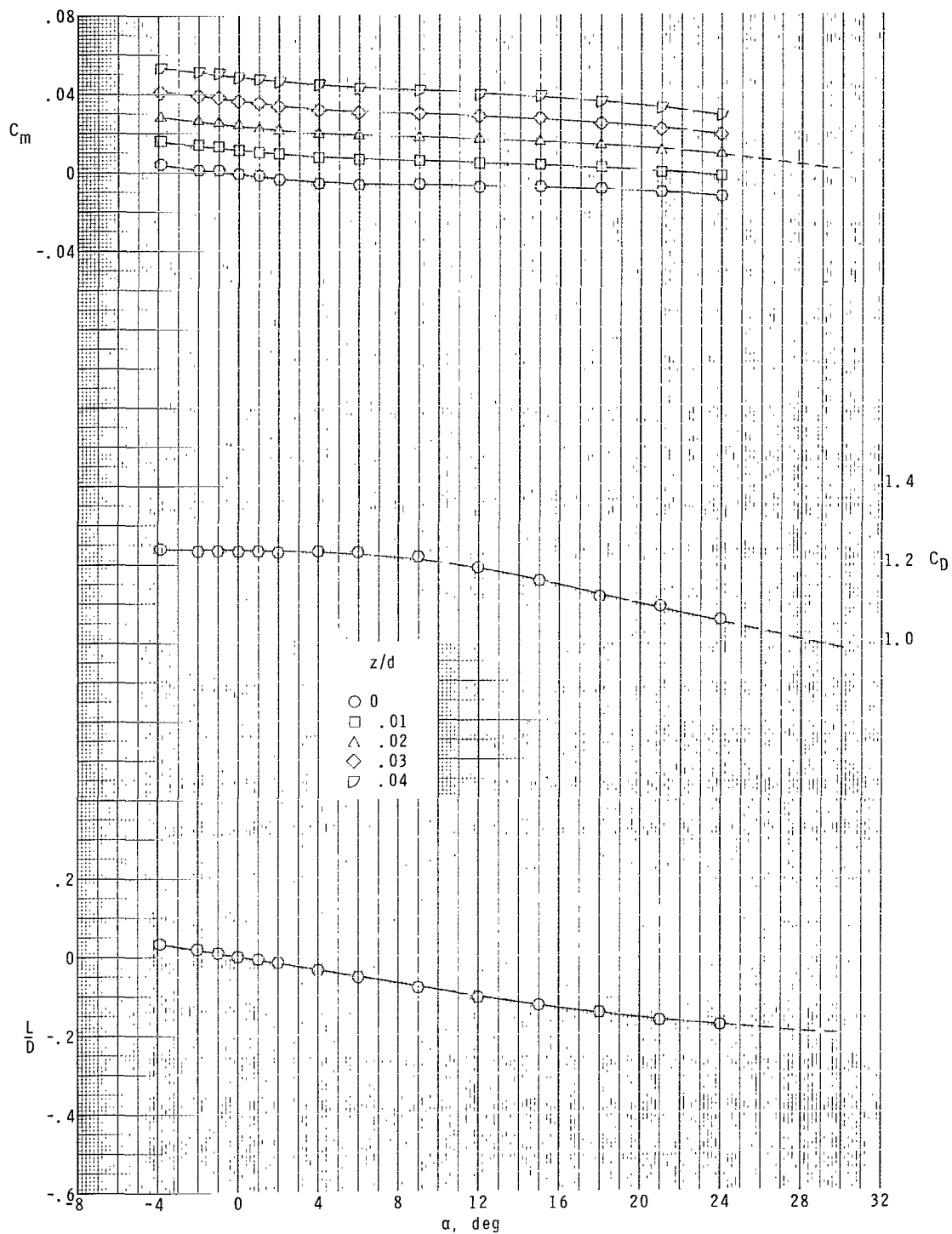


(a) Model details.  $\theta_c = 40^\circ, 50^\circ, 60^\circ, 70^\circ, 80^\circ, \text{ and } 90^\circ$ .



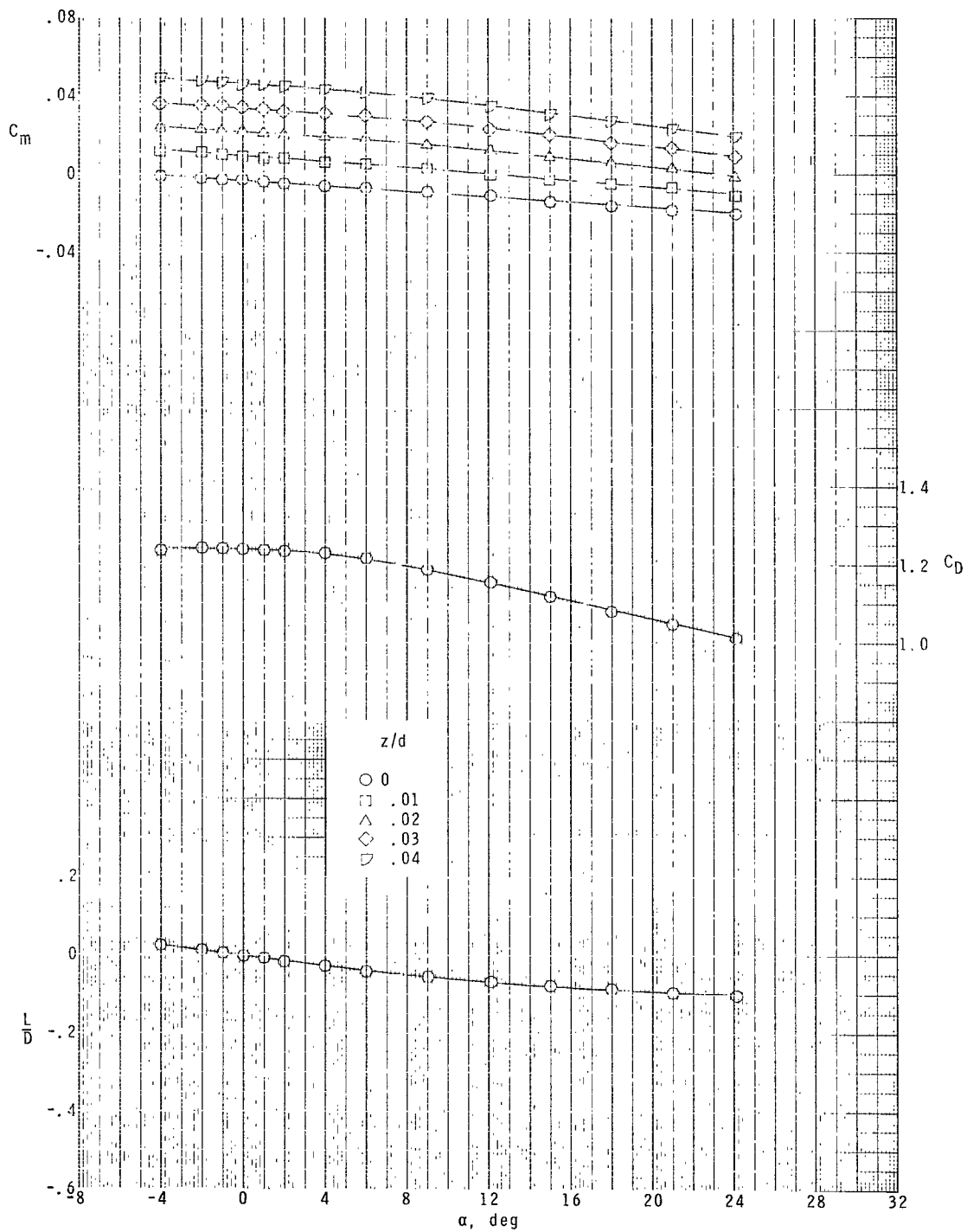
(b) Center-of-gravity locations as fractions of base diameter. For  $x/d = 0$ ,  $z/d = 0, 0.01, 0.02, 0.03, \text{ and } 0.04$ ; for  $z/d = 0$ ,  $x/d = 0, -0.05, \text{ and } -0.10$ .

Figure 1.- Schematic diagrams of cone models illustrating transverse and longitudinal center-of-gravity locations.  $d = 4.80 \text{ in. (12.19 cm)}$ .



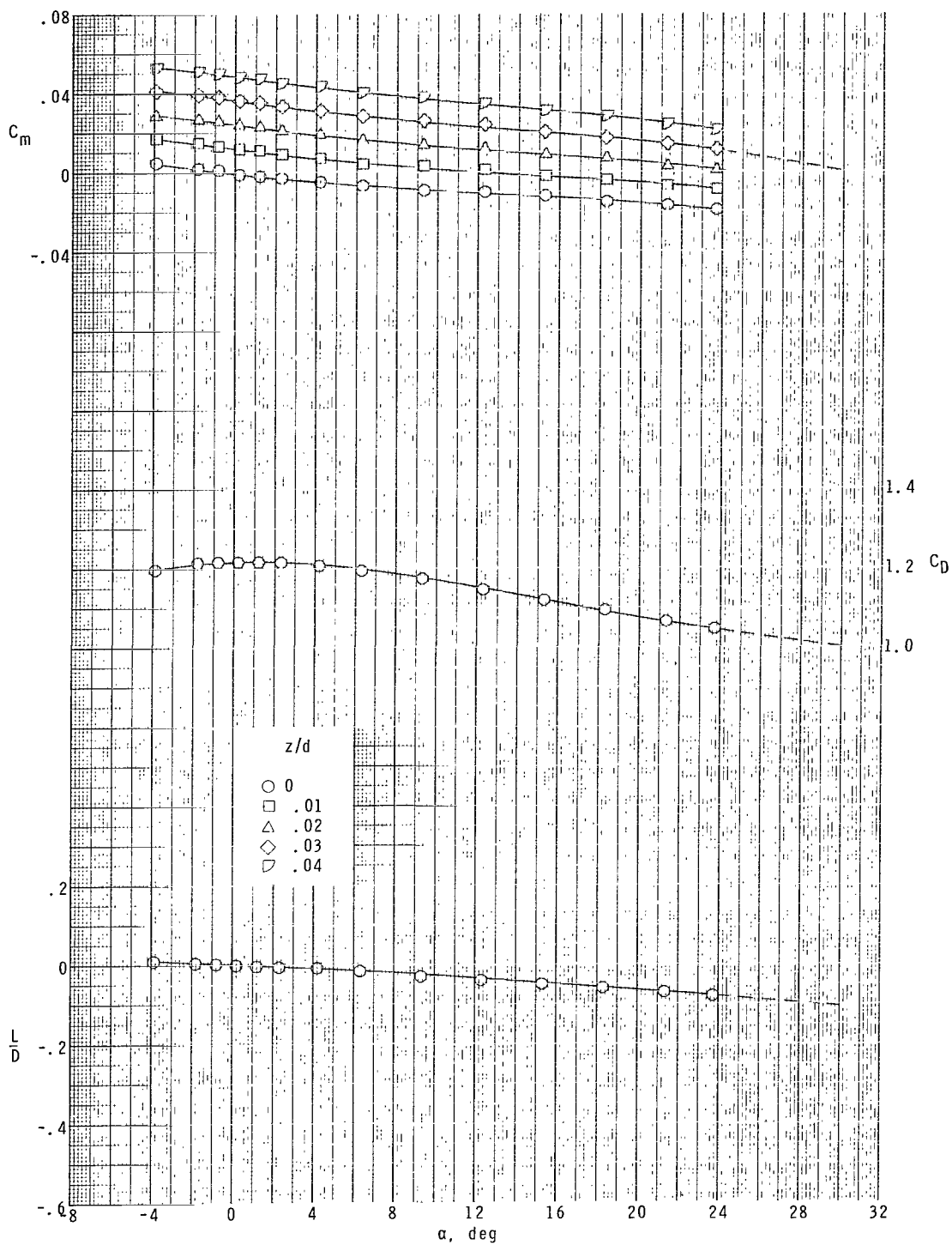
(a)  $M = 1.41$ .

Figure 2.- Longitudinal aerodynamic characteristics of the  $40^\circ$  semiapex-angle cone for the range of transverse center-of-gravity locations.  $x/d = 0$ . Dashed lines represent extrapolated data.



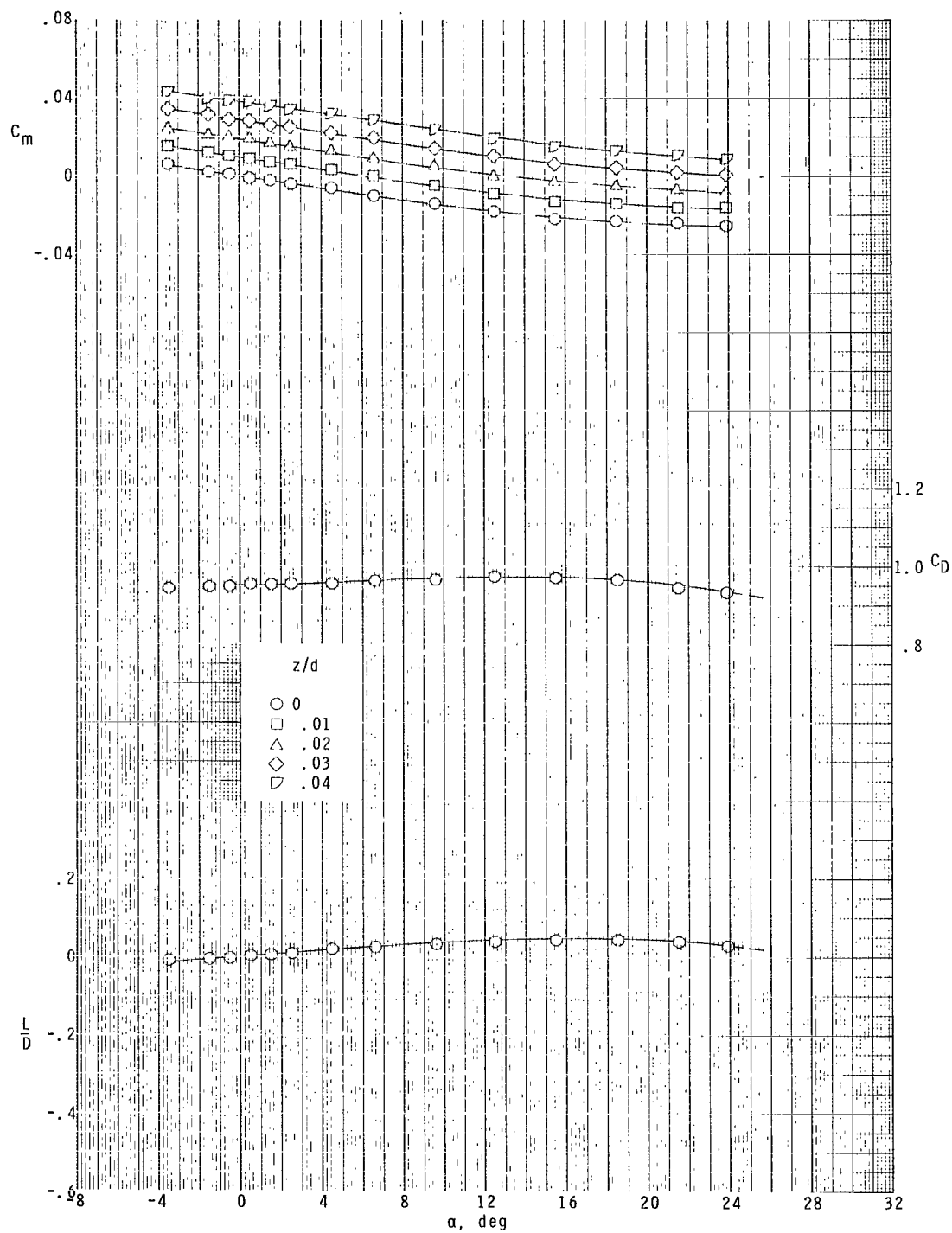
(b)  $M = 2.00$ .

Figure 2.- Continued.



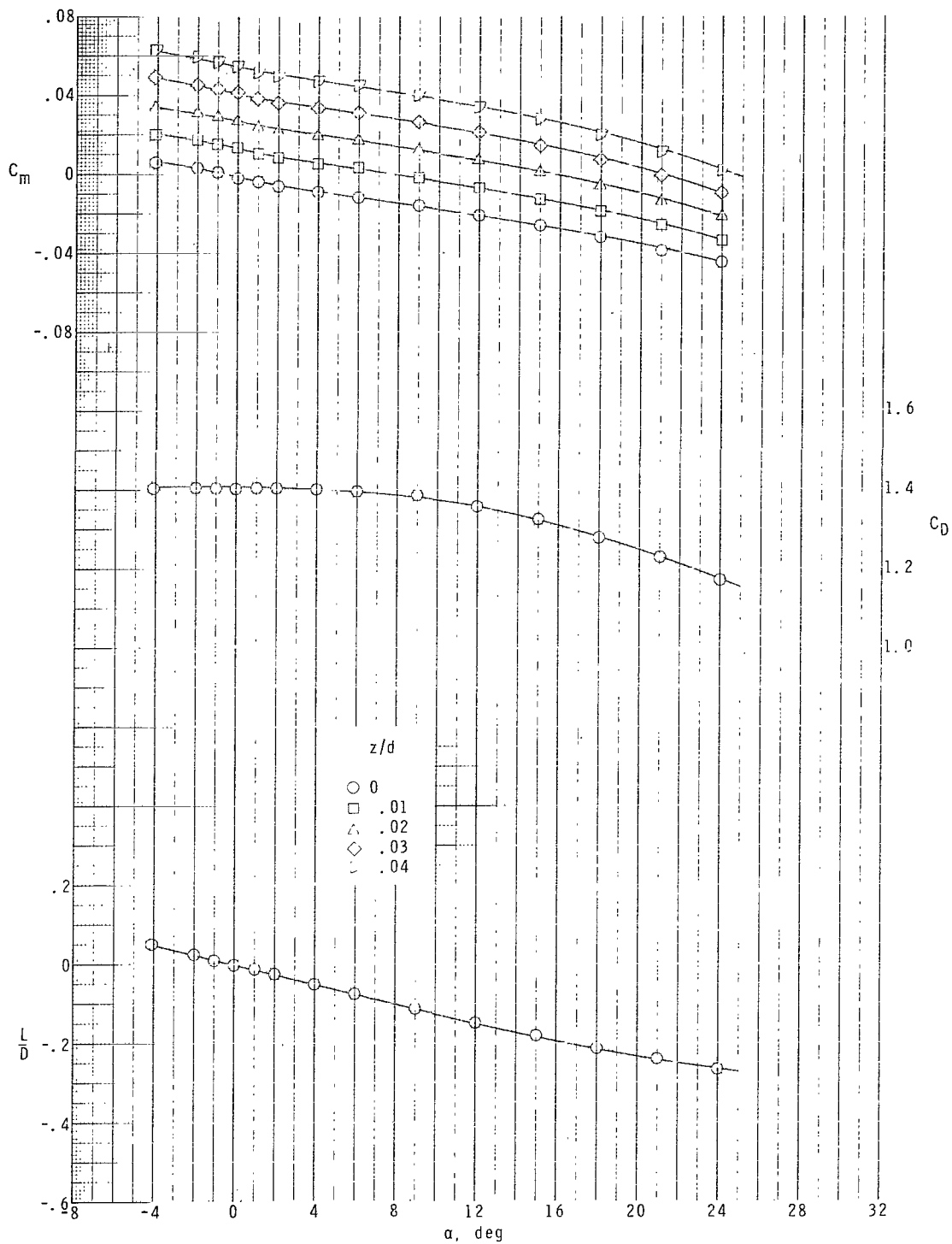
(c)  $M = 2.30$ .

Figure 2.- Continued.



(d)  $M = 4.63$ .

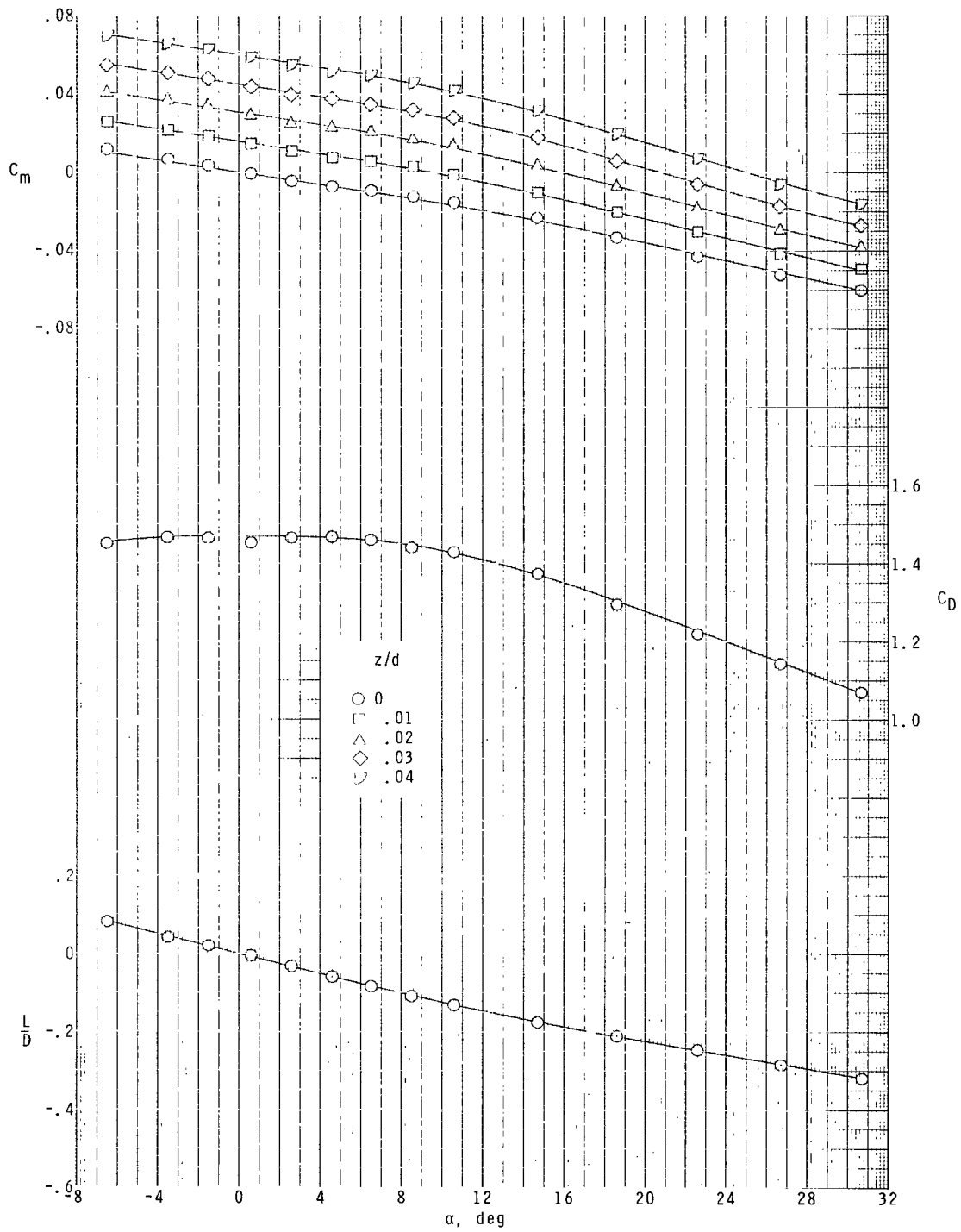
Figure 2.- Concluded.



(a)  $M = 2.00$ .

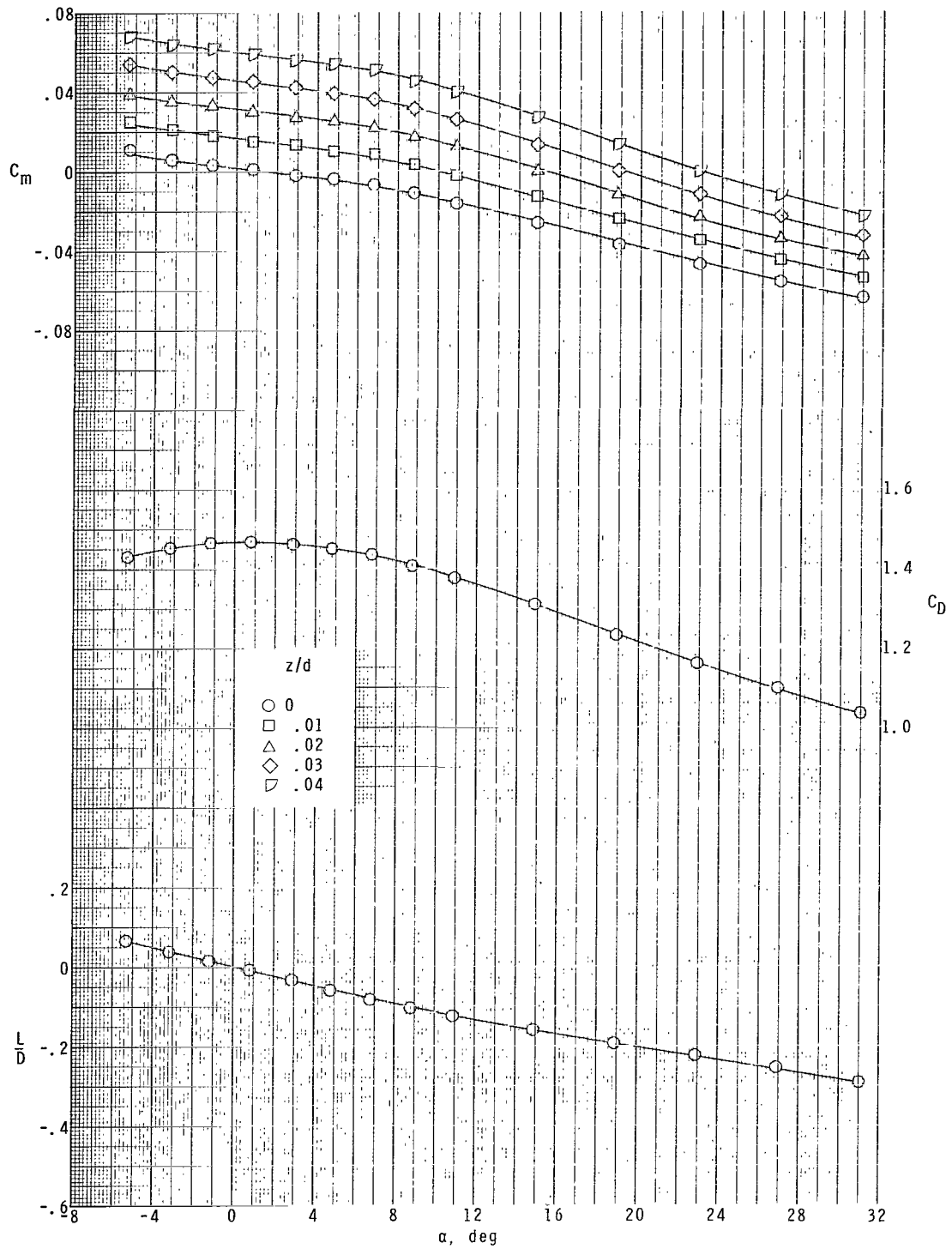
Figure 3.- Longitudinal aerodynamic characteristics of the  $50^\circ$  semiapex-angle cone for the range of transverse center-of-gravity locations.  $x/d = 0$ . Dashed lines represent extrapolated data.





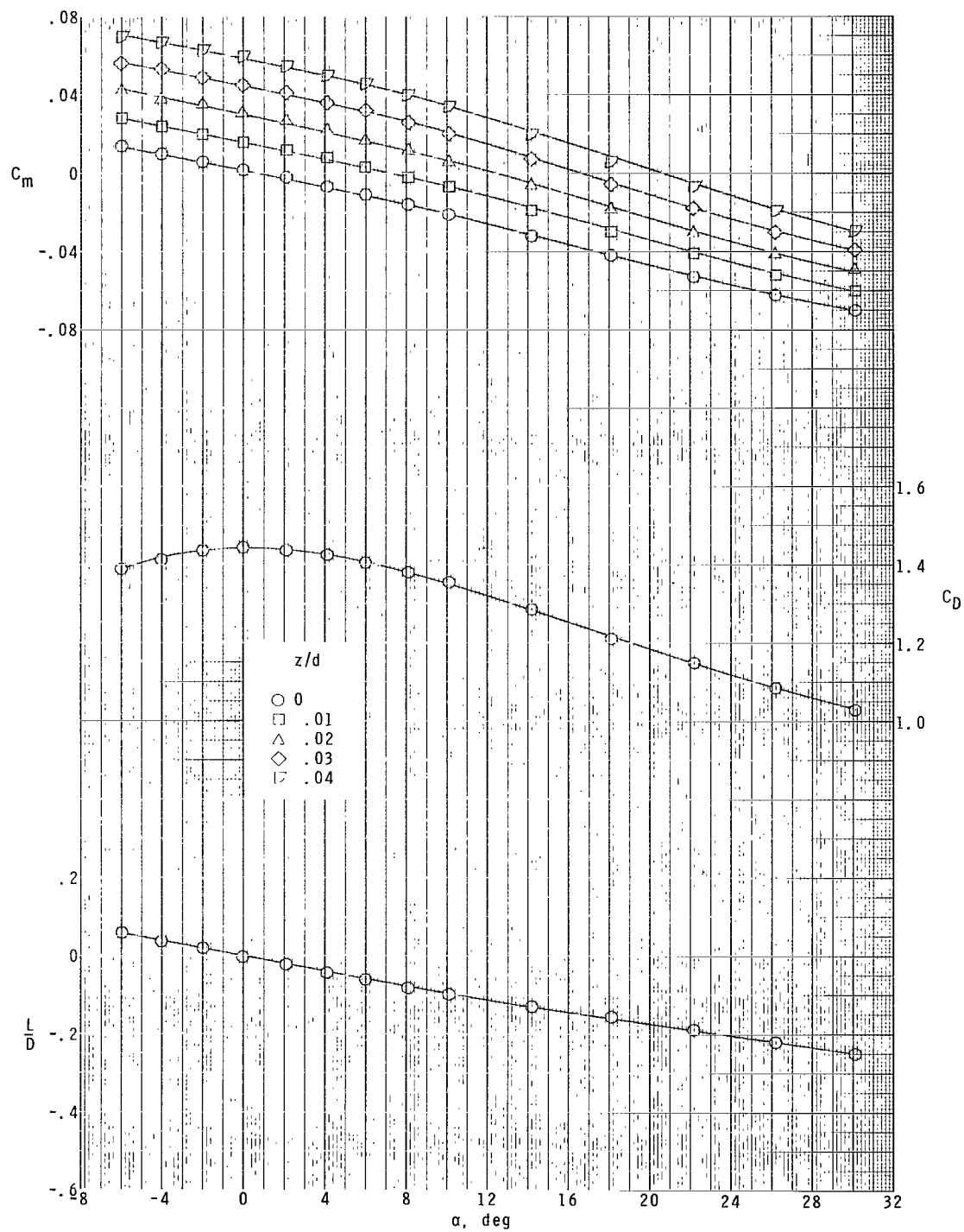
(b)  $M = 2.30$ .

Figure 3.- Continued.



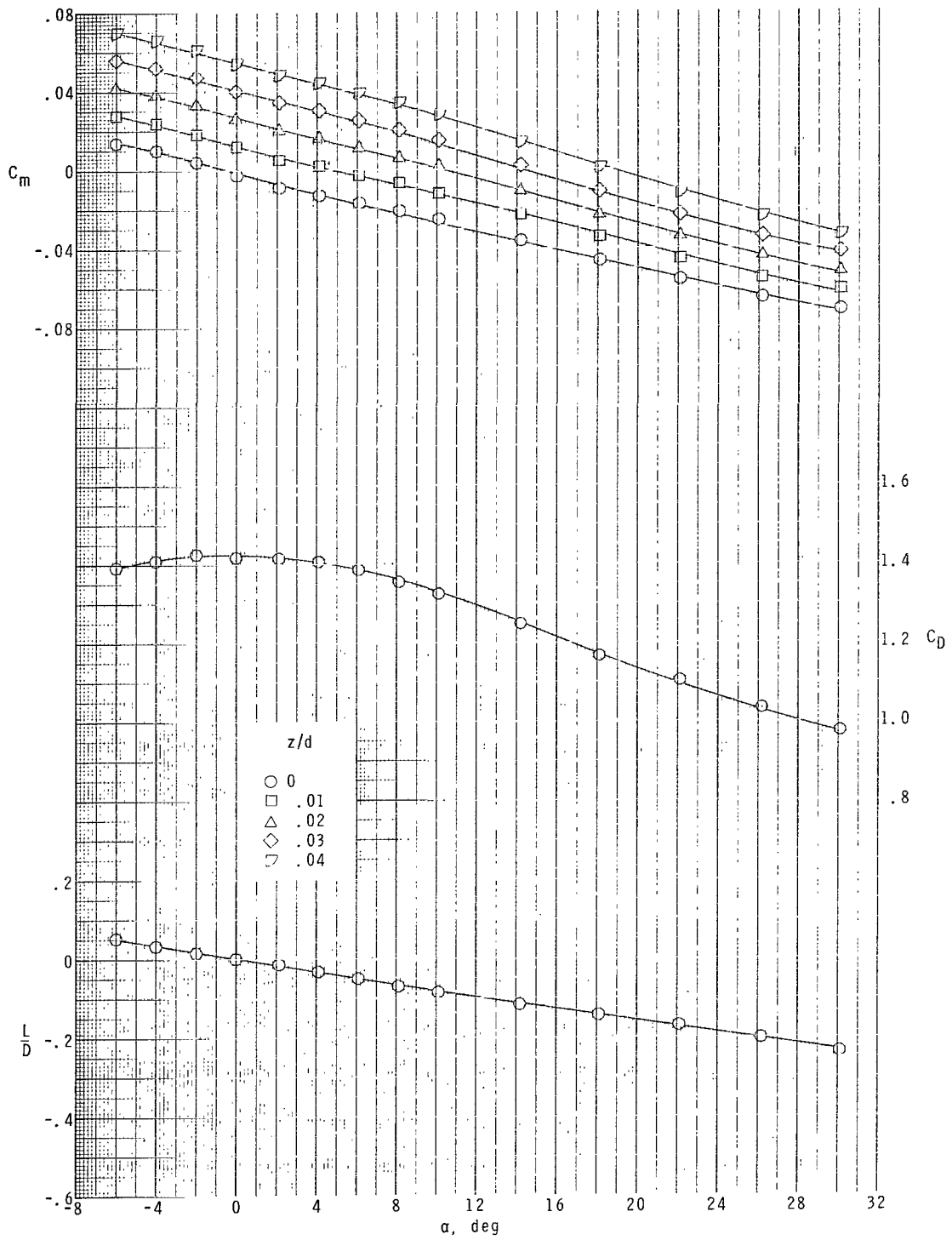
(c)  $M = 2.96$ .

Figure 3.- Continued.



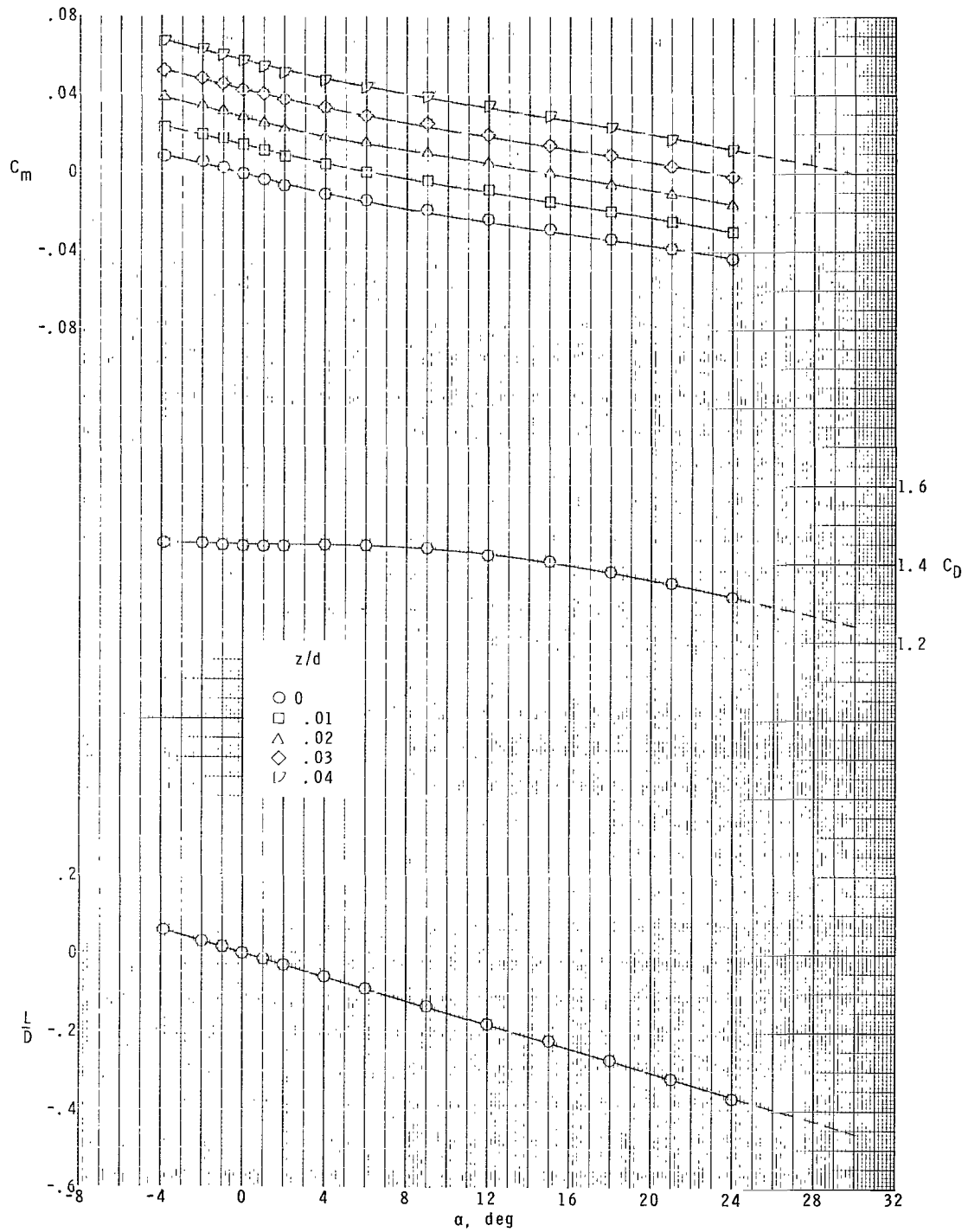
(d)  $M = 3.95$ .

Figure 3.- Continued.



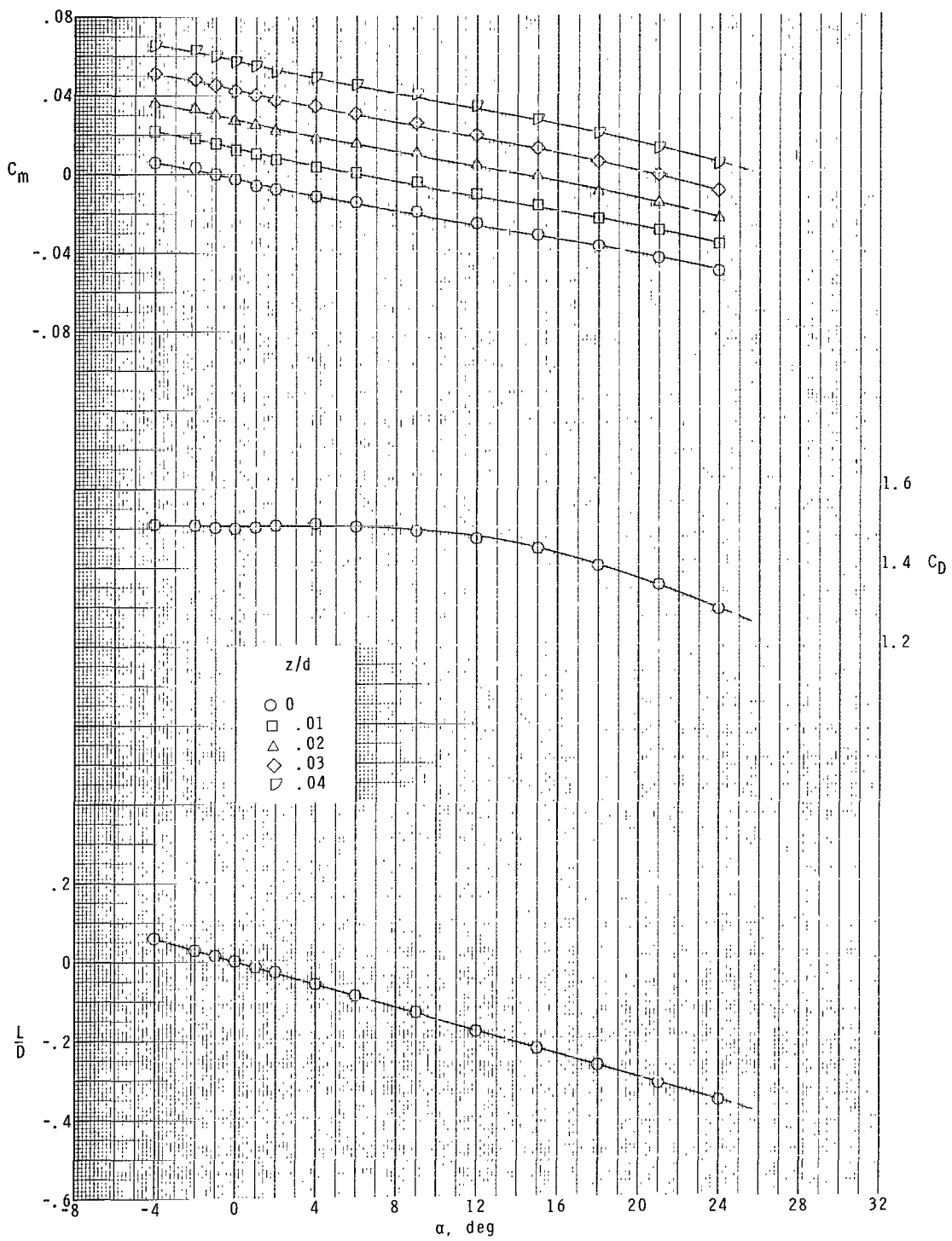
(e)  $M = 4.63$ .

Figure 3.- Concluded.



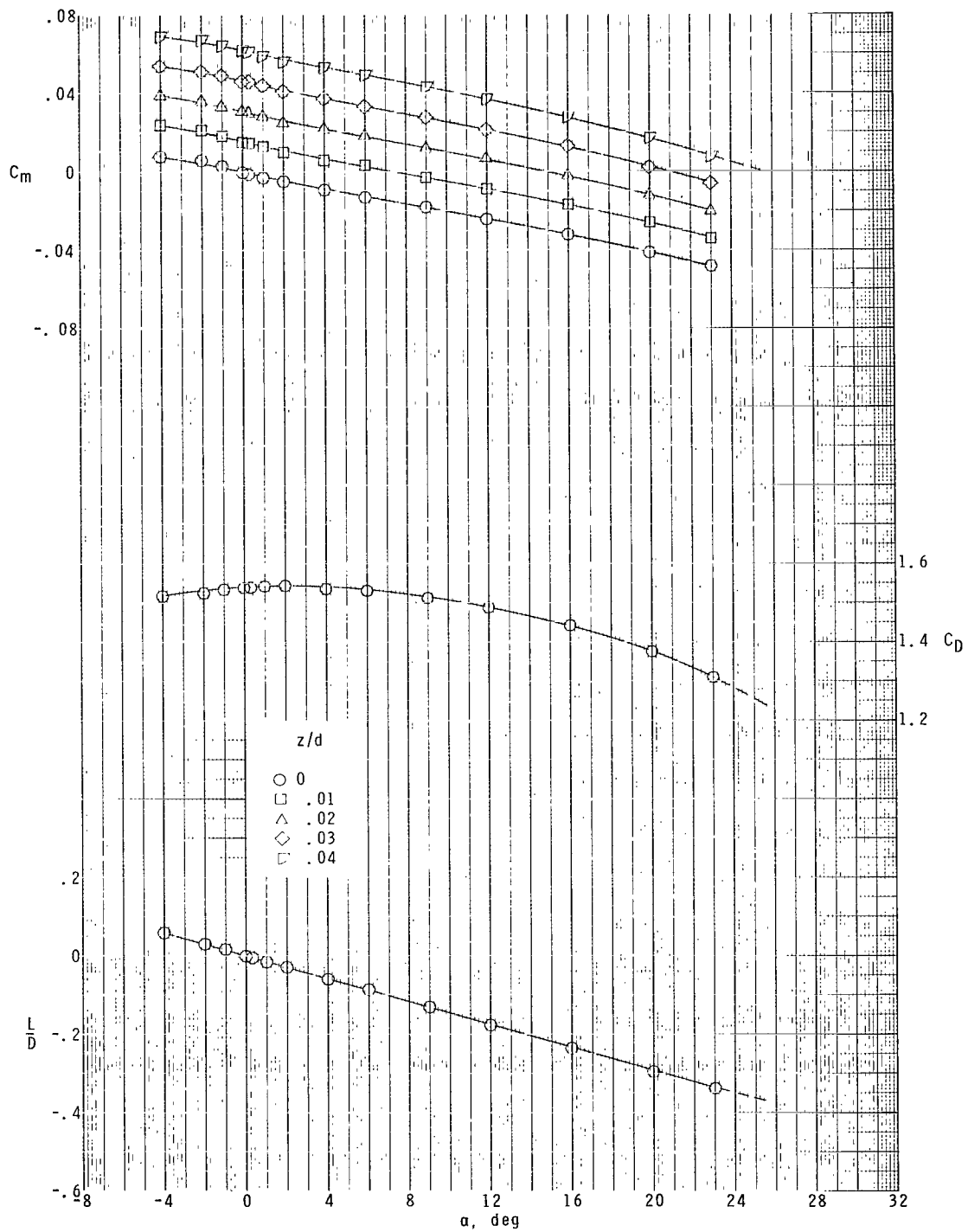
(a)  $M = 1.41$ .

Figure 4.- Longitudinal aerodynamic characteristics of the  $60^\circ$  semiapex-angle cone for the range of transverse center-of-gravity locations.  $x/d = 0$ . Dashed lines represent extrapolated data.



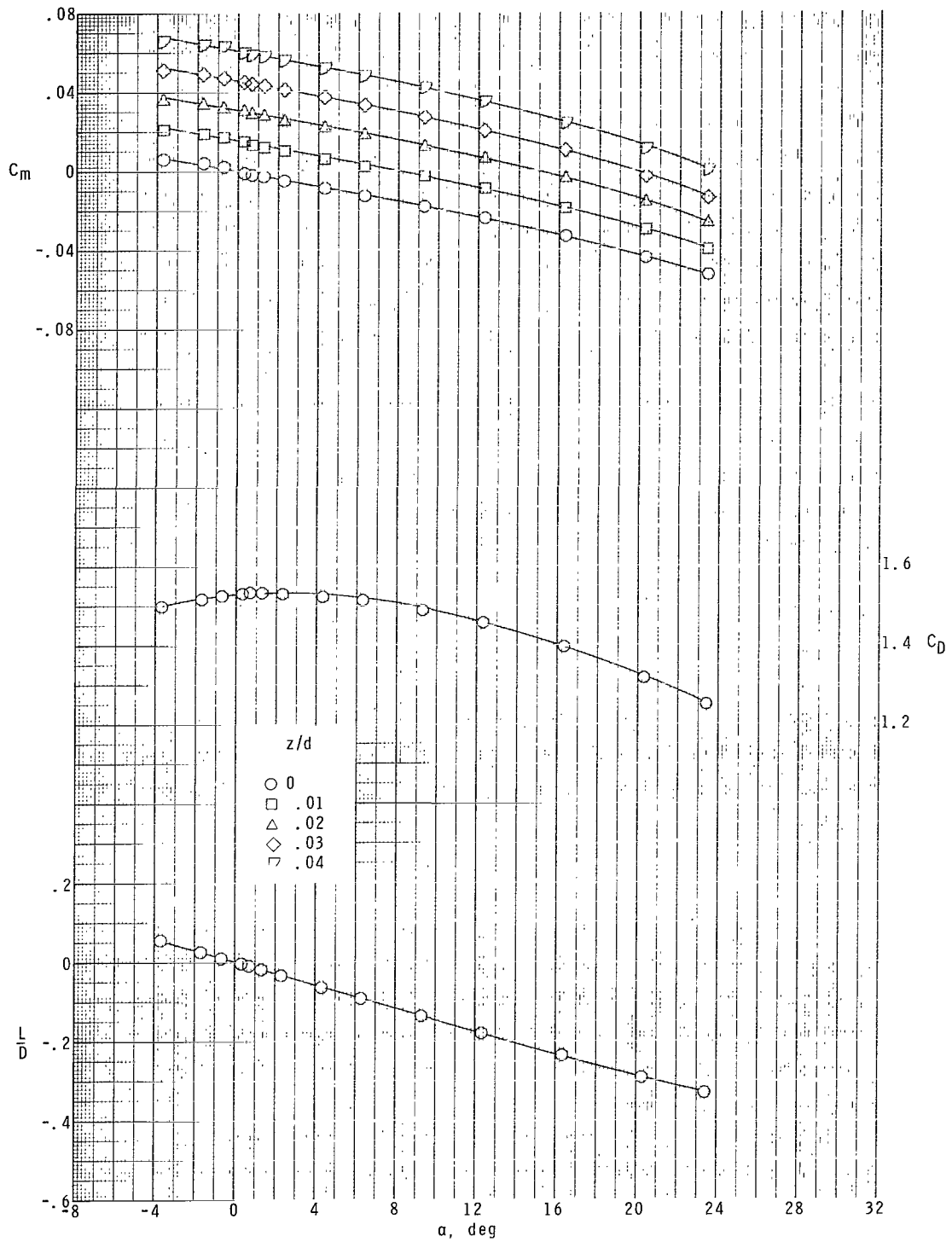
(b)  $M = 2.00$ .

Figure 4.- Continued.



(c)  $M = 2.30$ .

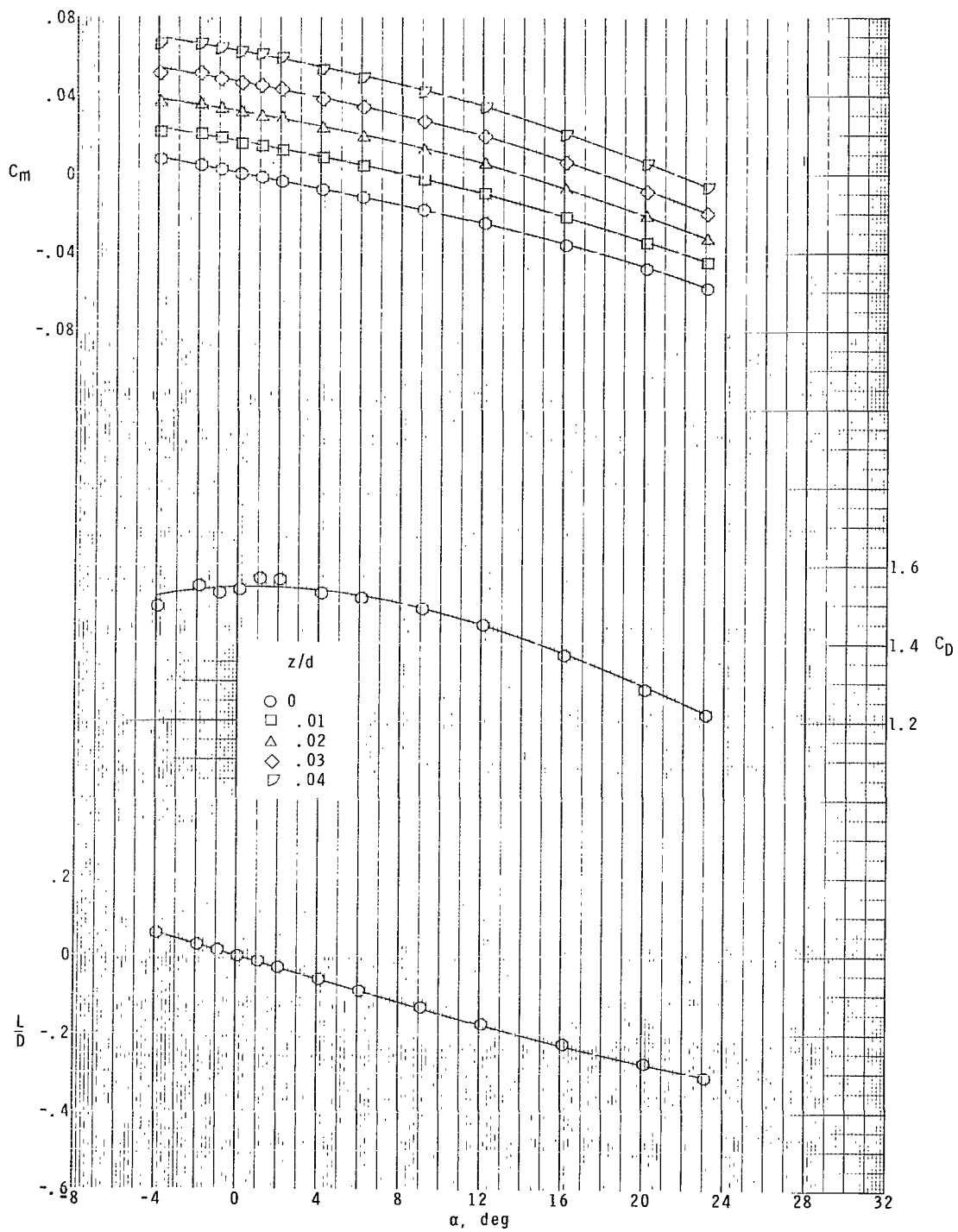
Figure 4.- Continued.



(d)  $M = 2.96$ .

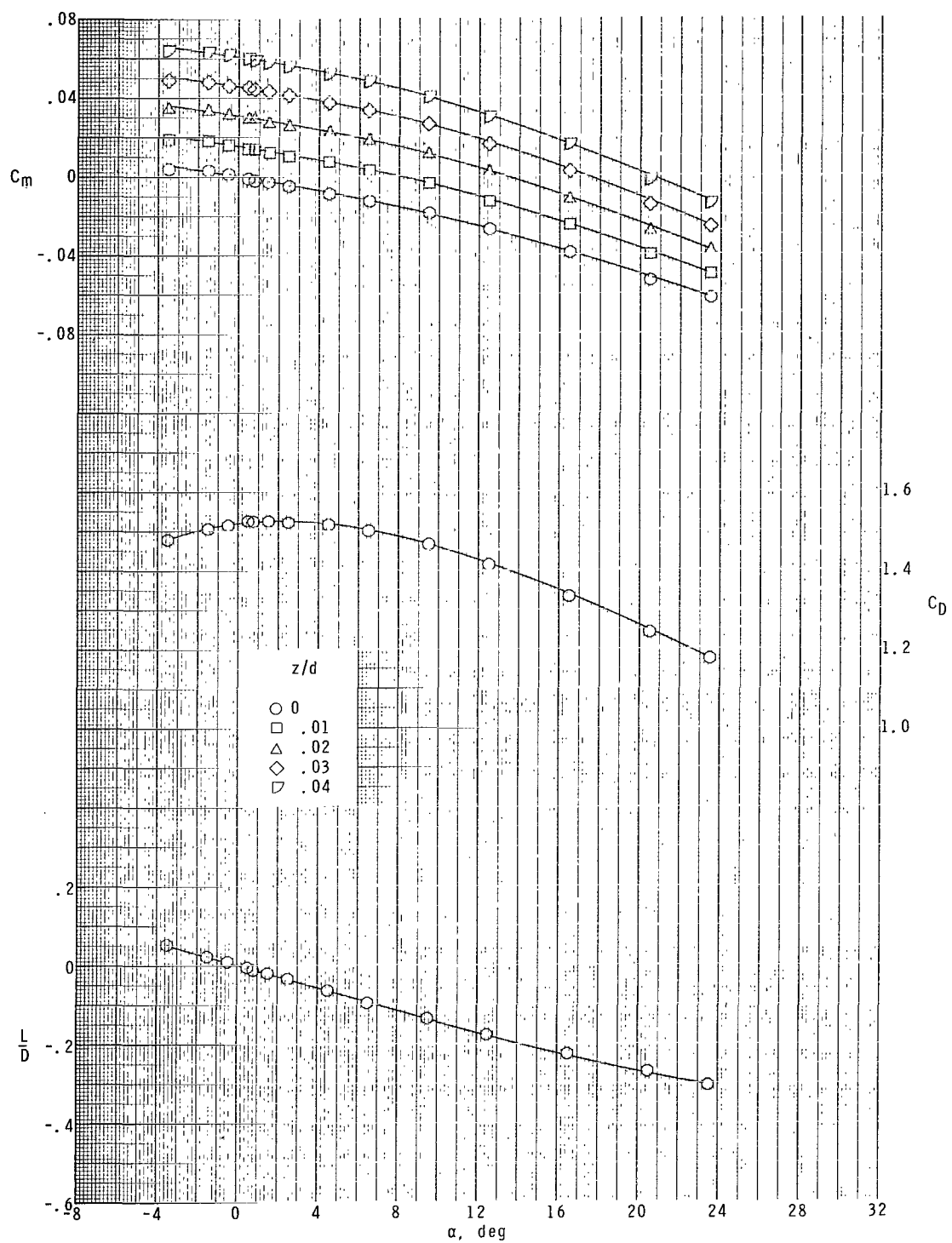
Figure 4.- Continued.





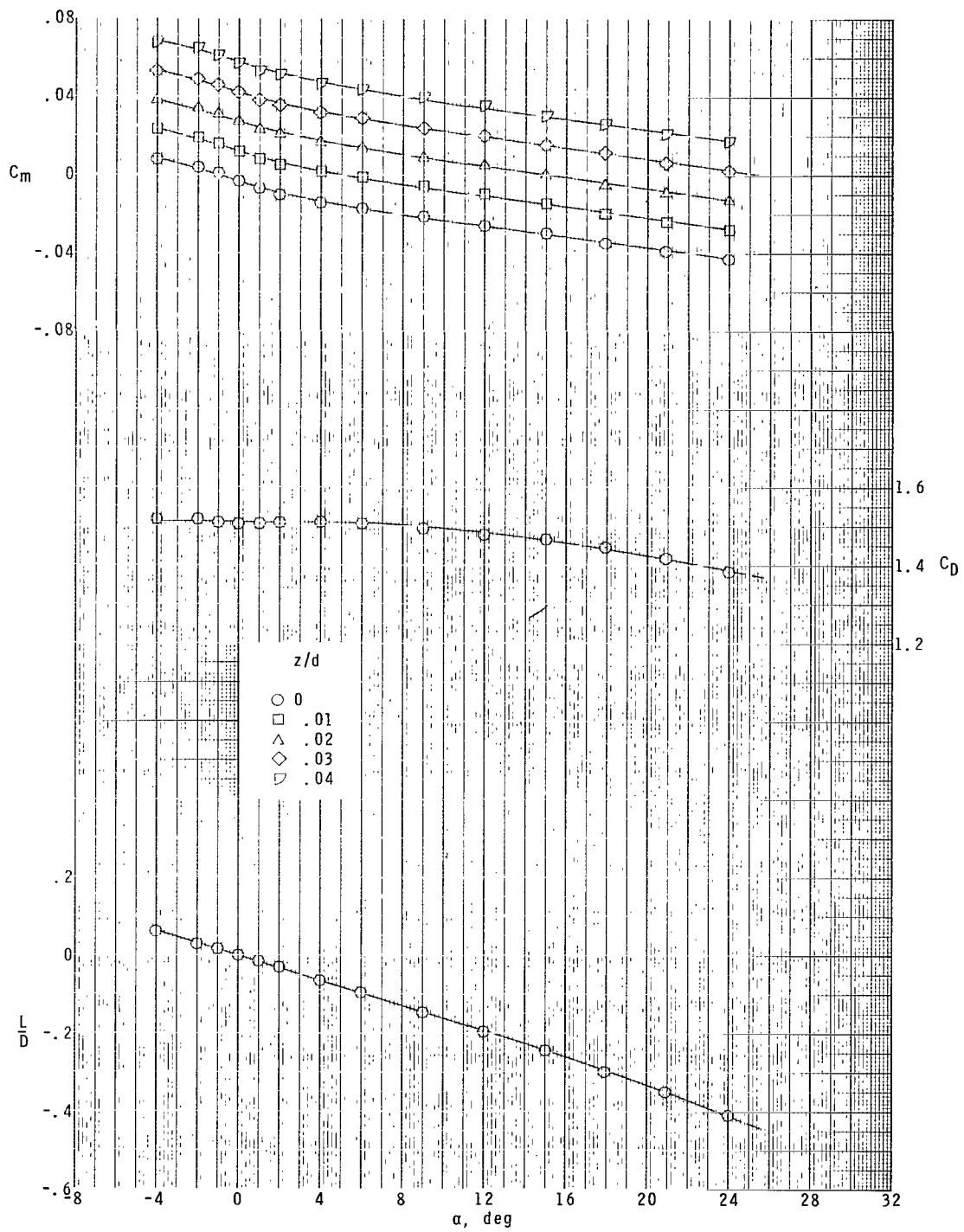
(e)  $M = 3.95$ .

Figure 4.- Continued.



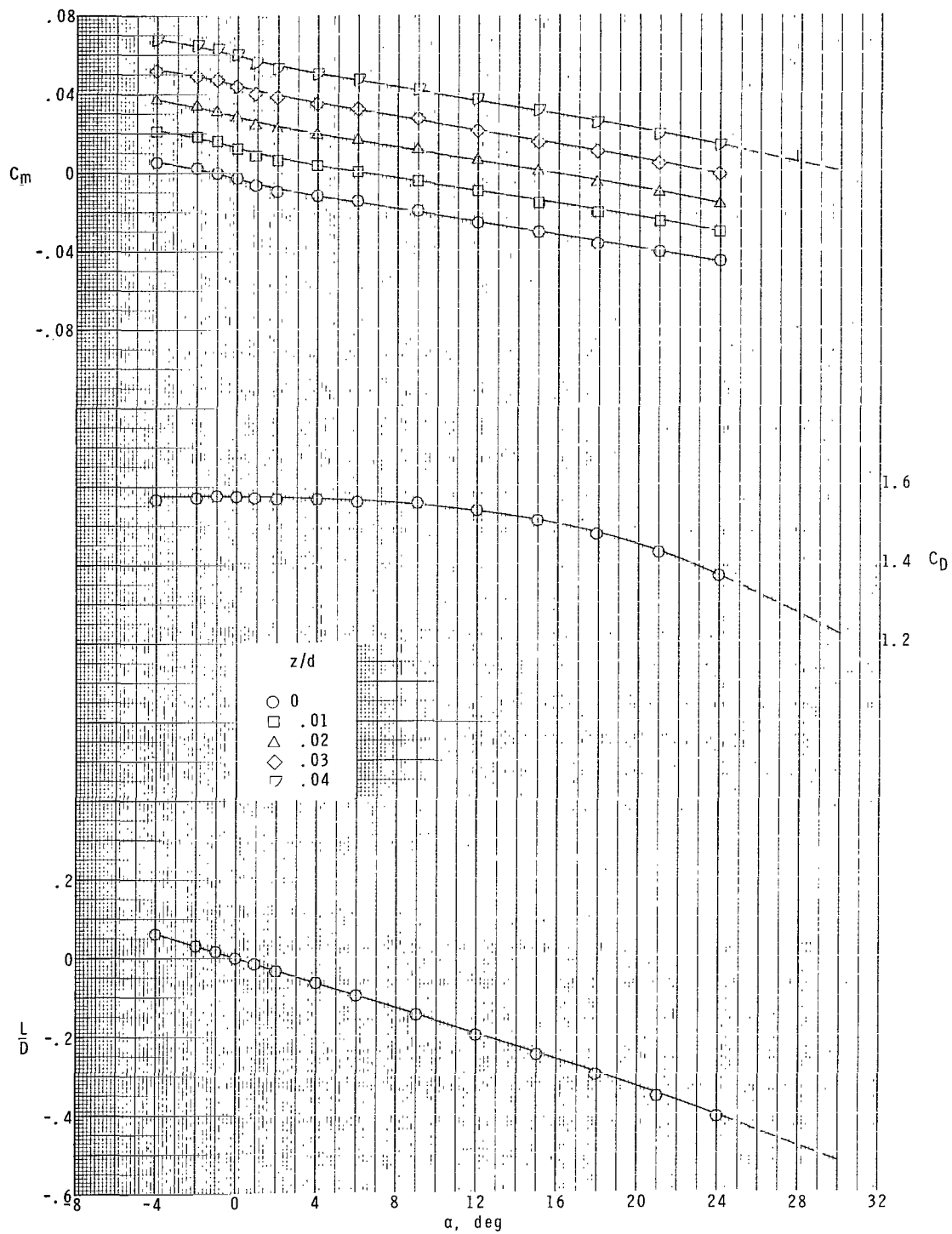
(f)  $M = 4.63$ .

Figure 4.- Concluded.



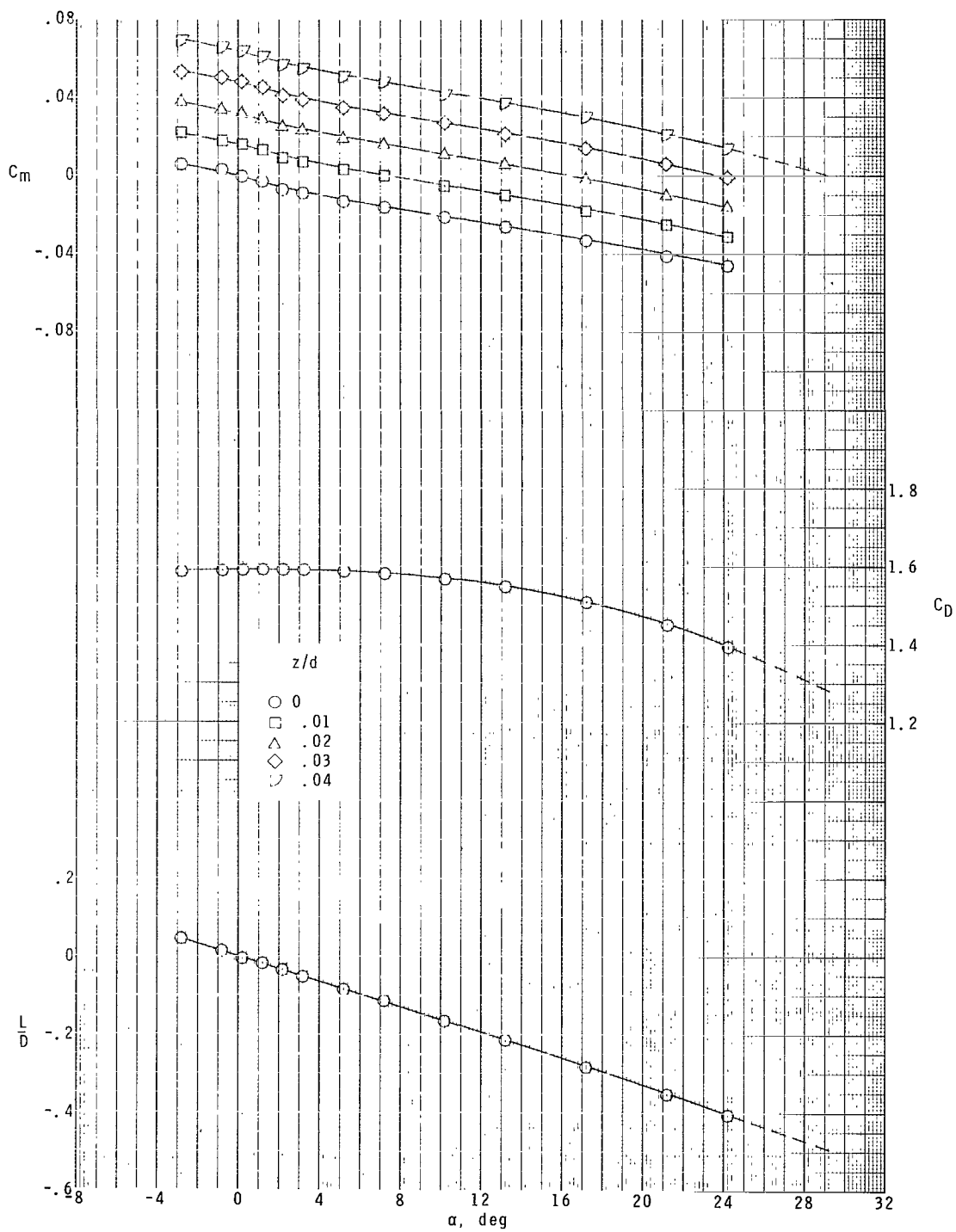
(a)  $M = 1.41$ .

Figure 5.- Longitudinal aerodynamic characteristics of the  $70^\circ$  semiapex-angle cone for the range of transverse center-of-gravity locations.  $x/d = 0$ . Dashed lines represent extrapolated data.



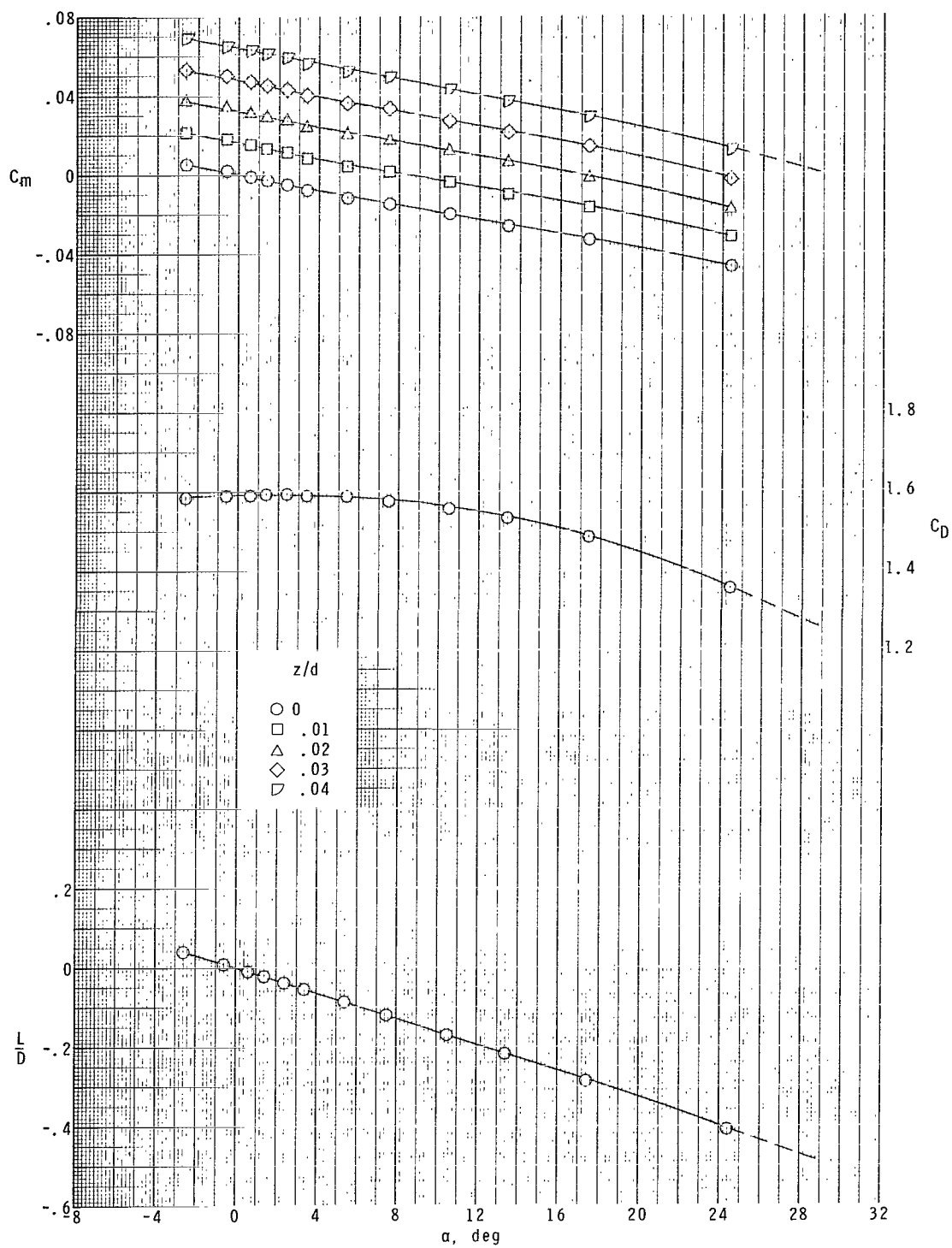
(b)  $M = 2.00$ .

Figure 5.- Continued.



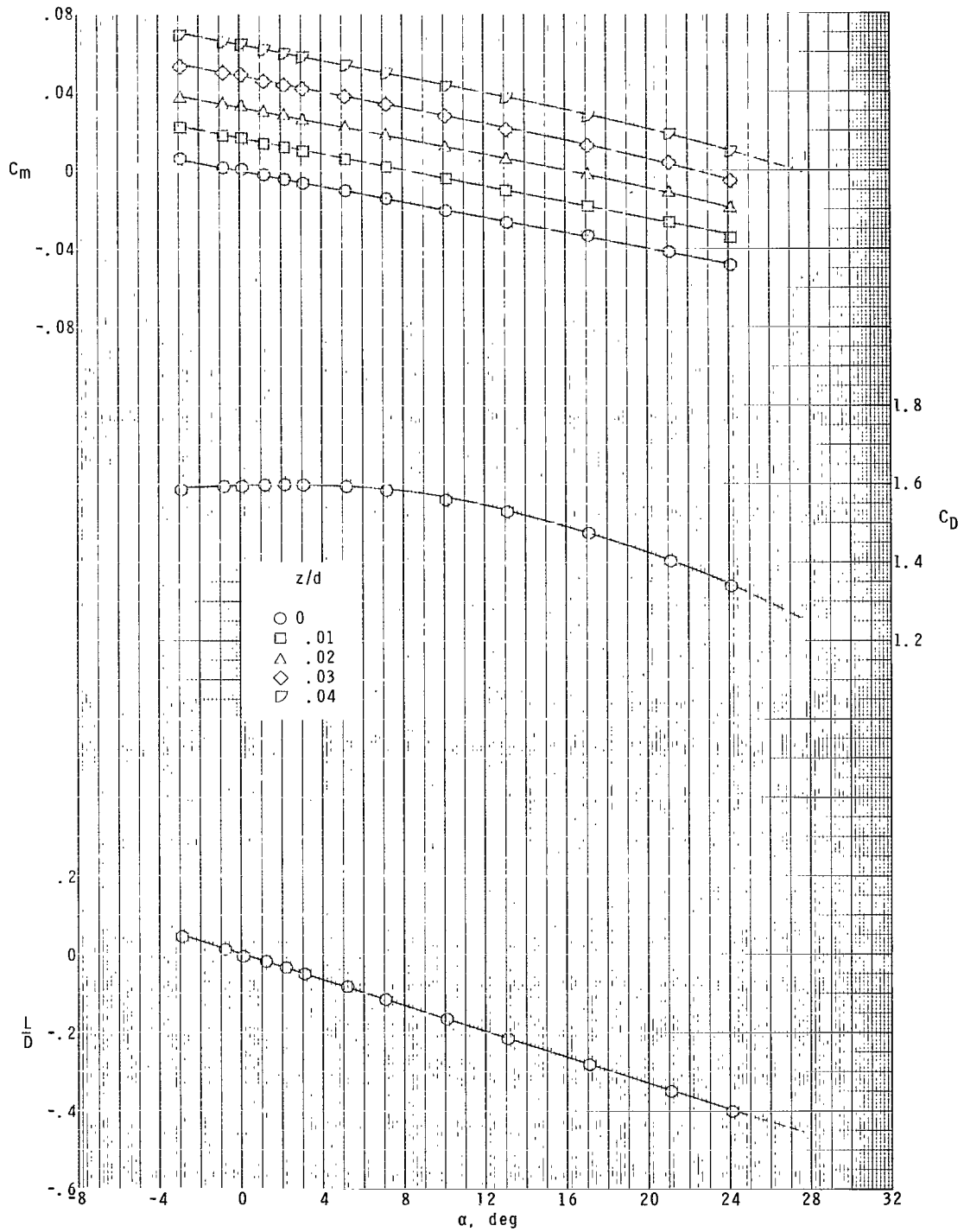
(c)  $M = 2.30$ .

Figure 5.- Continued.



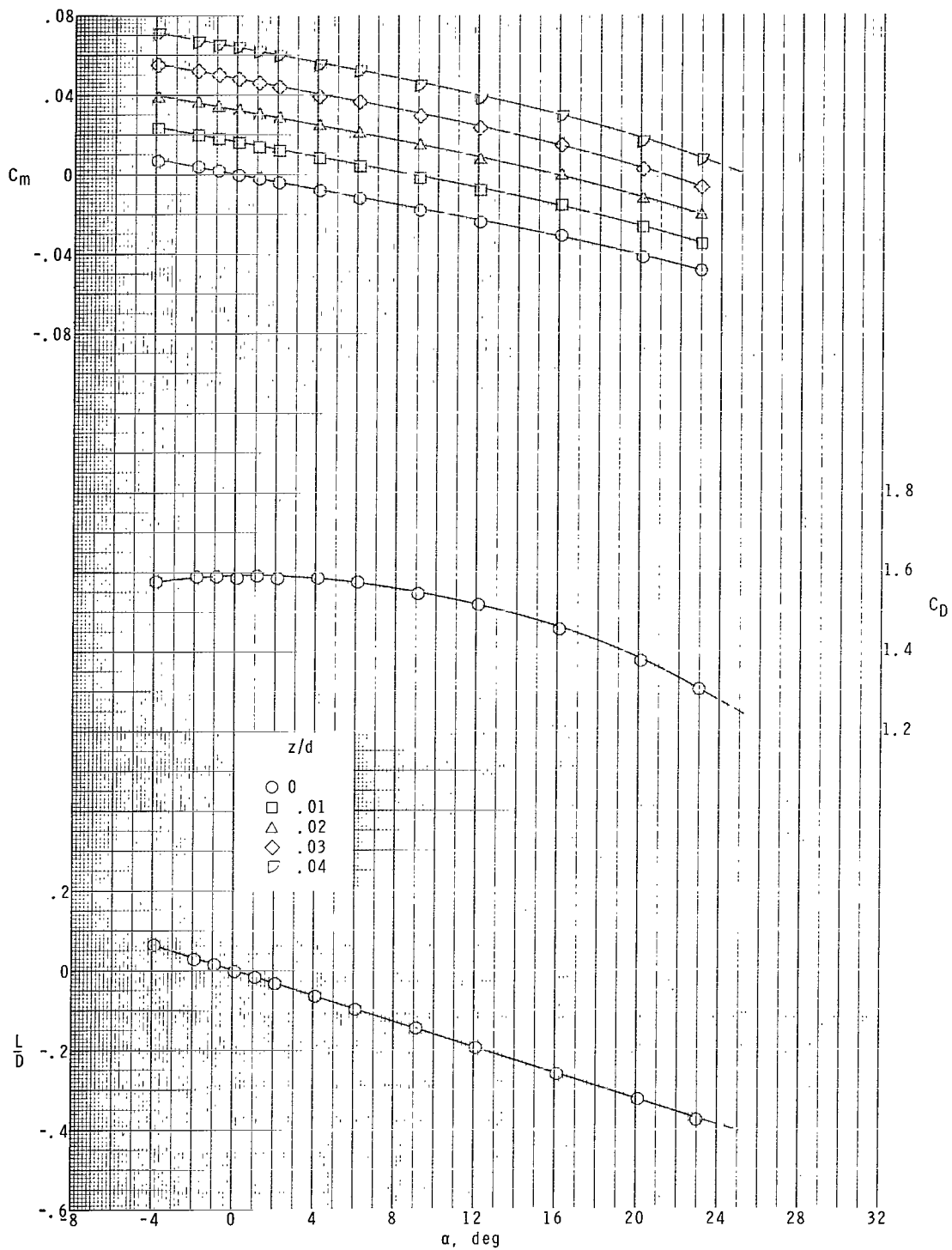
(d)  $M = 2.96$ .

Figure 5.- Continued.



(e)  $M = 3.95$ .

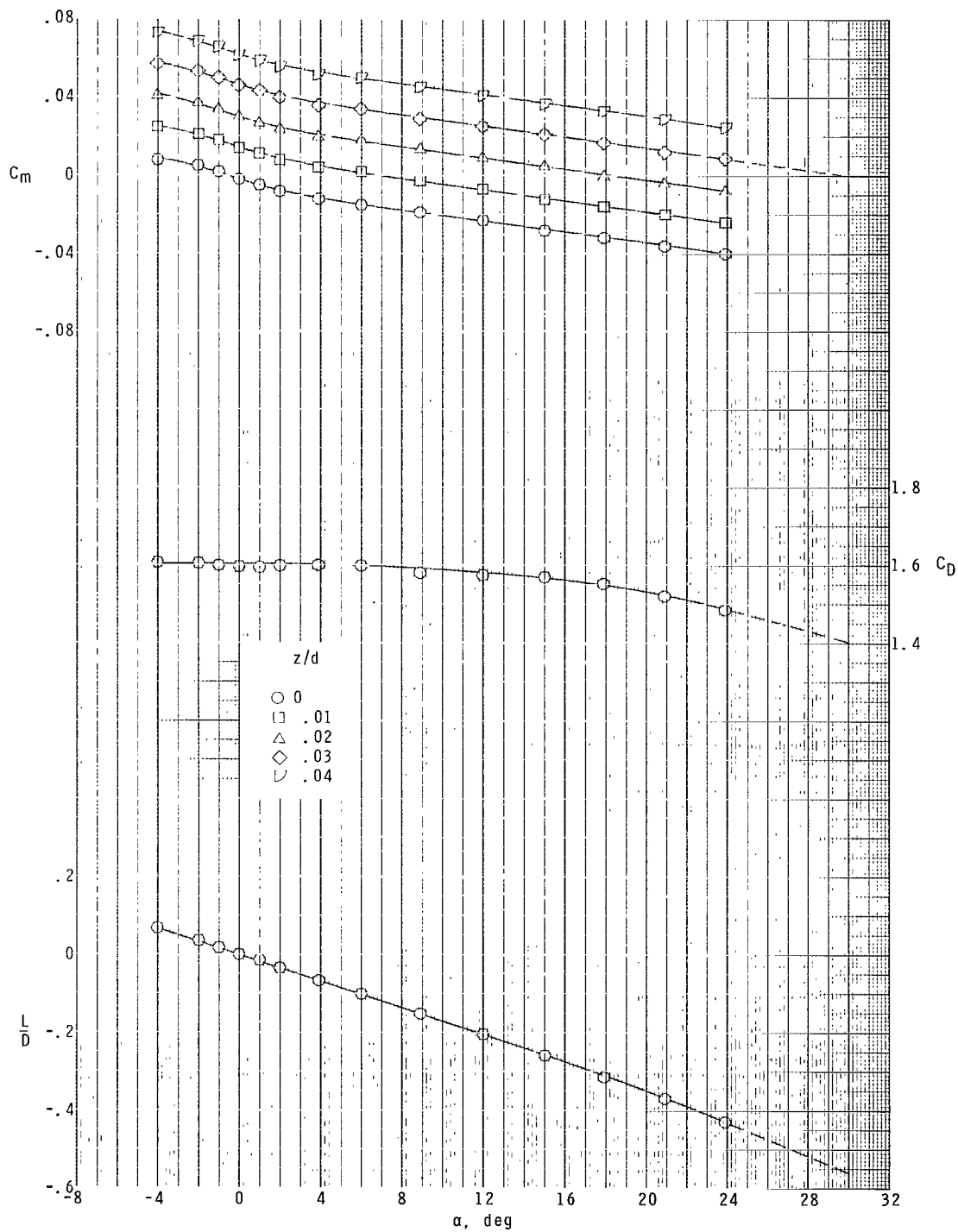
Figure 5.- Continued.



(f)  $M = 4.63$ .

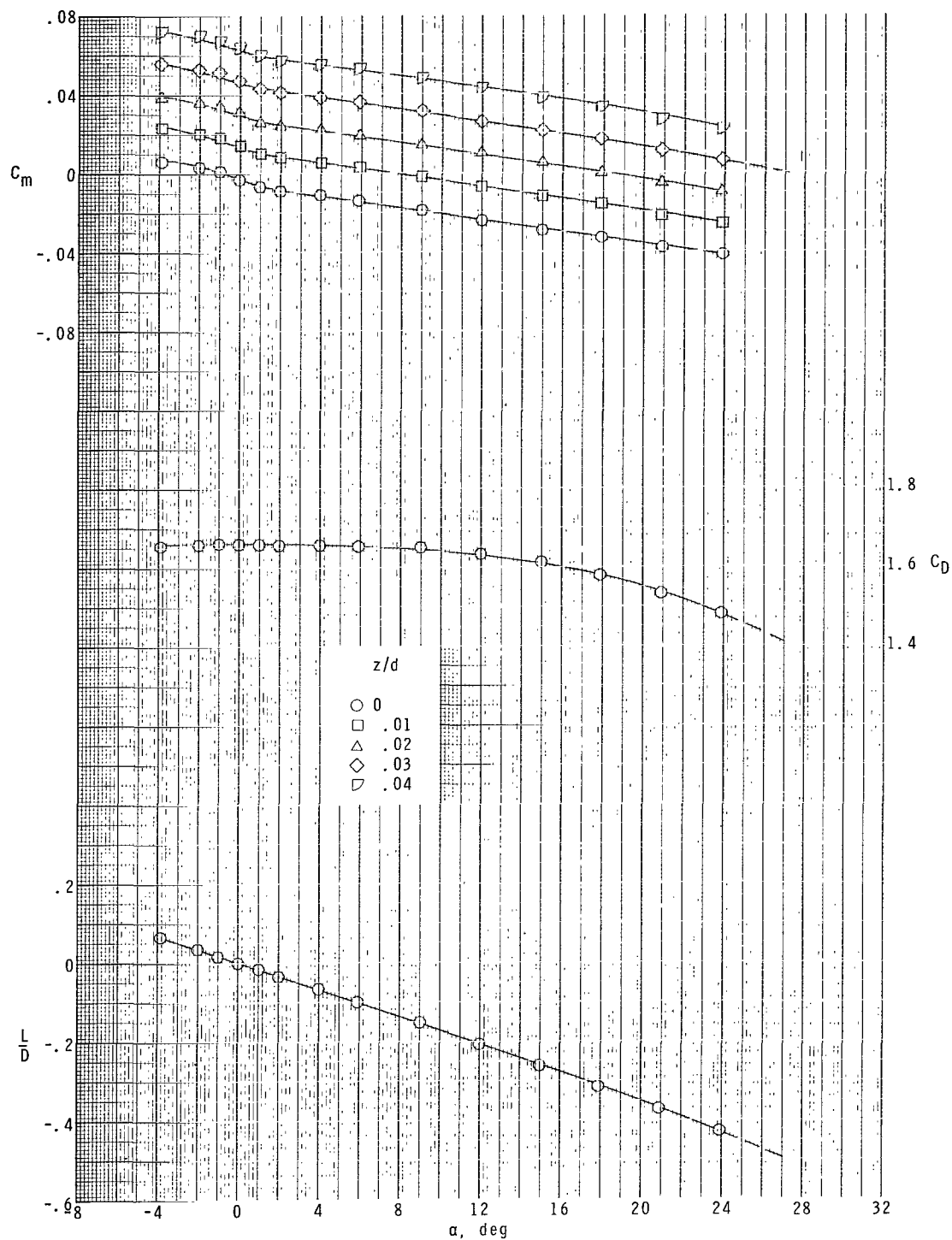
Figure 5.- Concluded.





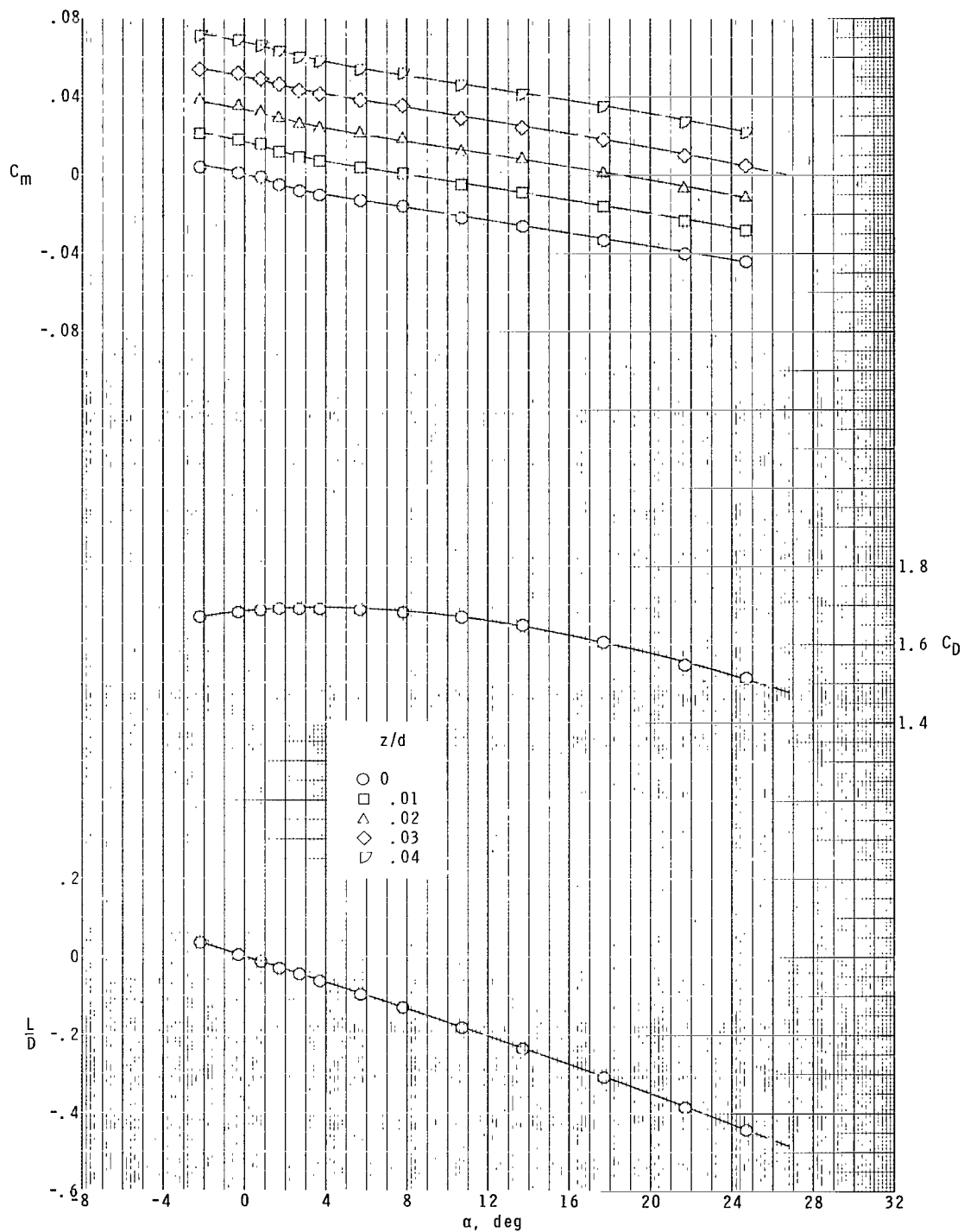
(a)  $M = 1.41$ .

Figure 6.- Longitudinal aerodynamic characteristics of the  $80^\circ$  semiapex-angle cone for the range of transverse center-of-gravity locations.  $x/d = 0$ . Dashed lines represent extrapolated data.



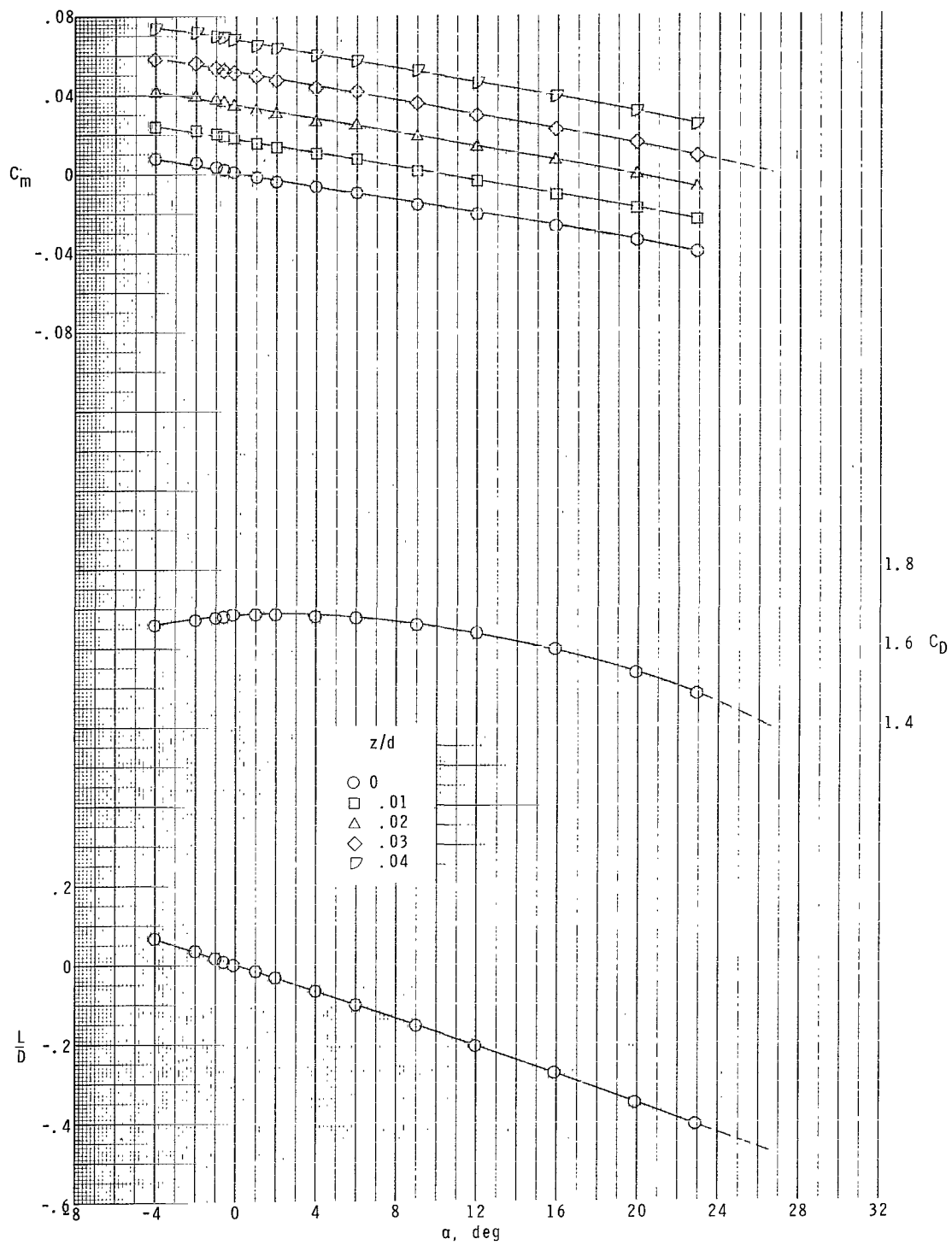
(b)  $M = 2.00$ .

Figure 6.- Continued.



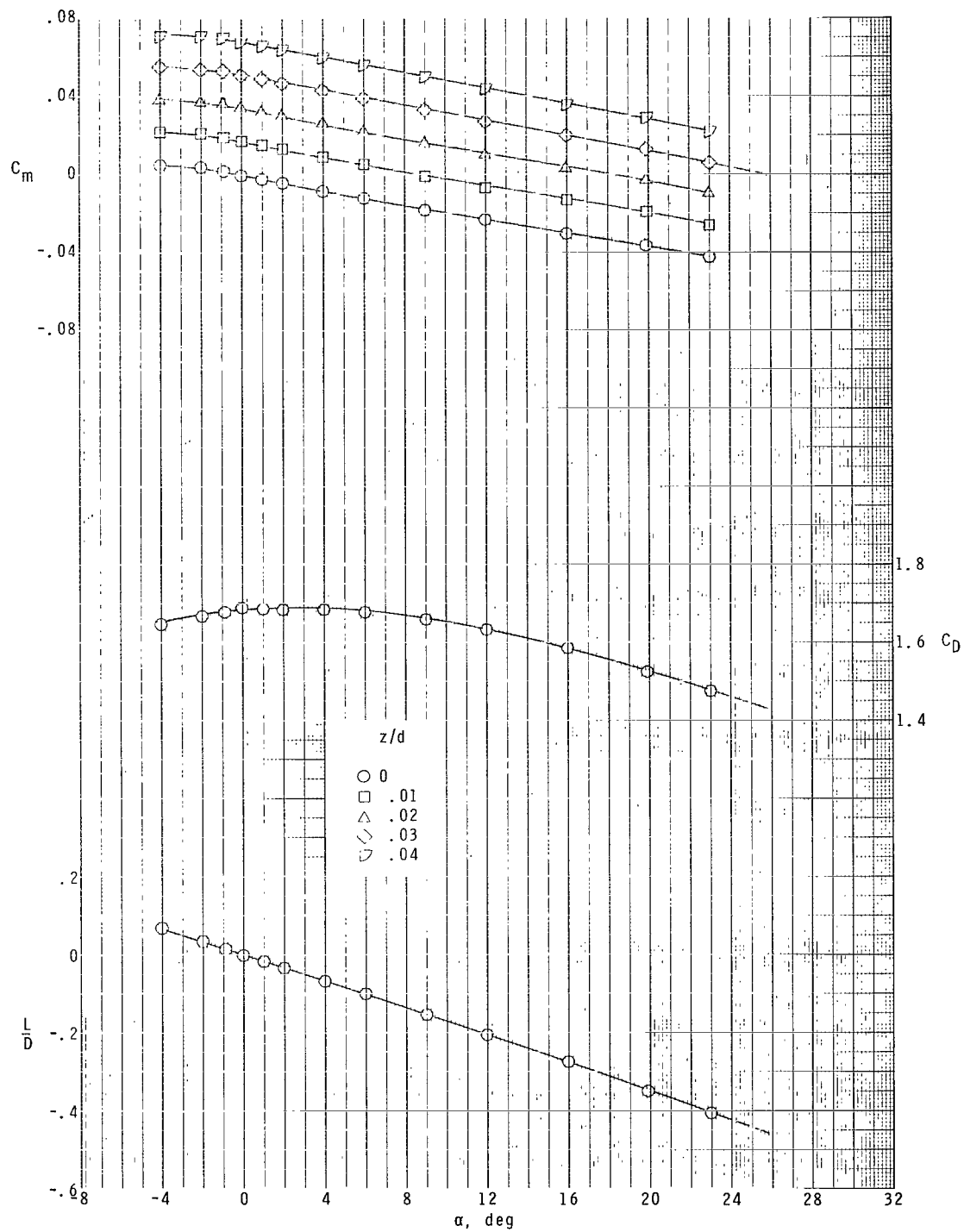
(c)  $M = 2.30$ .

Figure 6.- Continued.



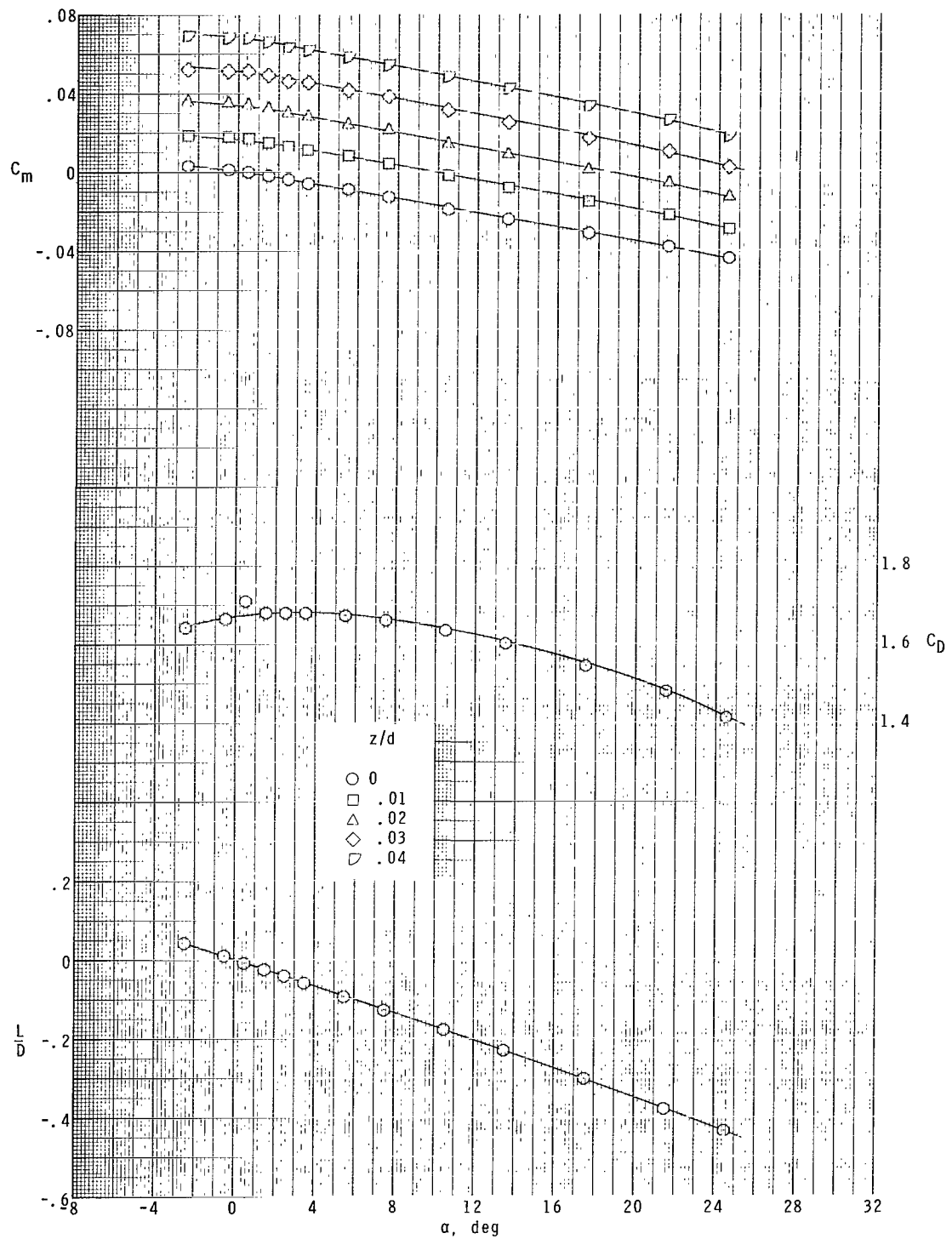
(d)  $M = 2.96$ .

Figure 6.- Continued.



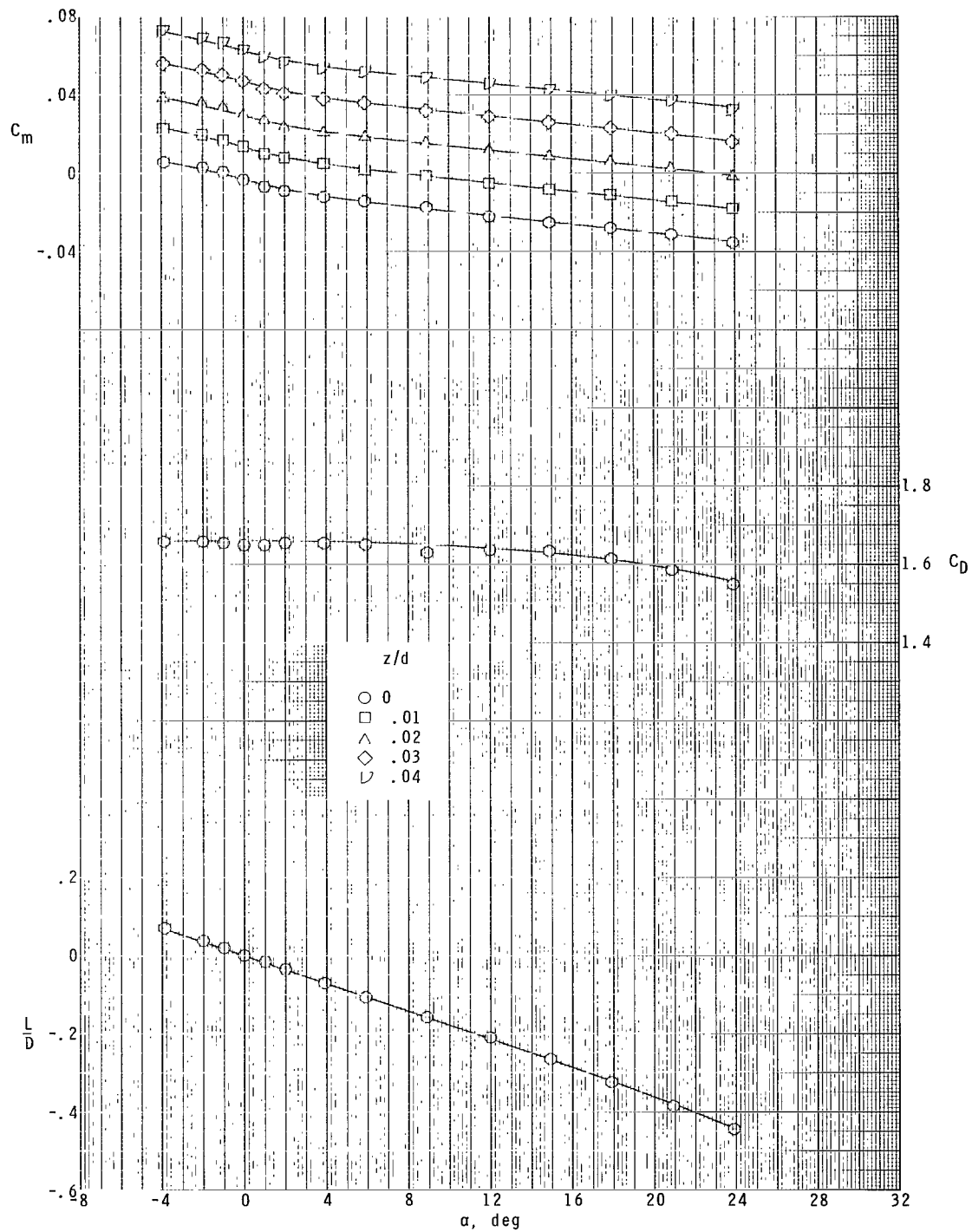
(e)  $M = 3.95$ .

Figure 6.- Continued.



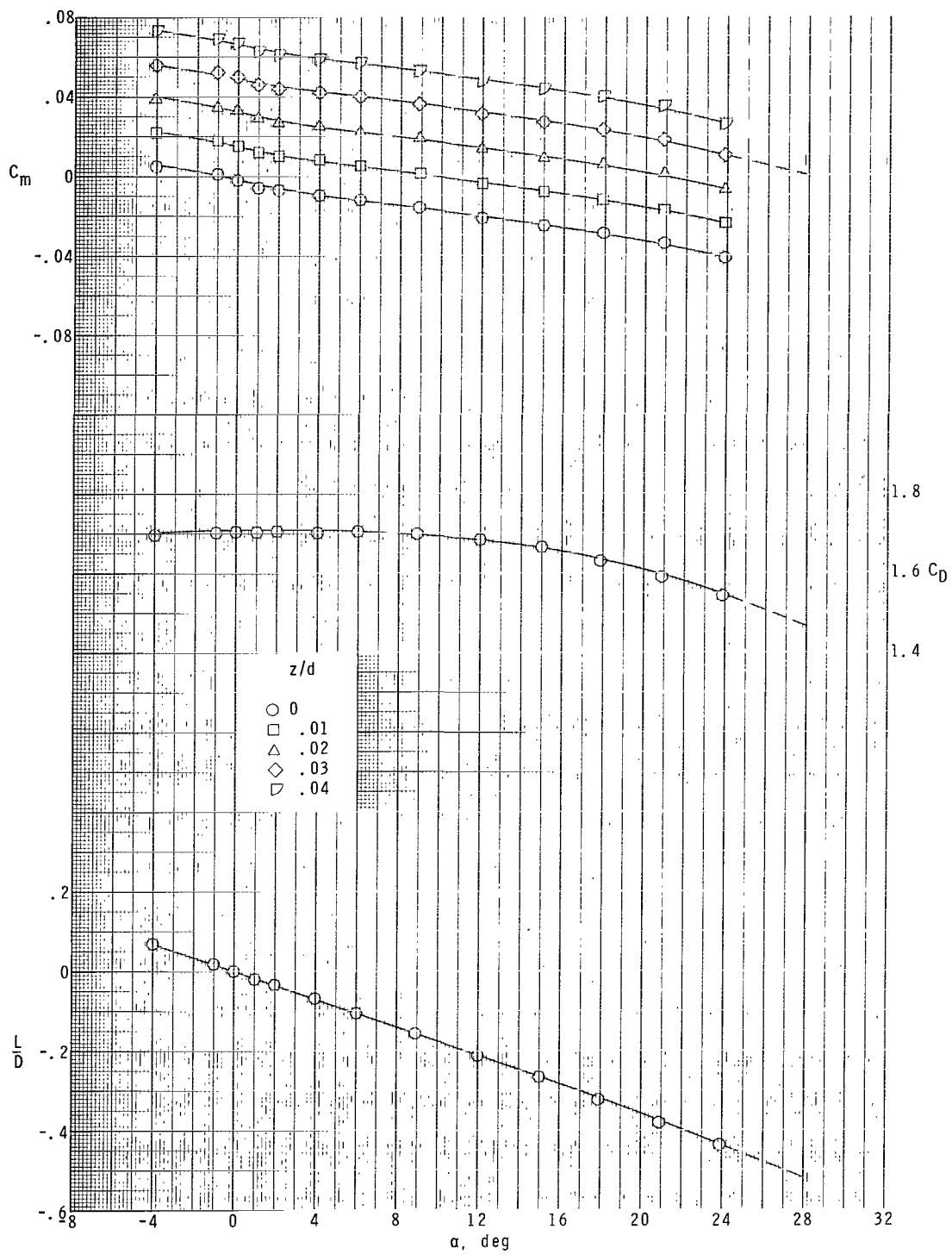
(f)  $M = 4.63$ .

Figure 6.- Concluded.



(a)  $M = 1.41$ .

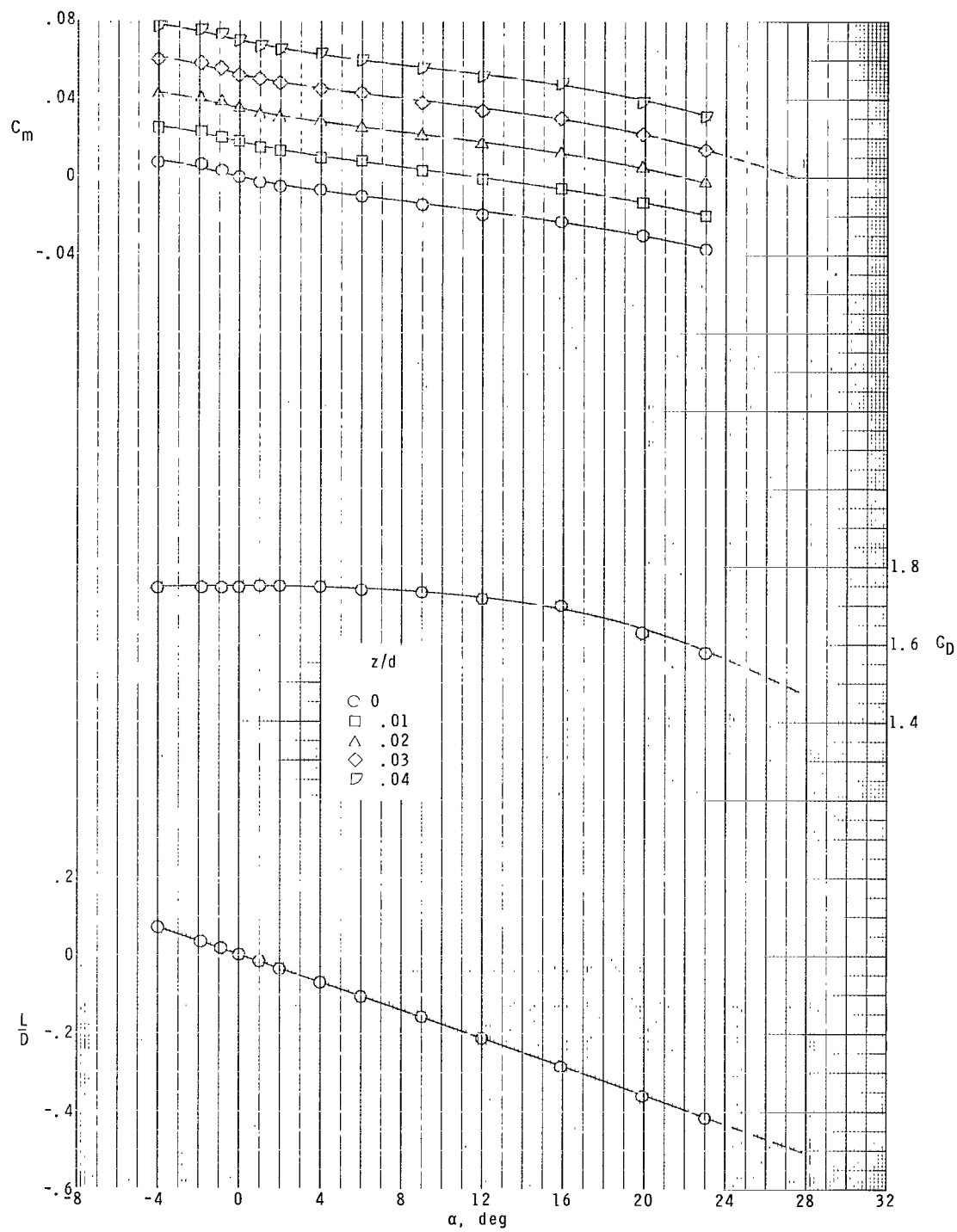
Figure 7.- Longitudinal aerodynamic characteristics of the  $90^\circ$  semiapex-angle cone for the range of transverse center-of-gravity locations,  $x/d = 0$ . Dashed lines represent extrapolated data.



(b)  $M = 2.00$ .

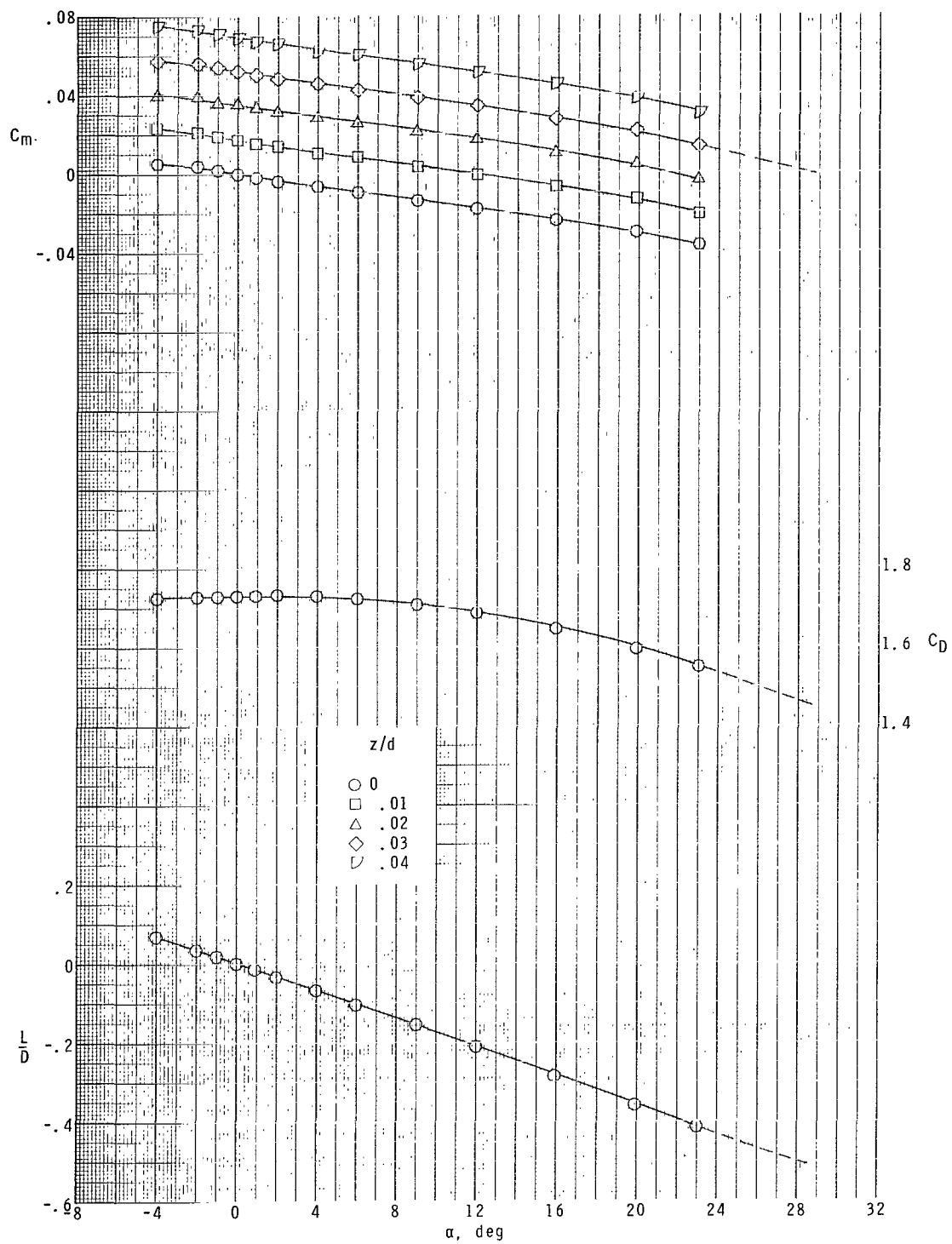
Figure 7.- Continued.





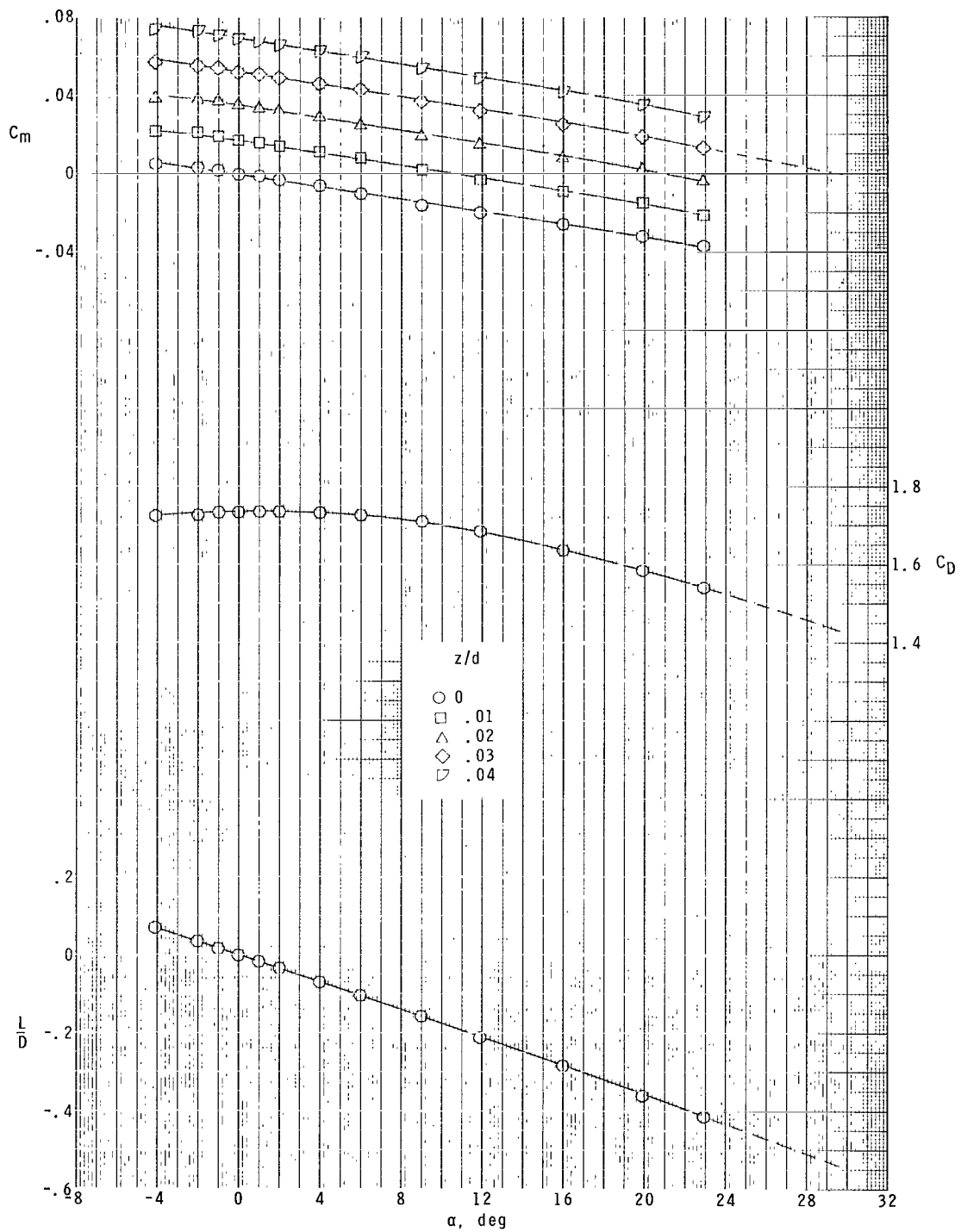
(c)  $M = 2.30$ .

Figure 7.- Continued.



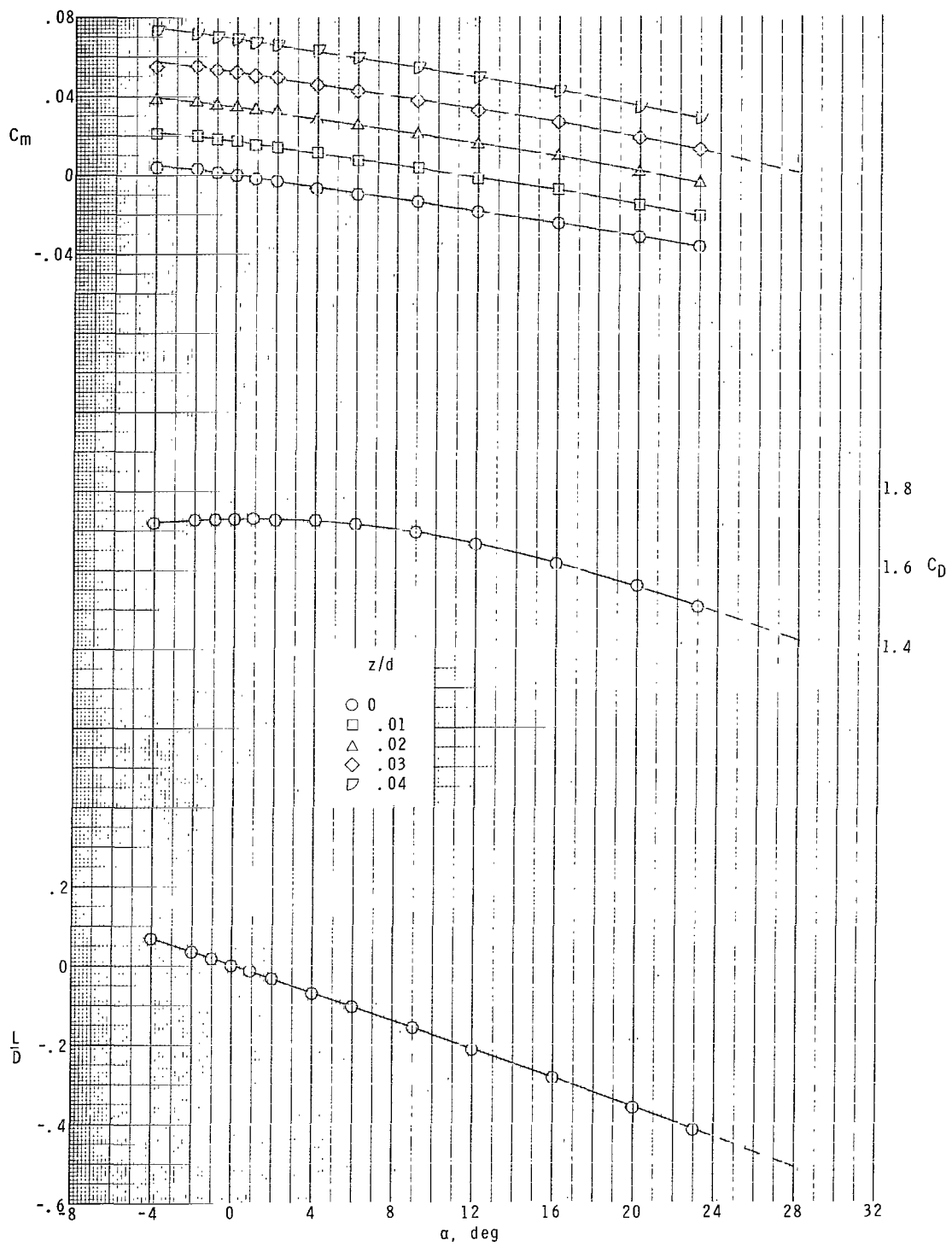
(d)  $M = 2.96$ .

Figure 7.- Continued.



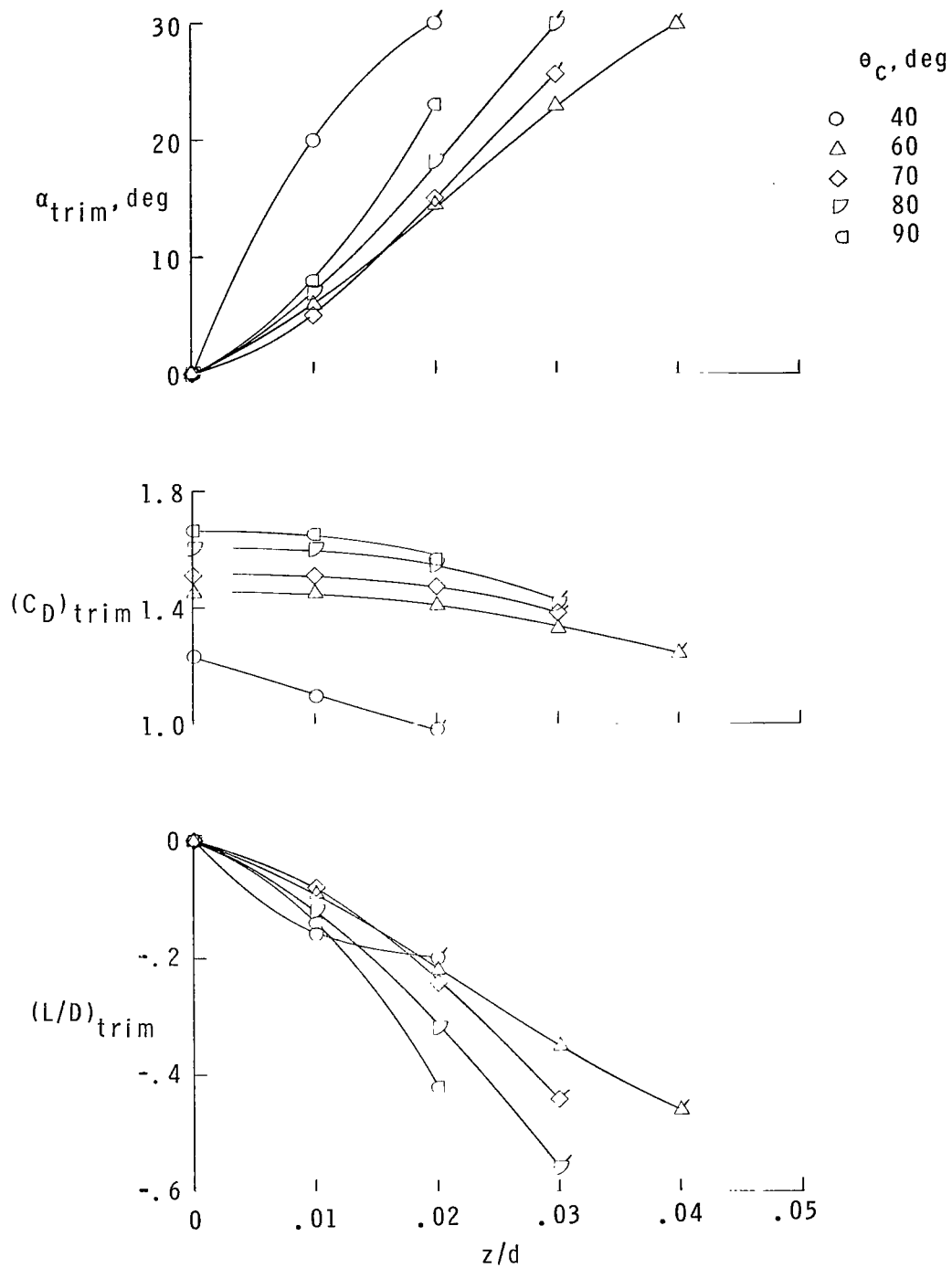
(e)  $M = 3.95$ .

Figure 7.- Continued.



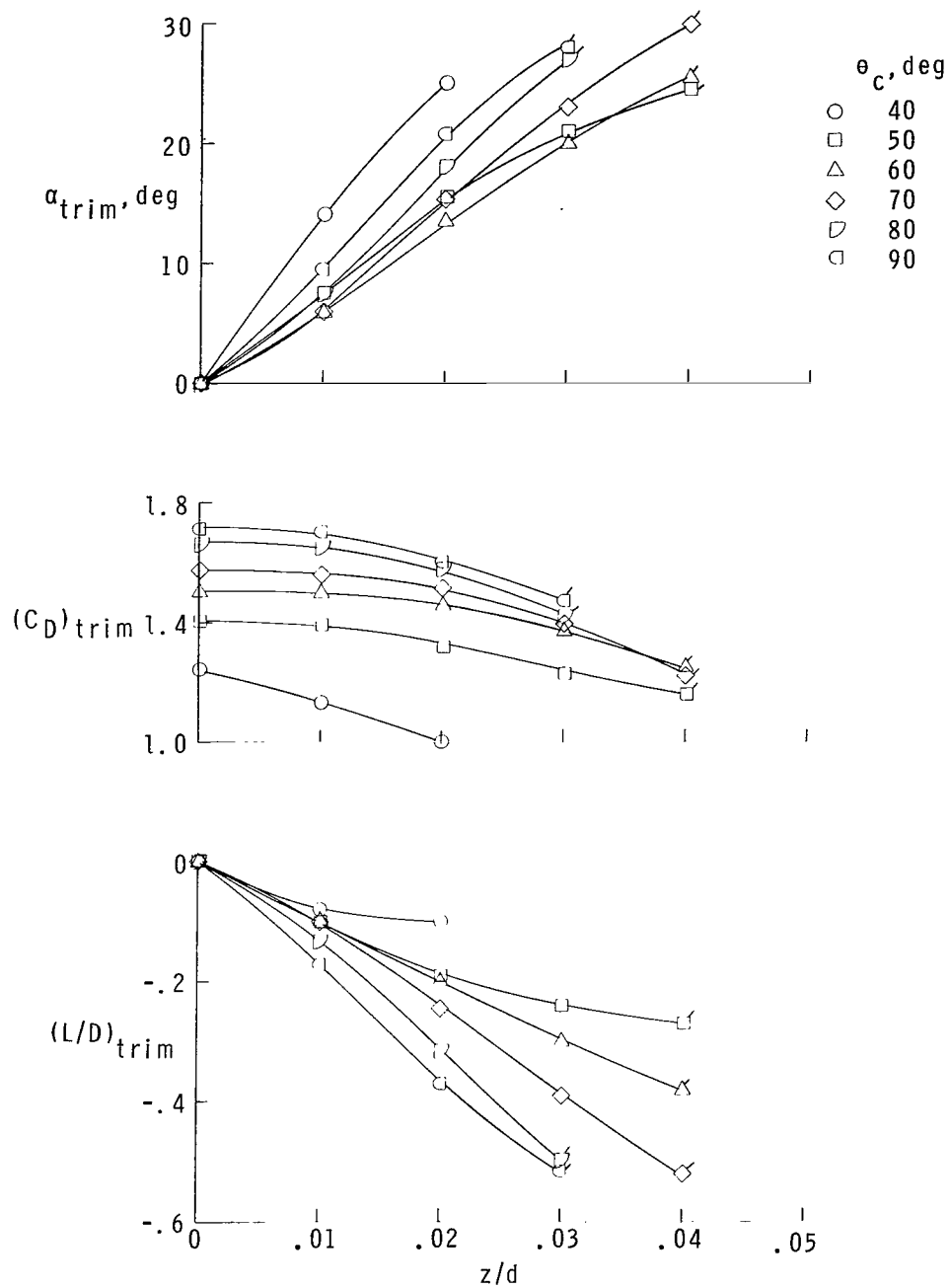
(f)  $M = 4.63$ .

Figure 7.- Concluded.



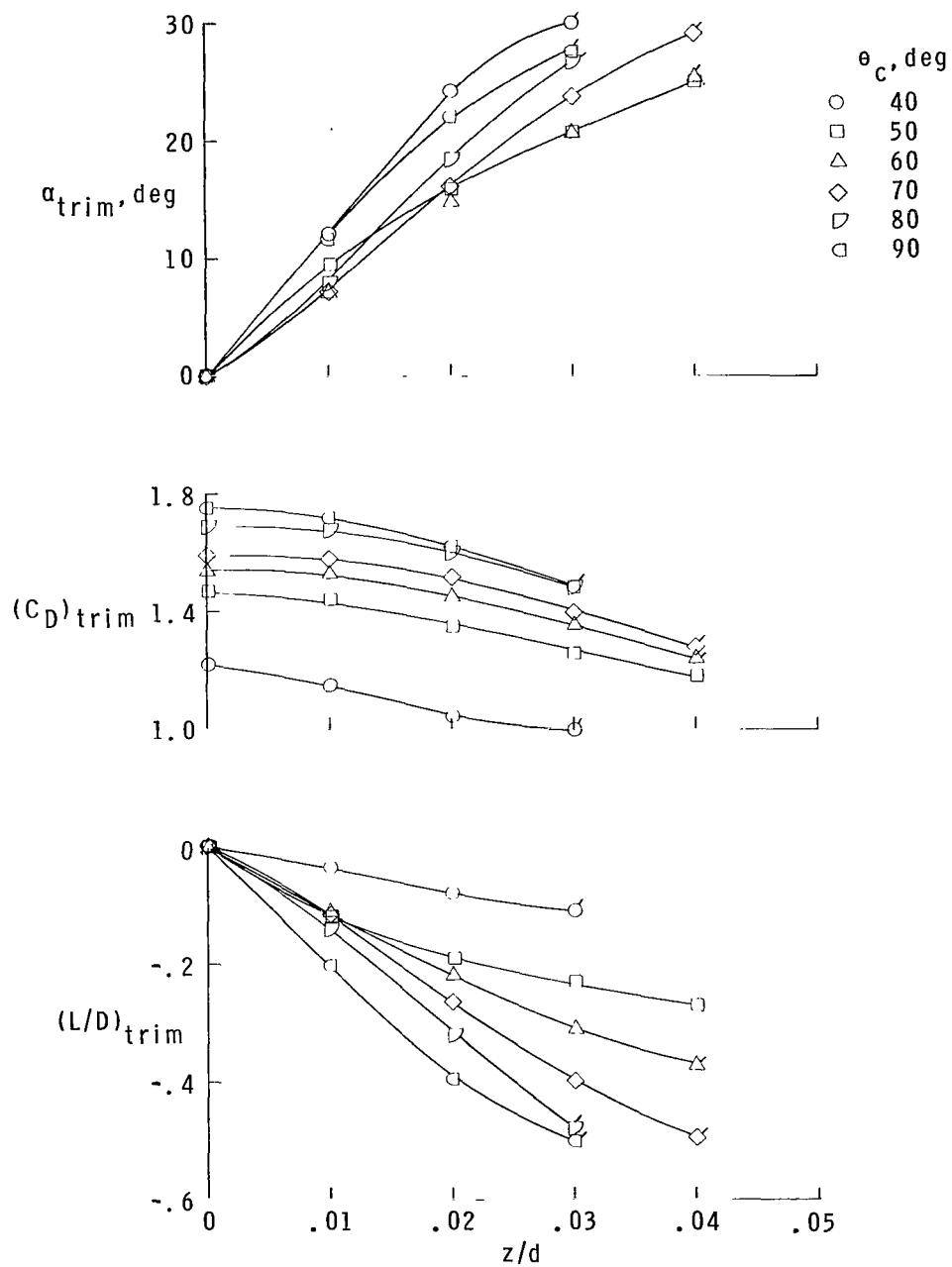
(a)  $M = 1.41$ . Flagged symbols represent extrapolated data.

Figure 8.- Variation of trim aerodynamic characteristics with transverse center-of-gravity location for family of cones.



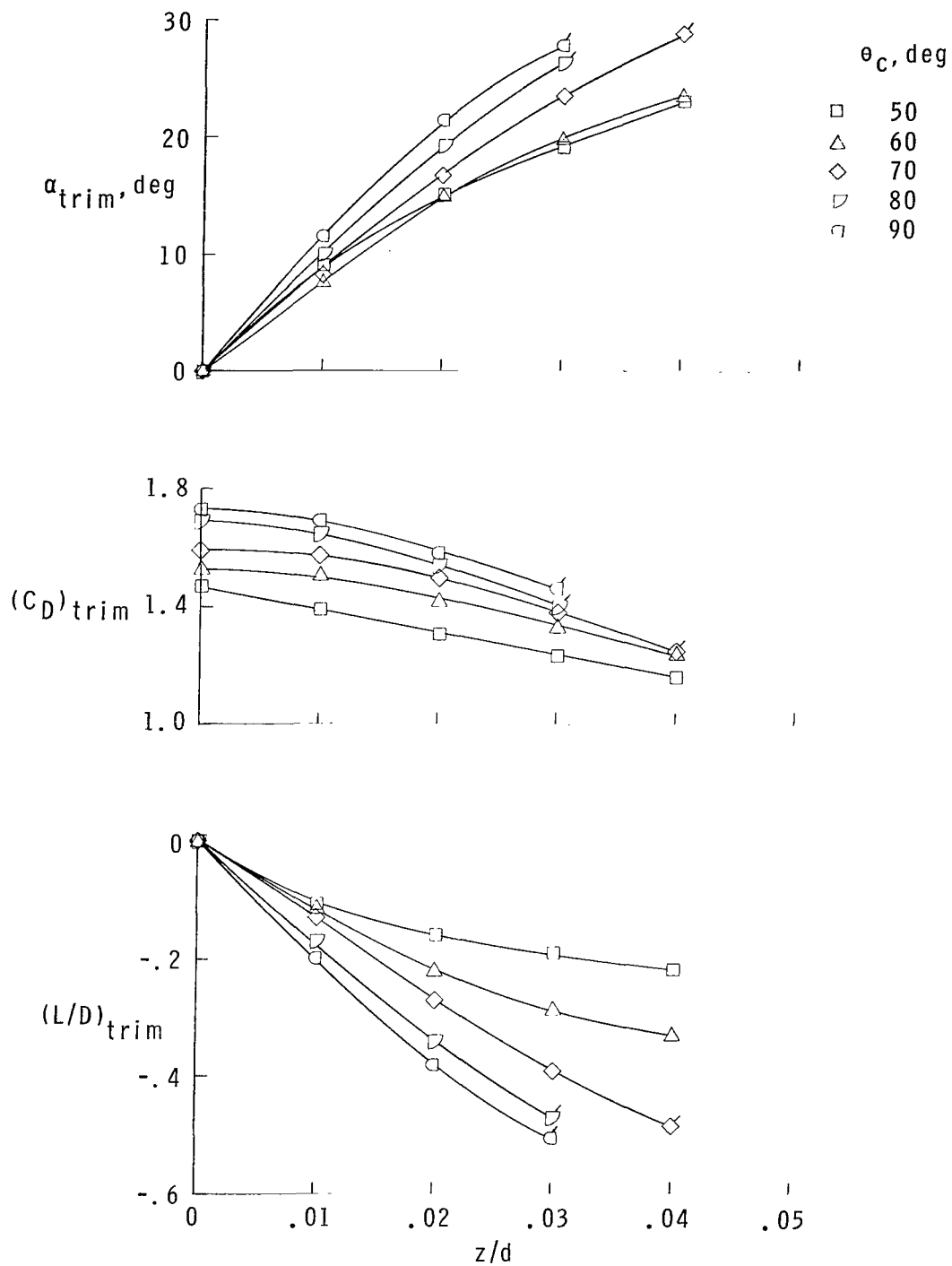
(b)  $M = 2.00$ . Flagged symbols represent extrapolated data.

Figure 8.- Continued.



(c)  $M = 2.30$ . Flagged symbols represent extrapolated data.

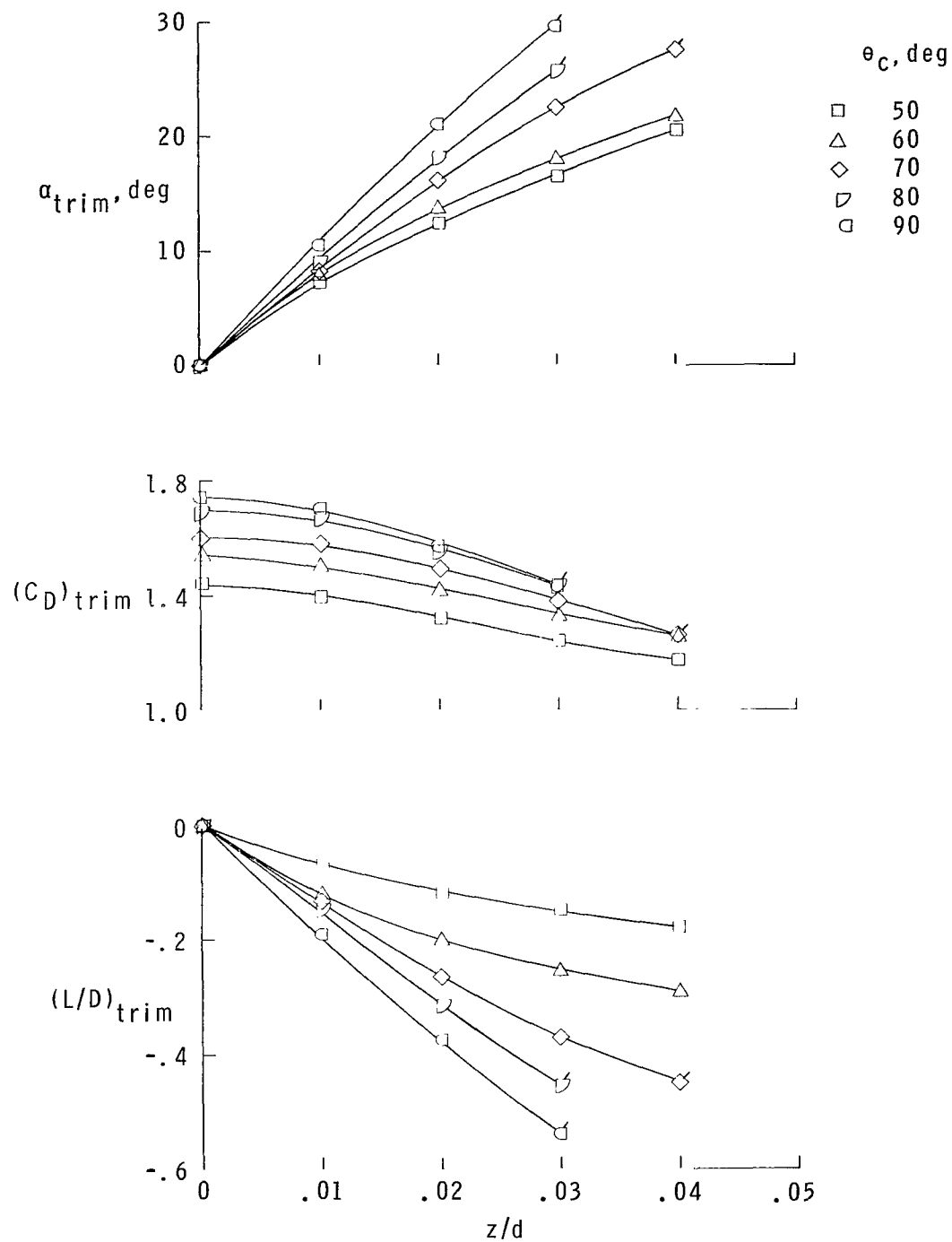
Figure 8.- Continued.



(d)  $M = 2.96$ . Flagged symbols represent extrapolated data.

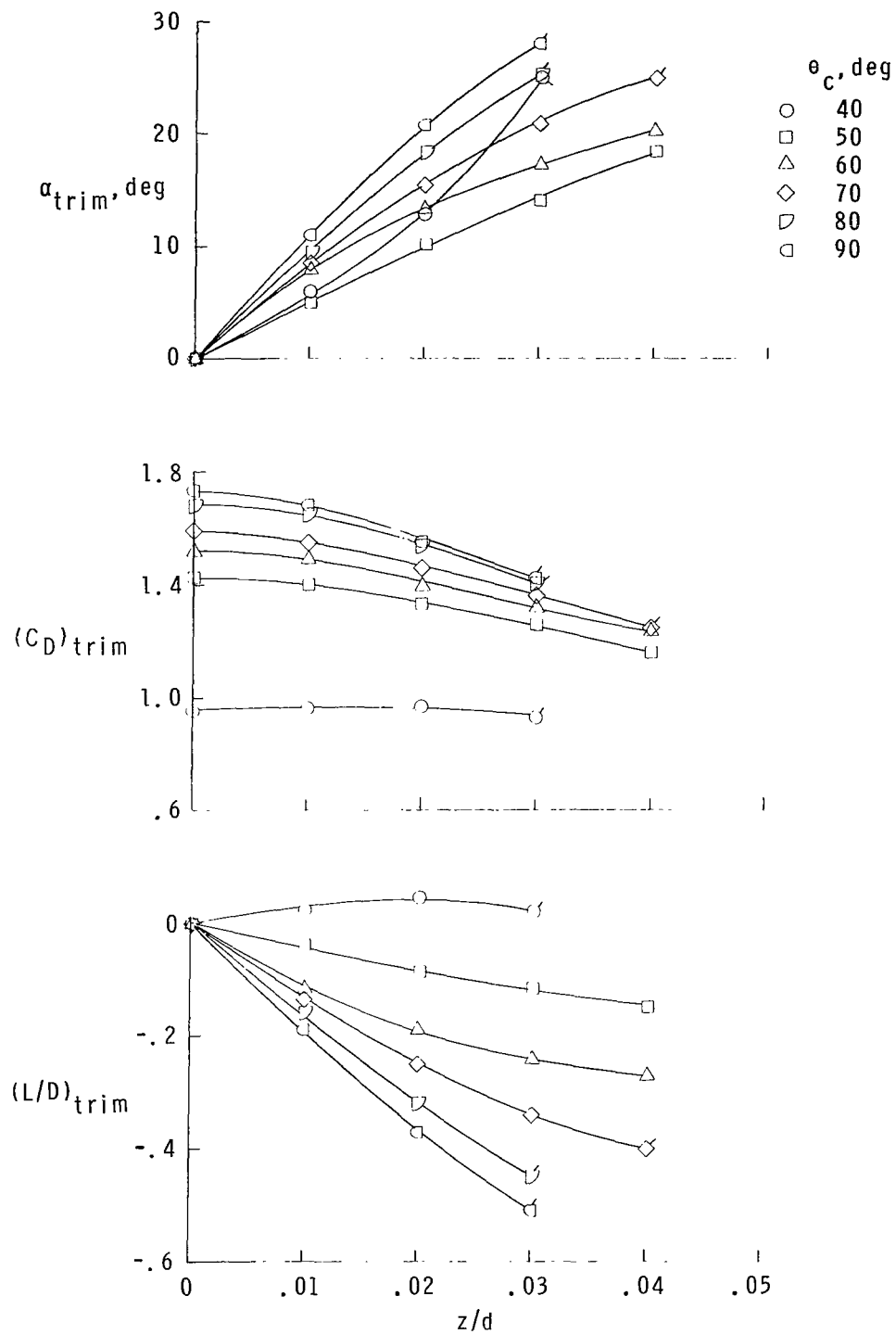
Figure 8.- Continued.





(e)  $M = 3.95$ . Flagged symbols represent extrapolated data.

Figure 8.- Continued.



(f)  $M = 4.63$ . Flagged symbols represent extrapolated data.

Figure 8.- Concluded.

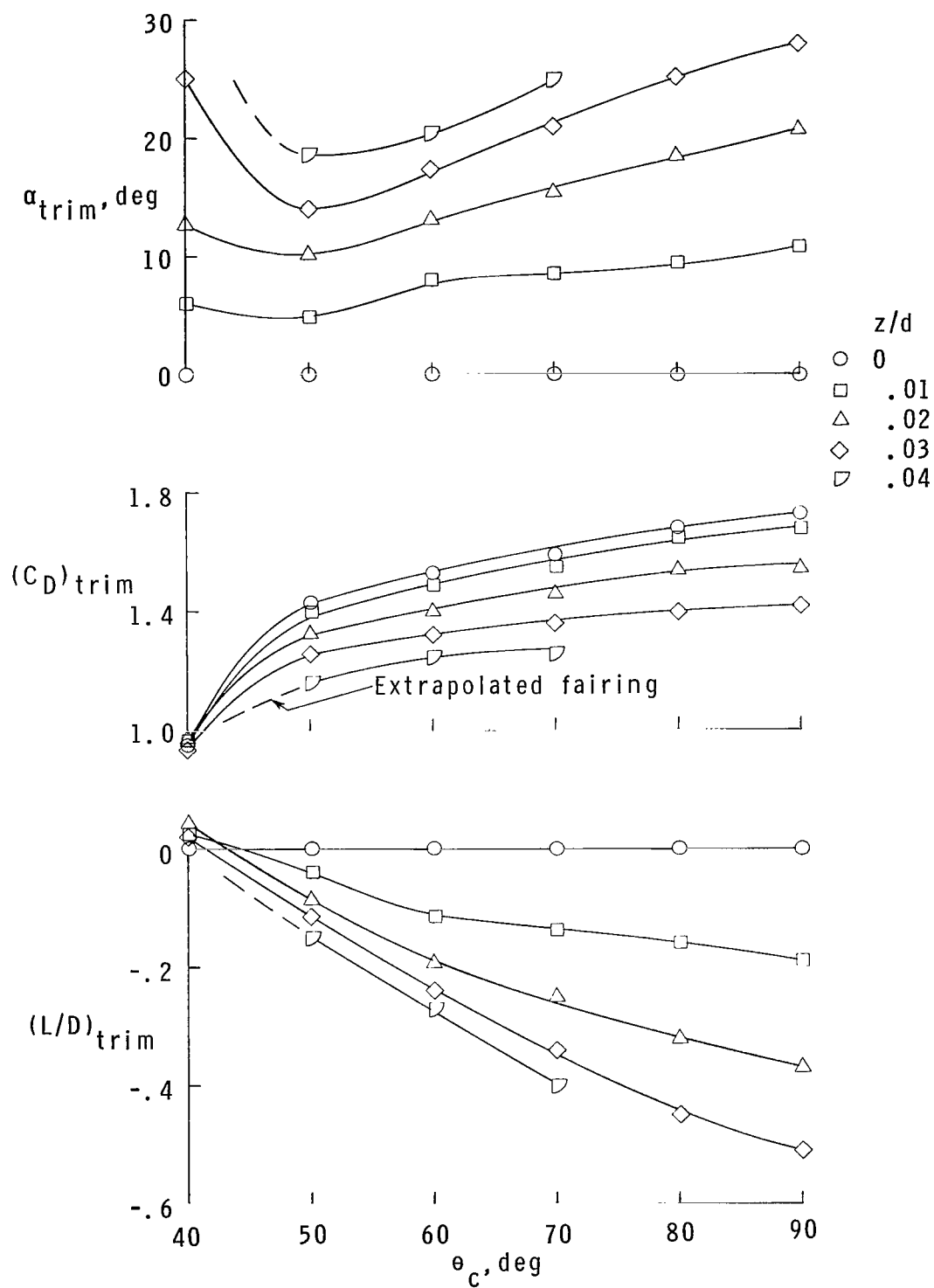
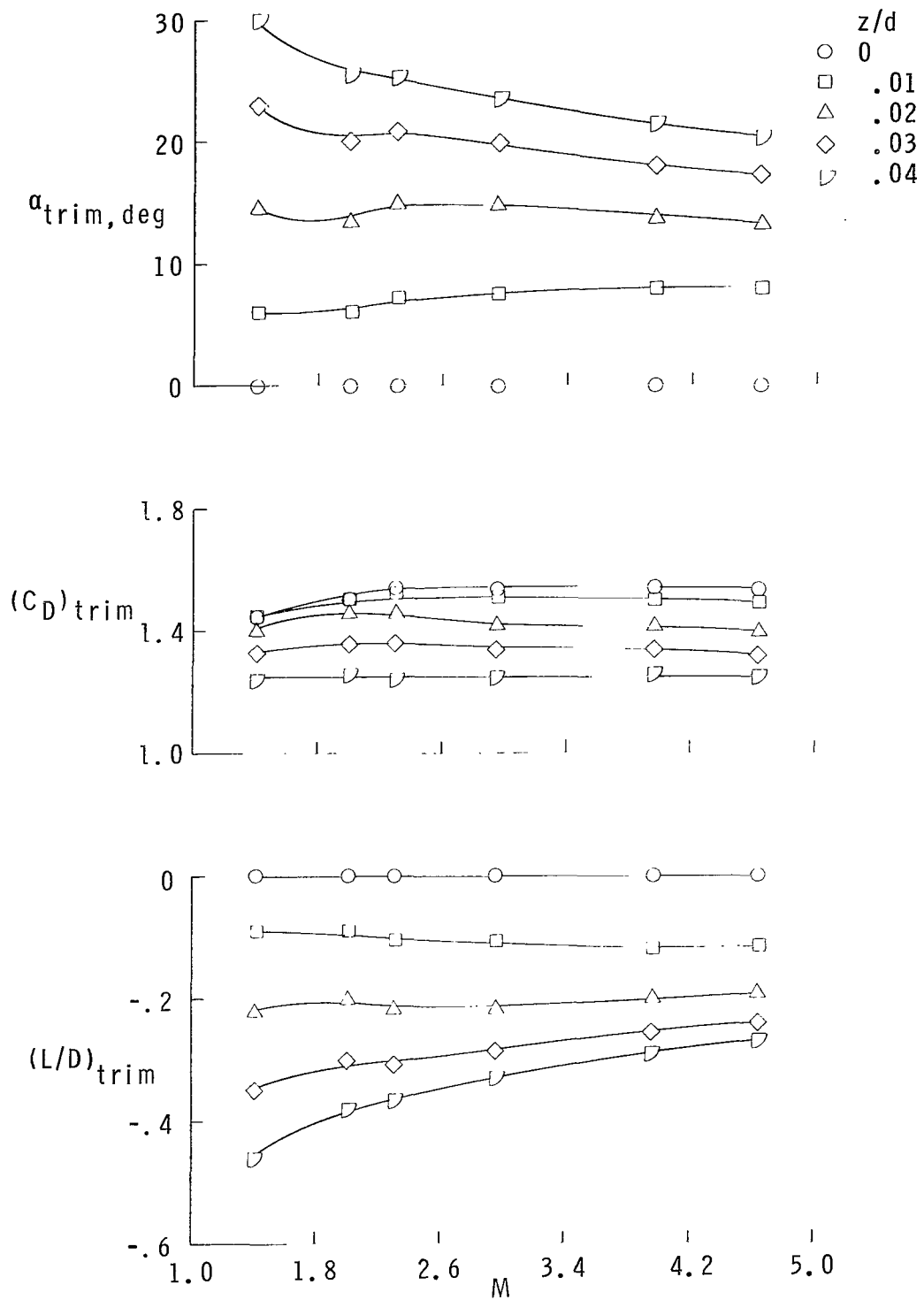
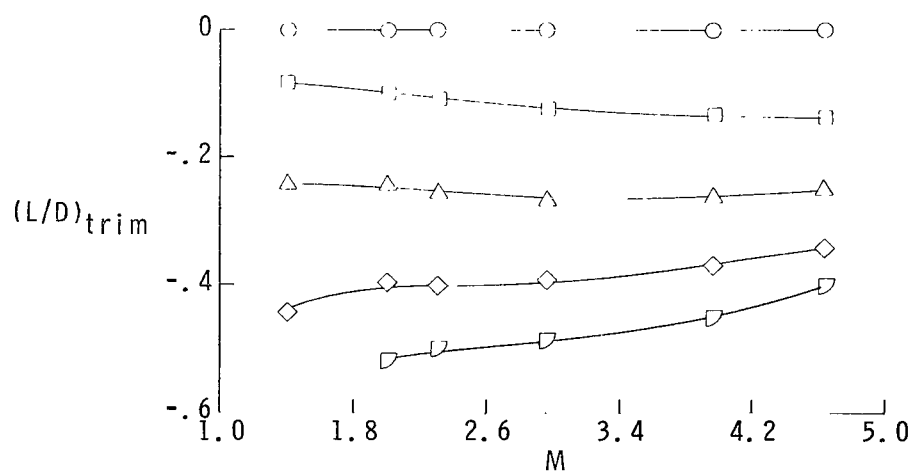
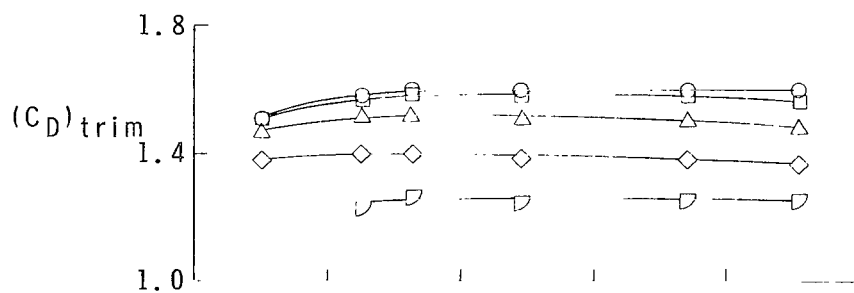
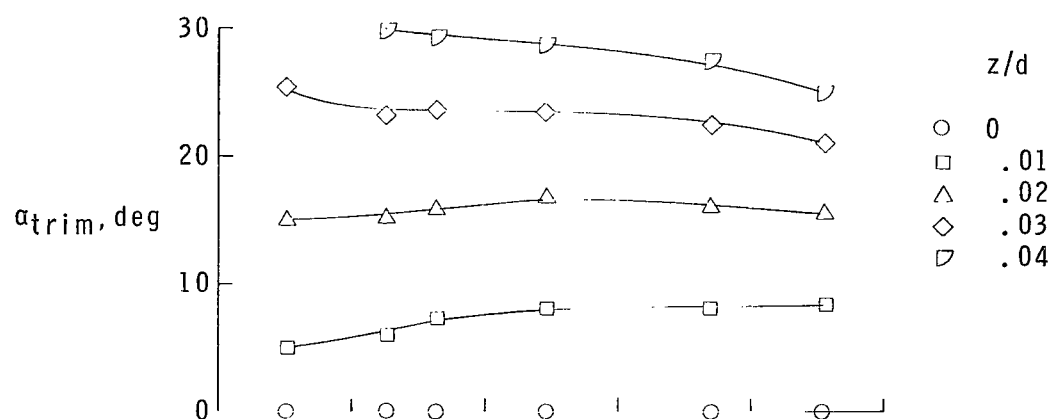


Figure 9.- Effect of transverse center-of-gravity location on variation of trim aerodynamic characteristics with cone semiapex angle.  $M = 4.63$ .



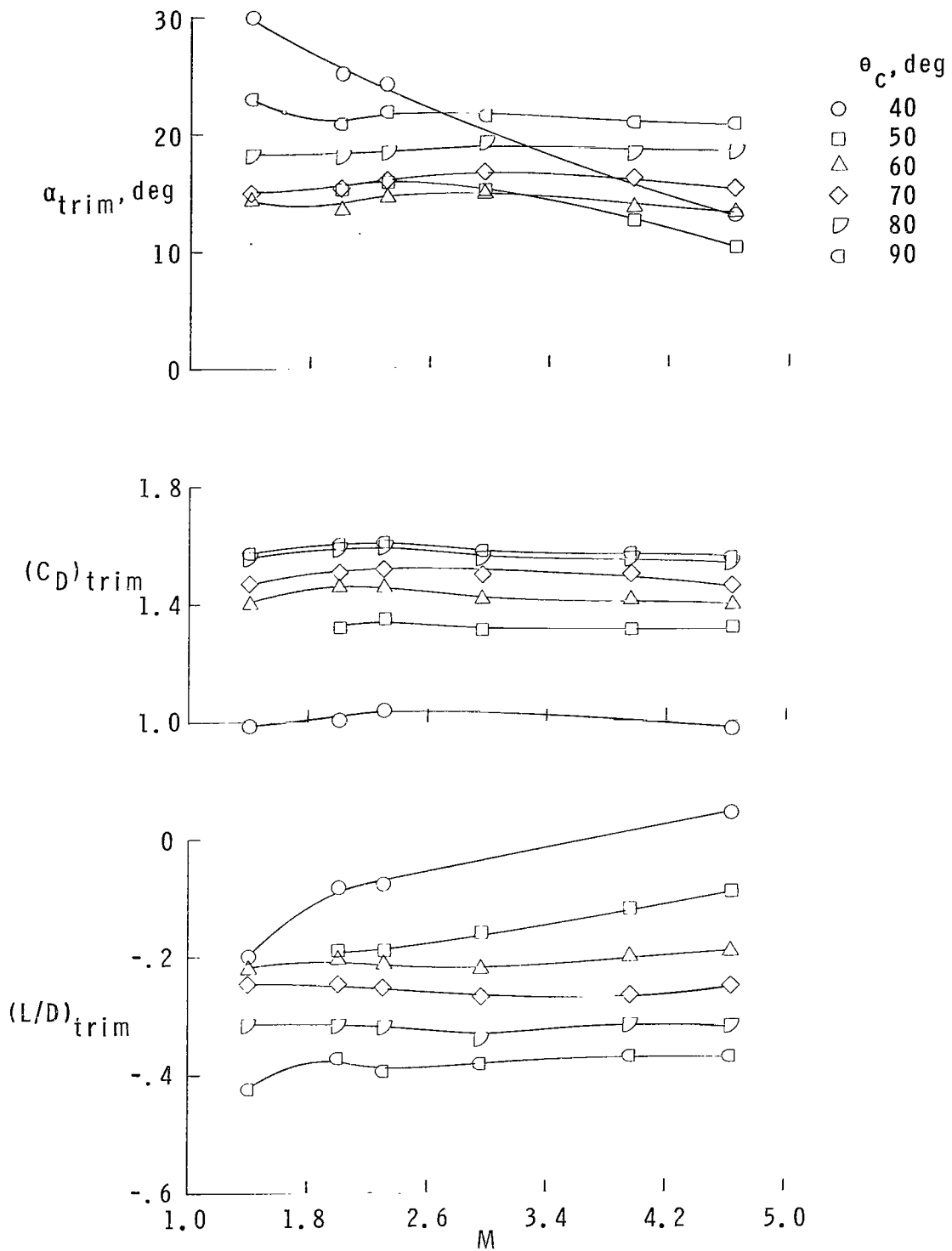
(a)  $\theta_c = 60^\circ$ .

Figure 10.- Effect of transverse center-of-gravity location on variation of trim aerodynamic characteristics with Mach number.



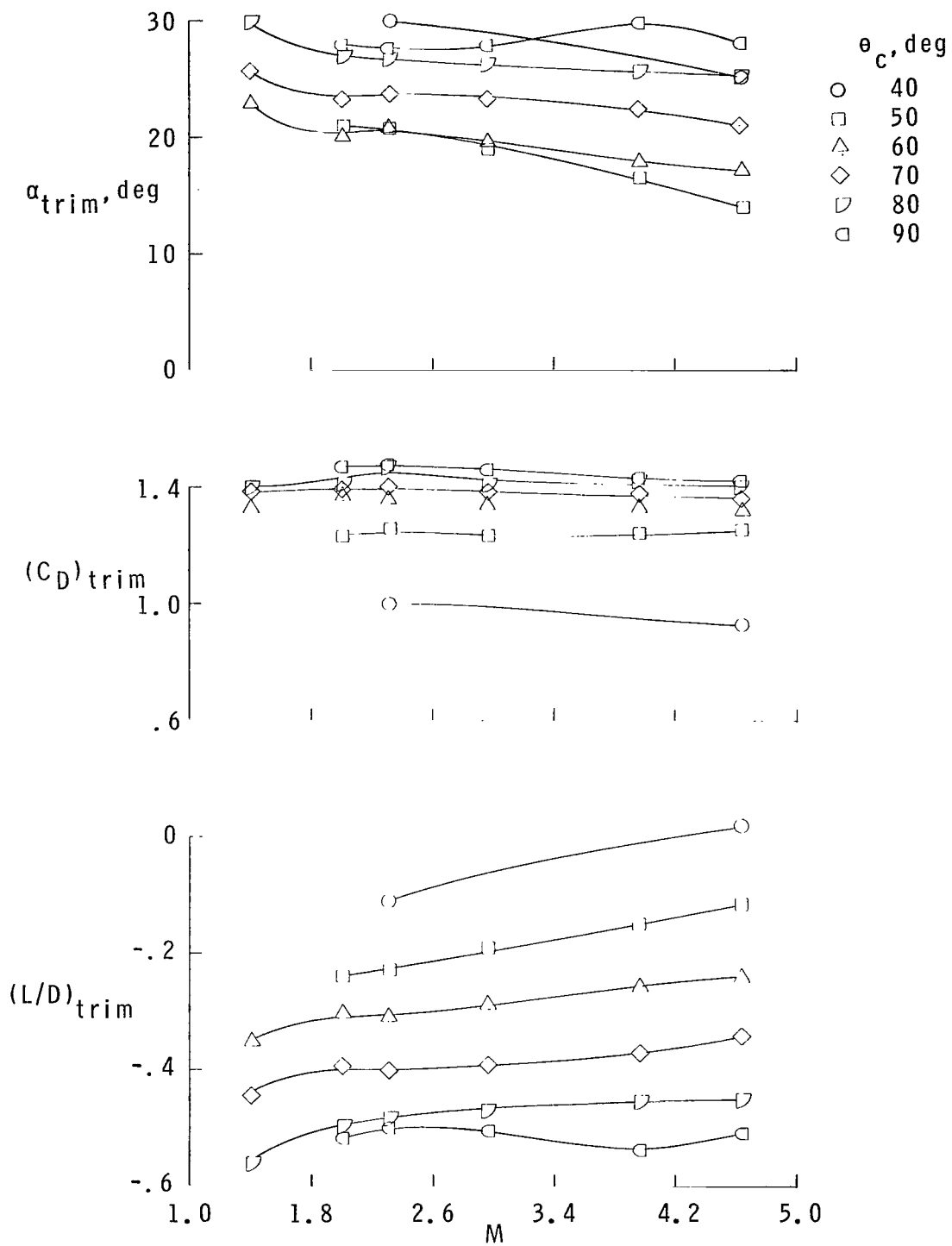
(b)  $\theta_c = 70^\circ$ .

Figure 10.- Concluded.



(a)  $z/d = 0.02$ .

Figure 11.- Variation of trim aerodynamic characteristics with Mach number for family of cones.



(b)  $z/d = 0.03$ .

Figure 11.- Concluded.

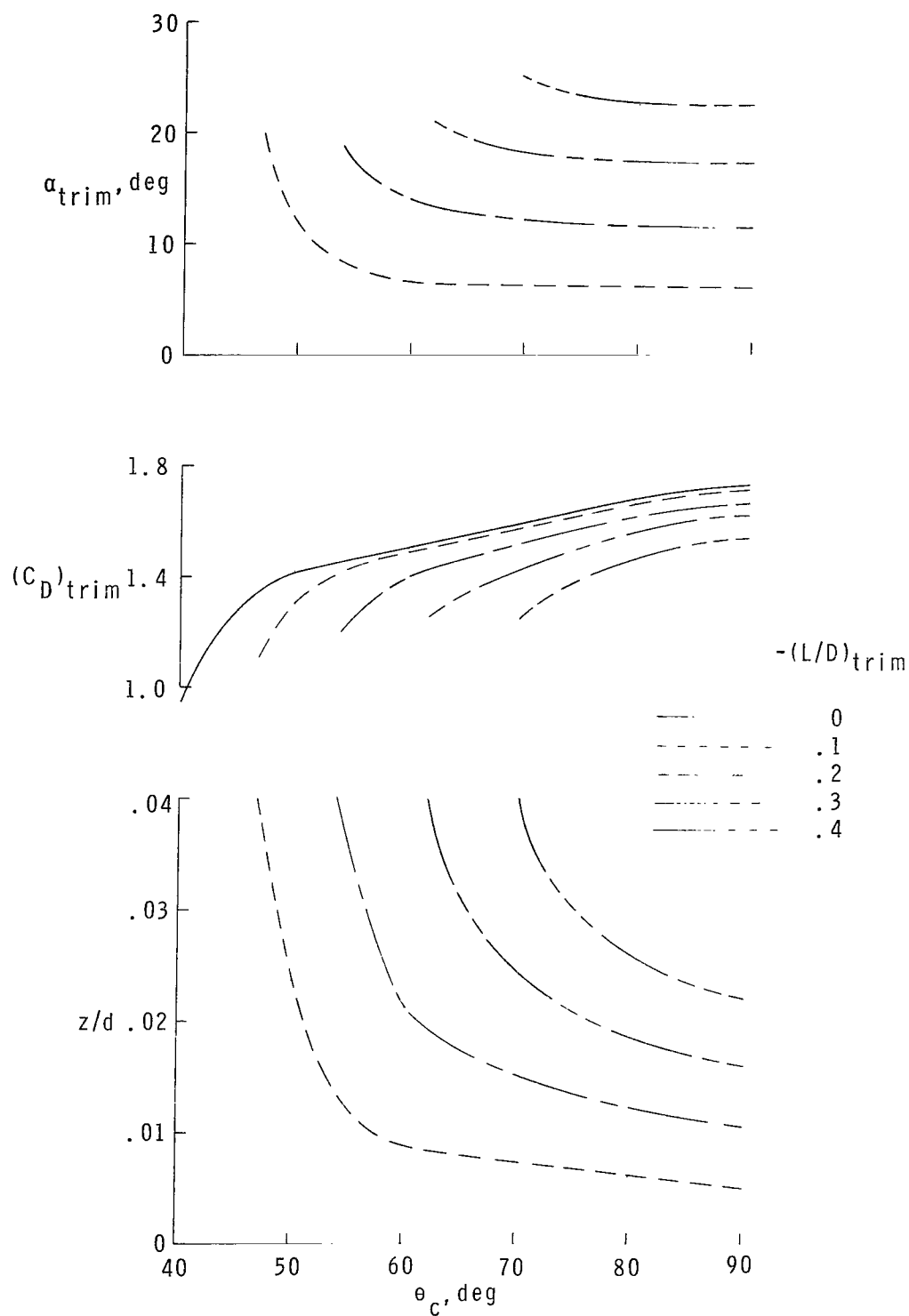


Figure 12.- Combinations of cone semiapex angle and transverse center-of-gravity location necessary to achieve a given trim  $L/D$ , with the resulting values of trim angle of attack and trim drag.  $M = 4.63$ .



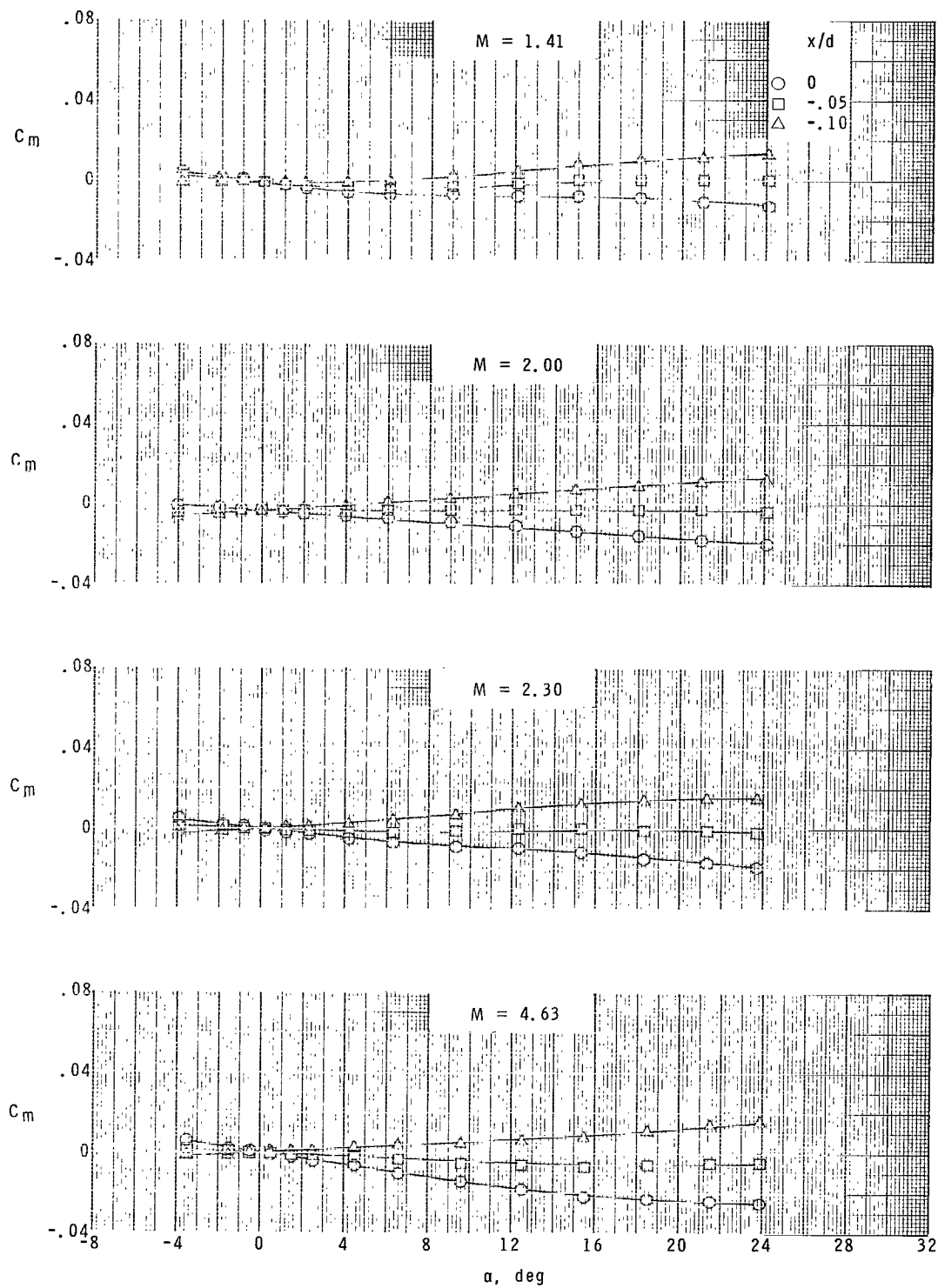


Figure 13.- Effect of longitudinal center-of-gravity location on pitching-moment characteristics of the  $40^\circ$  cone for range of Mach numbers.  $z/d = 0$ .

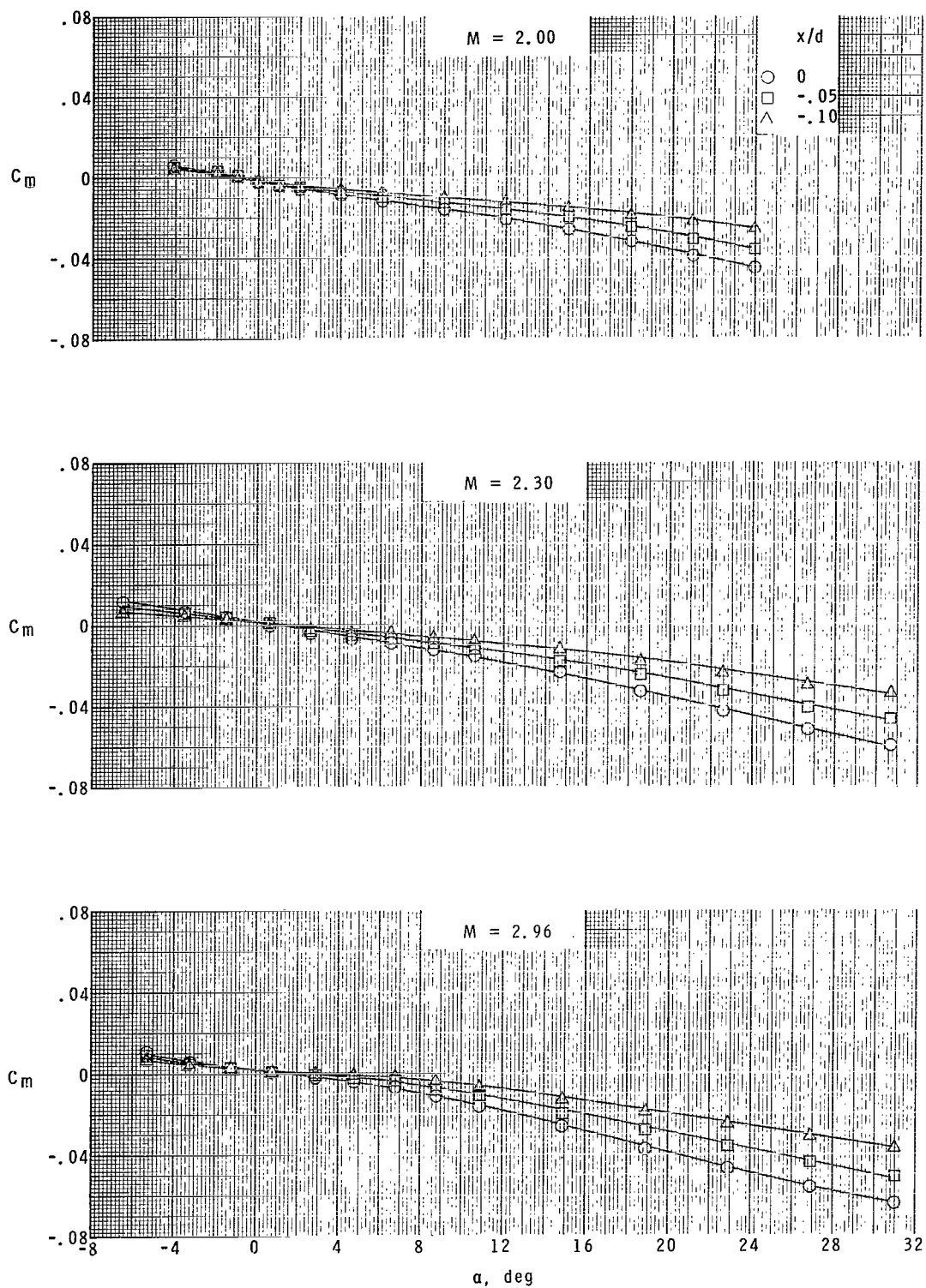


Figure 14.- Effect of longitudinal center-of-gravity location on pitching-moment characteristics of the  $50^\circ$  cone for range of Mach numbers.  $z/d = 0$ .

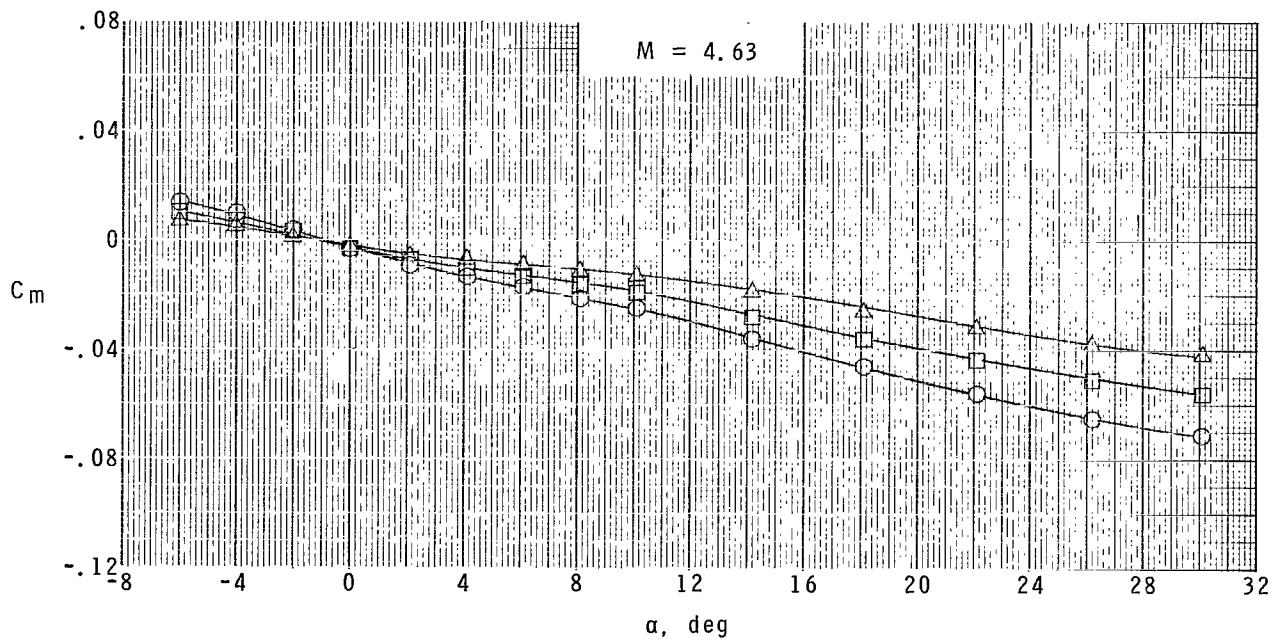
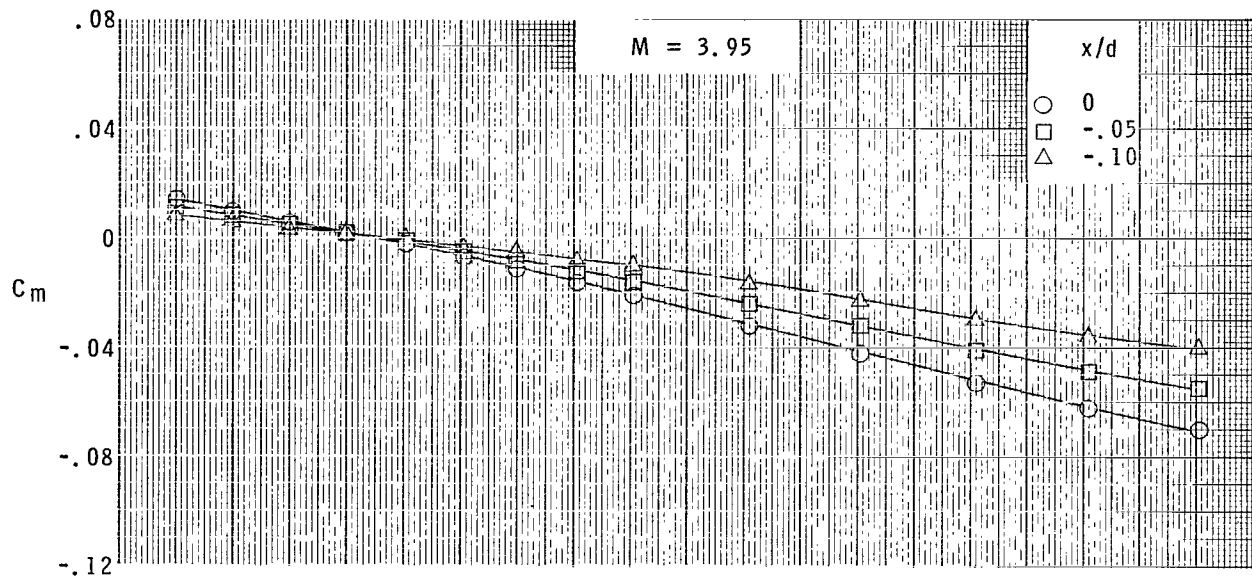


Figure 14.- Concluded.

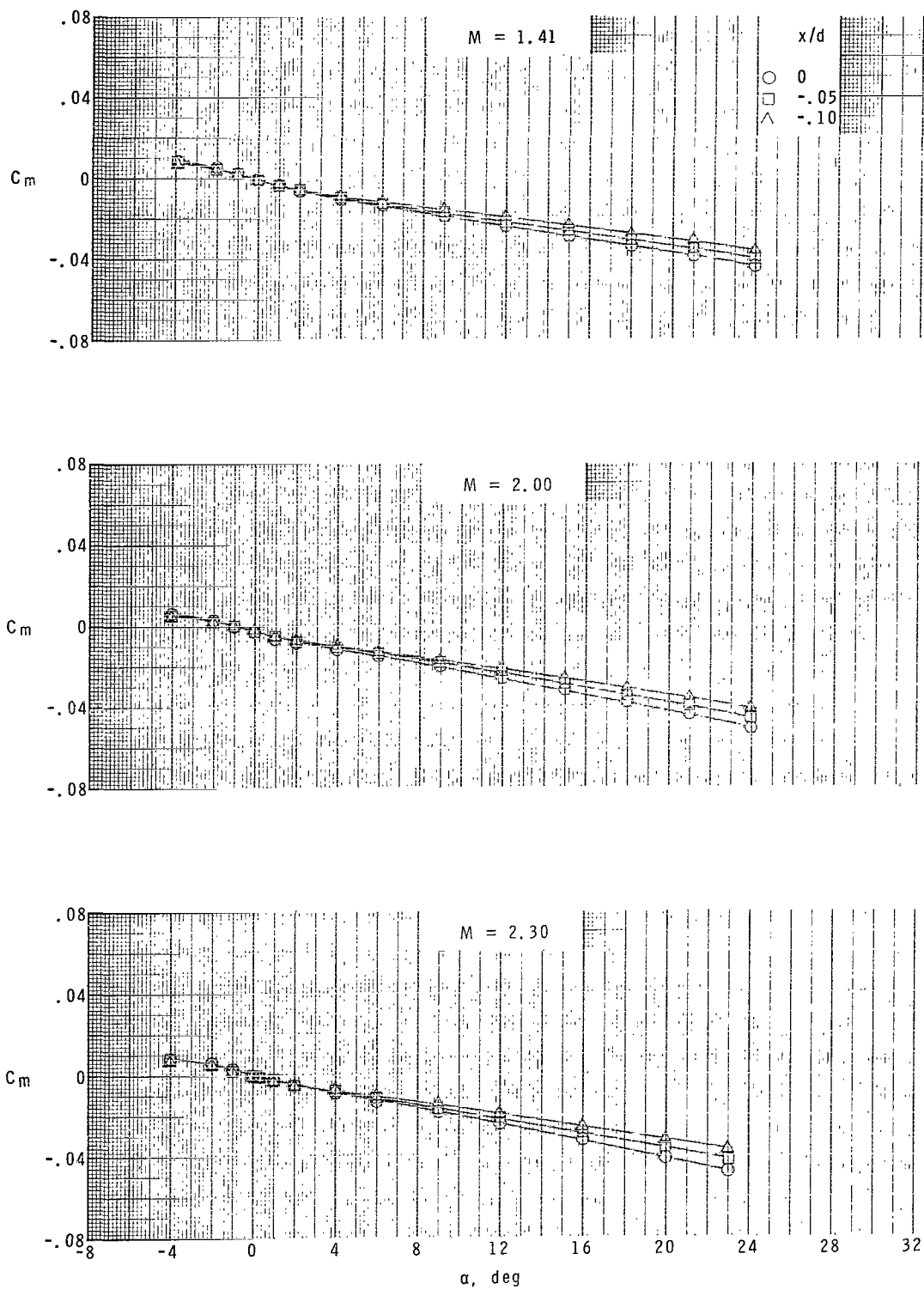


Figure 15.- Effect of longitudinal center-of-gravity location on pitching-moment characteristics of the  $60^\circ$  cone for range of Mach numbers.  $z/d = 0$ .

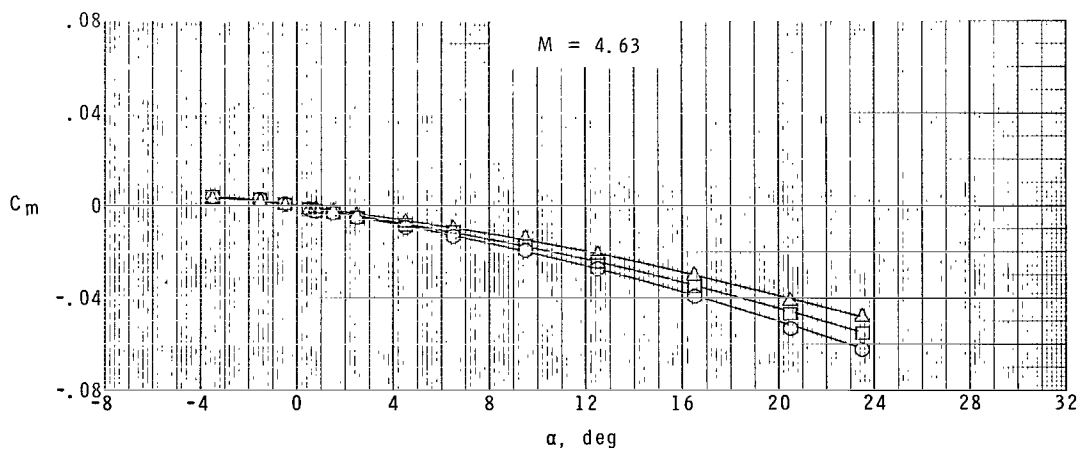
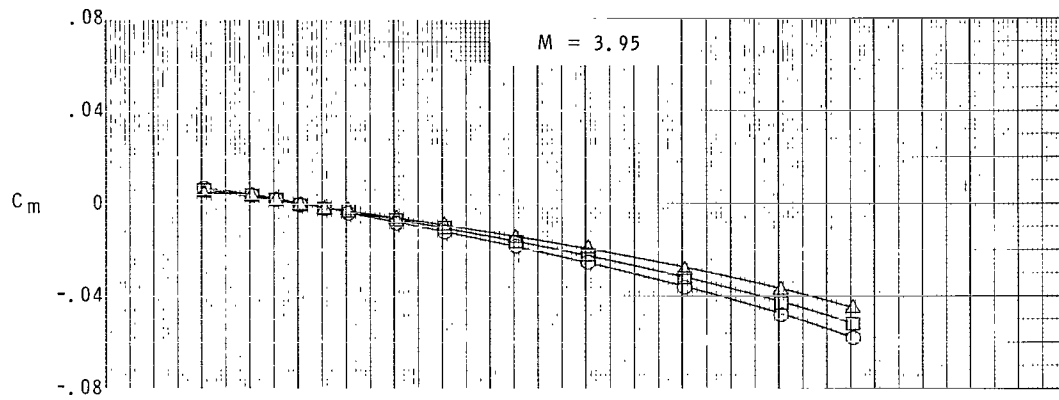
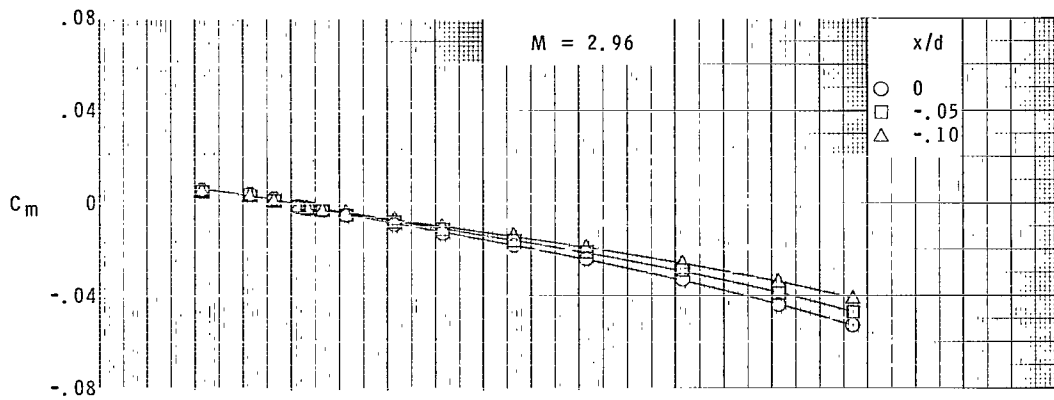


Figure 15.- Concluded.

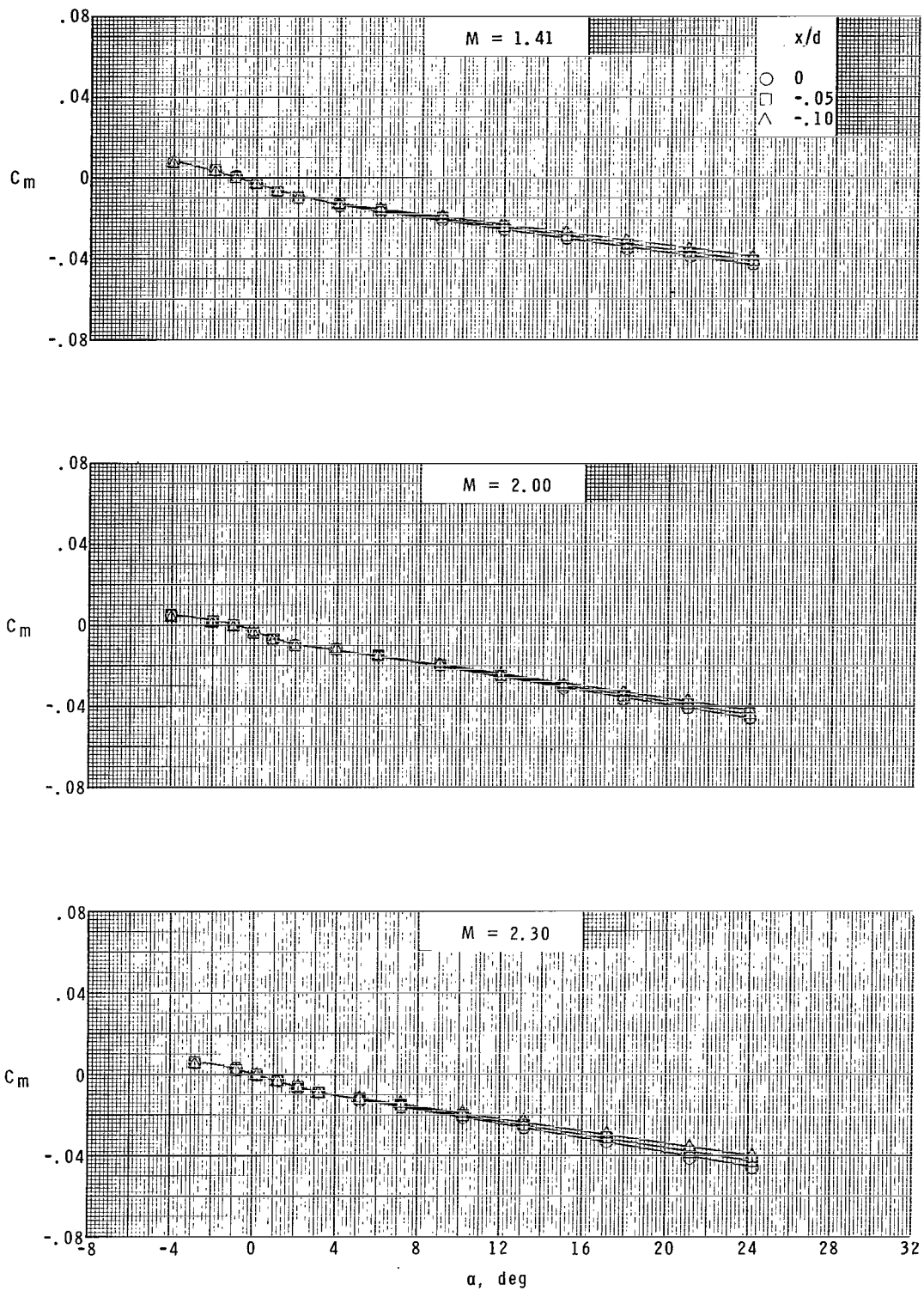


Figure 16.- Effect of longitudinal center-of-gravity location on pitching-moment characteristics of the  $70^\circ$  cone for range of Mach numbers.  $z/d = 0$ .

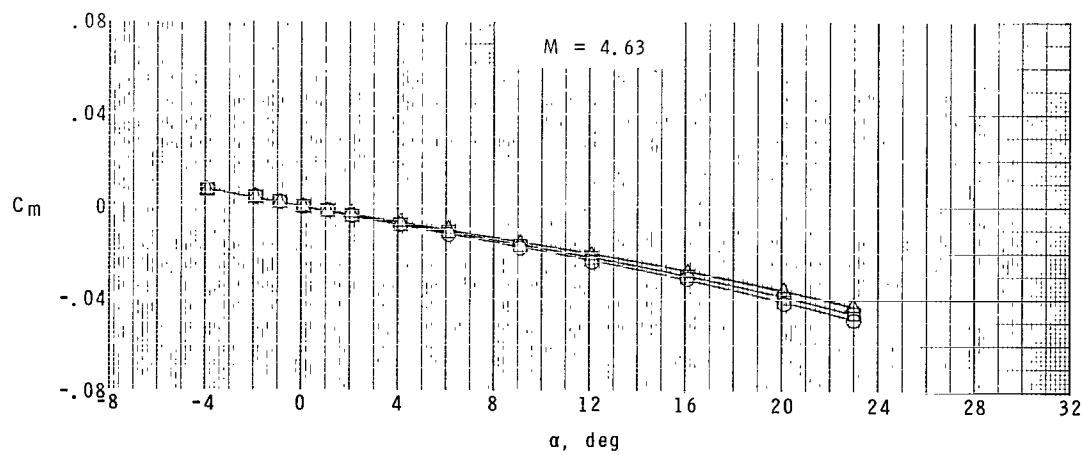
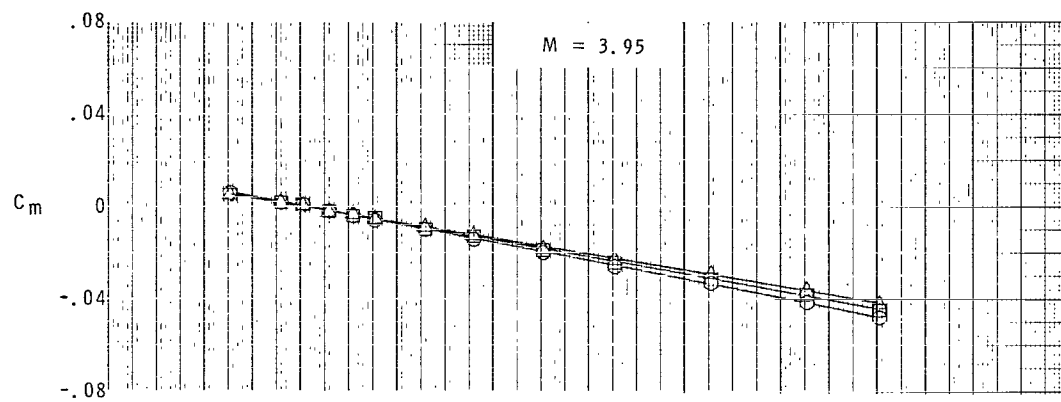
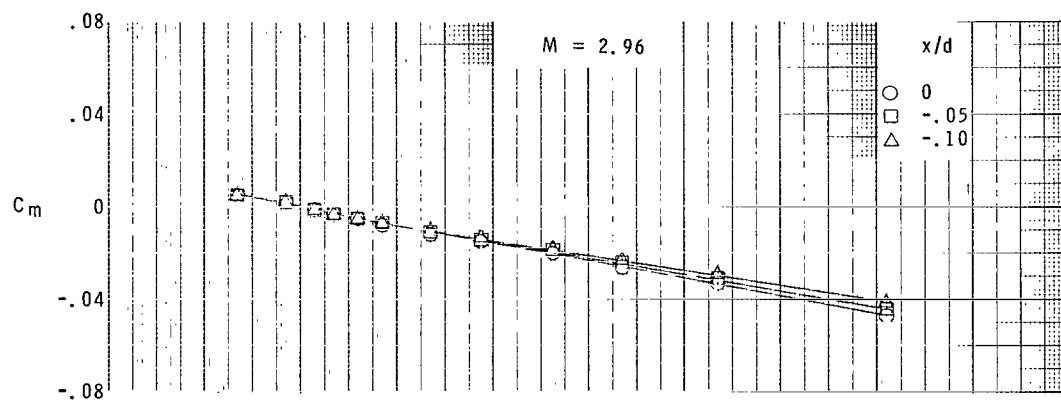


Figure 16.- Concluded.

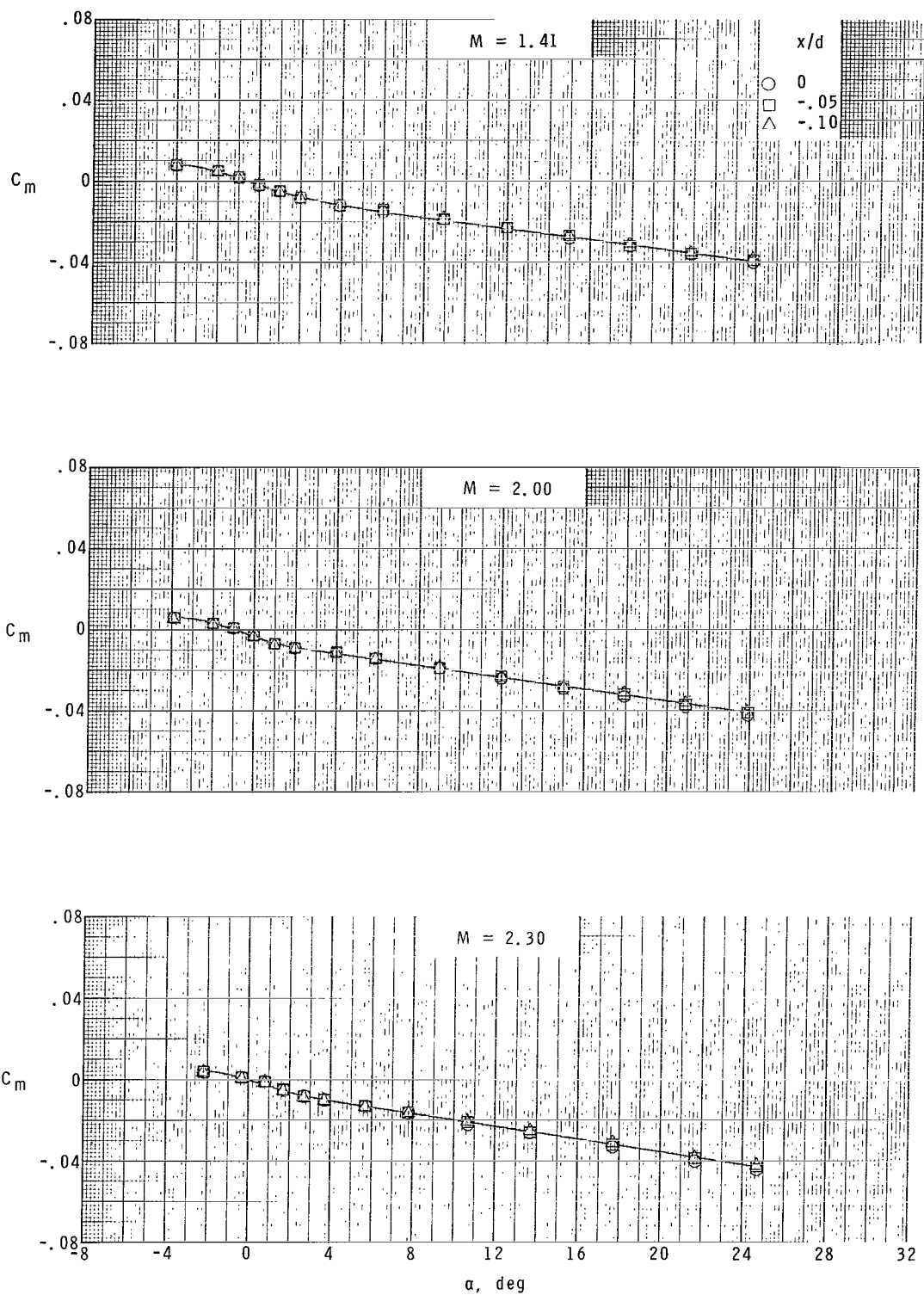


Figure 17.- Effect of longitudinal center-of-gravity location on pitching-moment characteristics of the  $80^\circ$  cone for range of Mach numbers.  $z/d = 0$ .



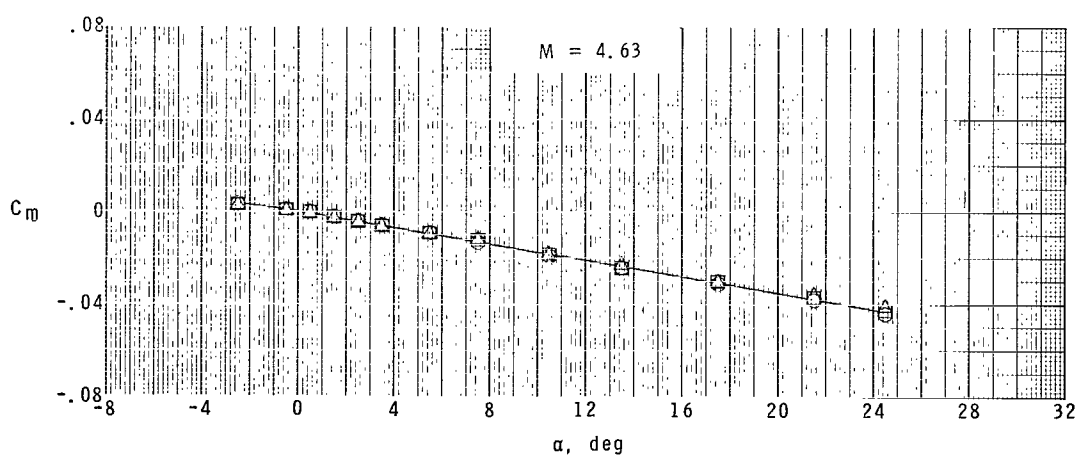
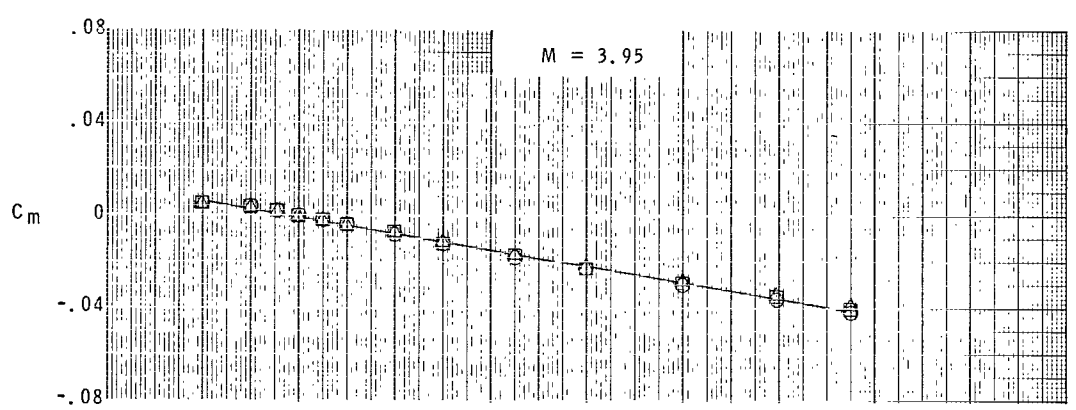
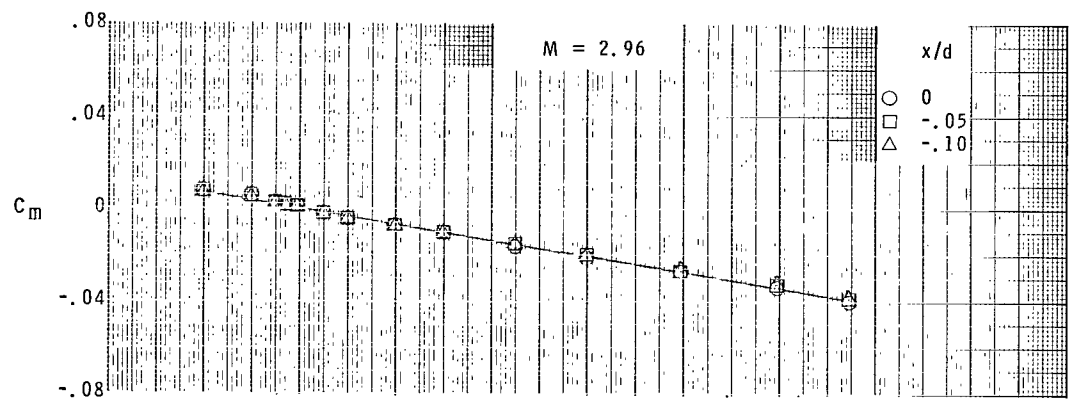


Figure 17.- Concluded.

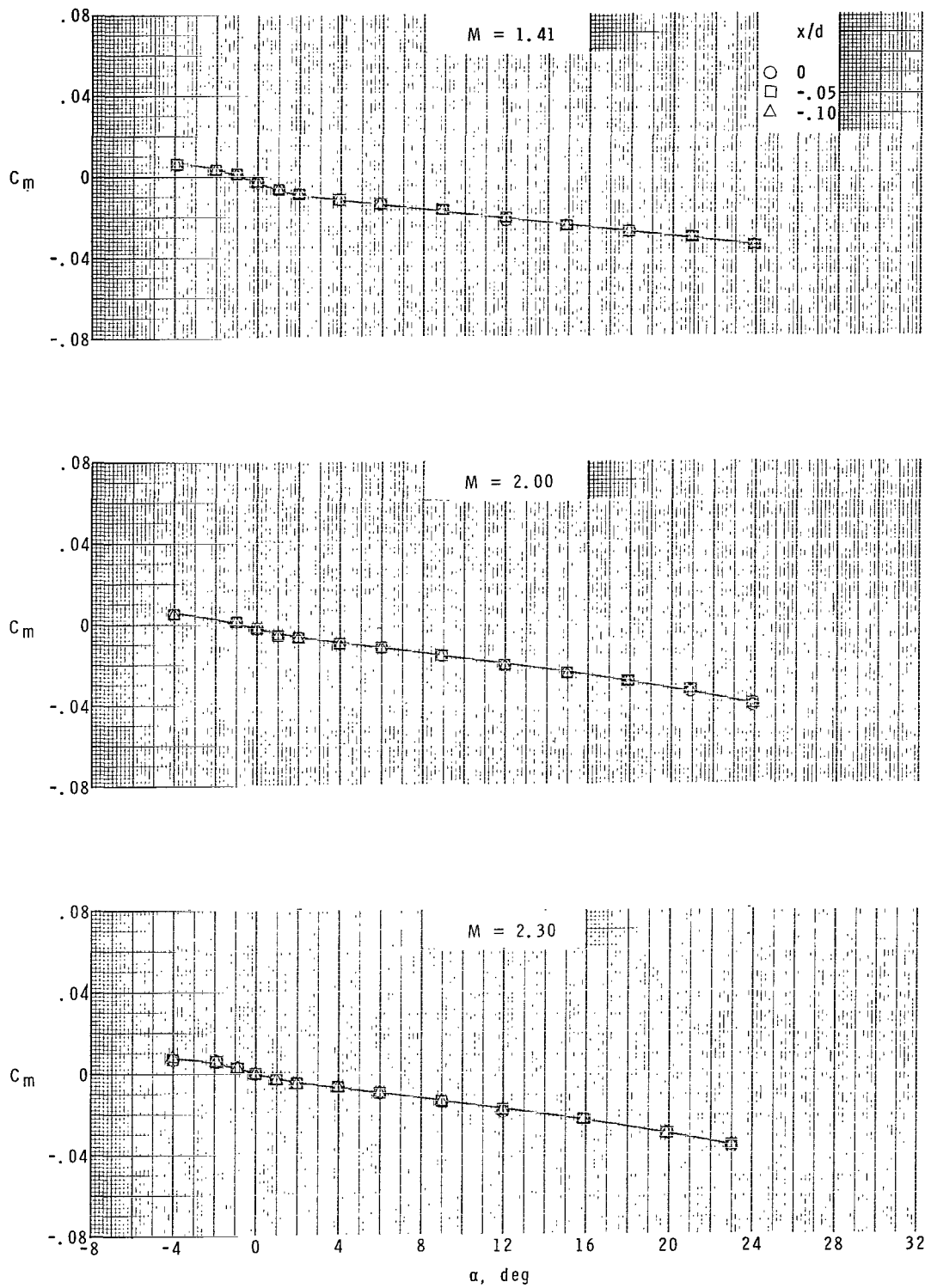


Figure 18.- Effect of longitudinal center-of-gravity location on pitching-moment characteristics of the  $90^\circ$  cone for range of Mach numbers.  $z/d = 0$ .

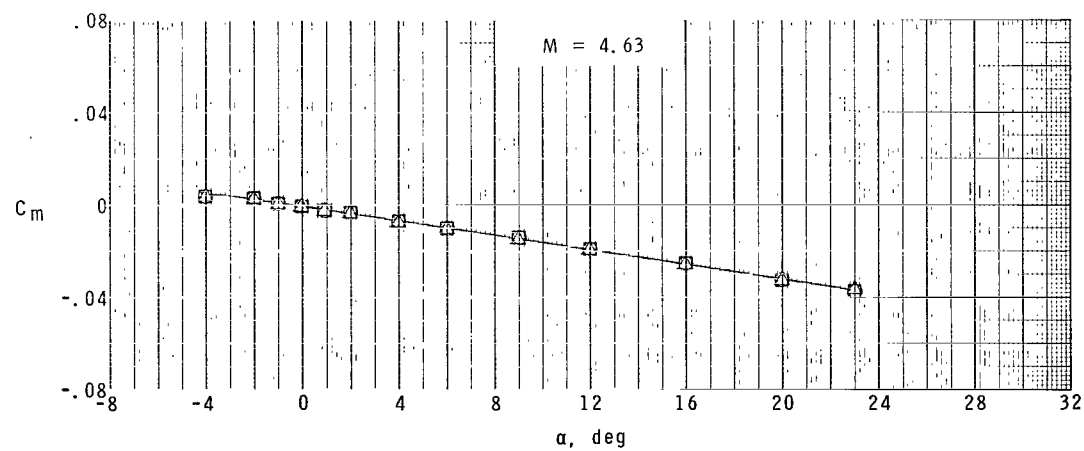
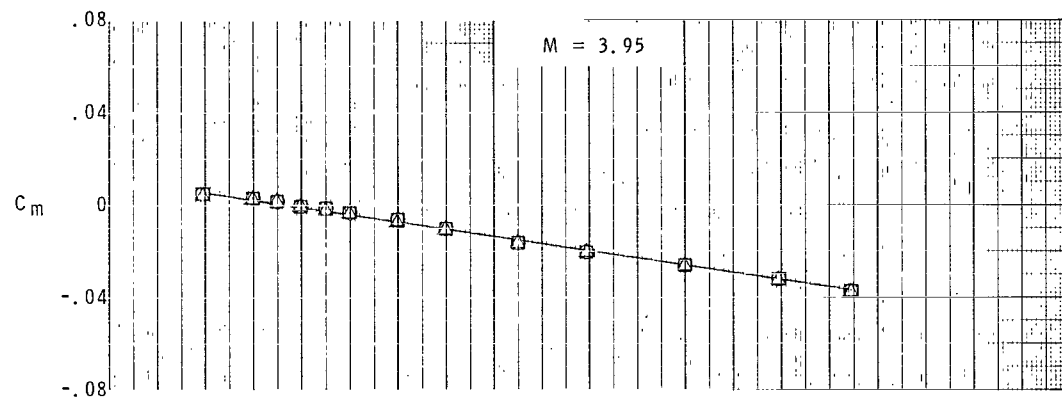
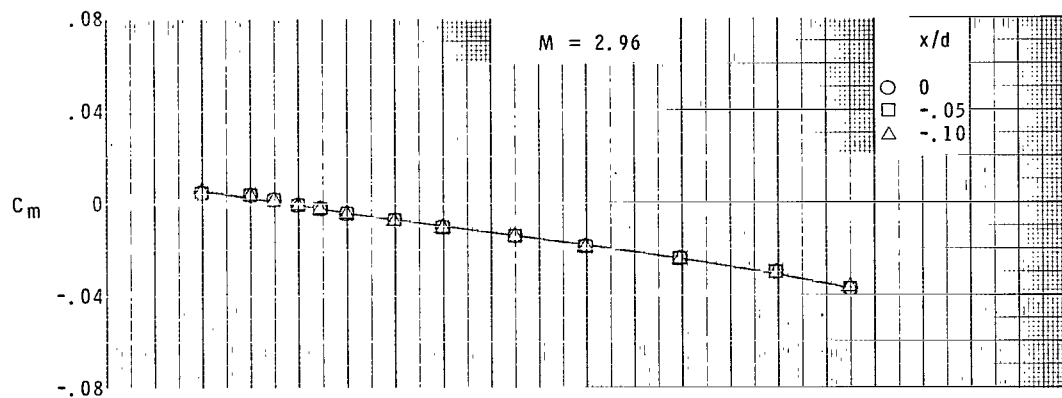


Figure 18.- Concluded.

NATIONAL AERONAUTICS AND SPACE ADMINISTRATION  
WASHINGTON, D. C. 20546  
OFFICIAL BUSINESS

FIRST CLASS MAIL



POSTAGE AND FEES PAID  
NATIONAL AERONAUTICS AND  
SPACE ADMINISTRATION

070 DPL 20 01 305 67286 00903  
RECEIVED OFFICE OF AERONAUTICS AND SPACE ADMINISTRATION  
KENTLAND AIR FORCE BASE, NEW MEXICO 87111

ALL INFORMATION CONTAINED HEREIN IS UNCLASSIFIED

POSTMASTER: If Undeliverable (Section 158  
Postal Manual) Do Not Return

*"The aeronautical and space activities of the United States shall be conducted so as to contribute . . . to the expansion of human knowledge of phenomena in the atmosphere and space. The Administration shall provide for the widest practicable and appropriate dissemination of information concerning its activities and the results thereof."*

—NATIONAL AERONAUTICS AND SPACE ACT OF 1958

## NASA SCIENTIFIC AND TECHNICAL PUBLICATIONS

**TECHNICAL REPORTS:** Scientific and technical information considered important, complete, and a lasting contribution to existing knowledge.

**TECHNICAL NOTES:** Information less broad in scope but nevertheless of importance as a contribution to existing knowledge.

**TECHNICAL MEMORANDUMS:** Information receiving limited distribution because of preliminary data, security classification, or other reasons.

**CONTRACTOR REPORTS:** Scientific and technical information generated under a NASA contract or grant and considered an important contribution to existing knowledge.

**TECHNICAL TRANSLATIONS:** Information published in a foreign language considered to merit NASA distribution in English.

**SPECIAL PUBLICATIONS:** Information derived from or of value to NASA activities. Publications include conference proceedings, monographs, data compilations, handbooks, sourcebooks, and special bibliographies.

**TECHNOLOGY UTILIZATION PUBLICATIONS:** Information on technology used by NASA that may be of particular interest in commercial and other non-aerospace applications. Publications include Tech Briefs, Technology Utilization Reports and Notes, and Technology Surveys.

*Details on the availability of these publications may be obtained from:*

SCIENTIFIC AND TECHNICAL INFORMATION DIVISION  
NATIONAL AERONAUTICS AND SPACE ADMINISTRATION  
Washington, D.C. 20546